Winter 2010

# Mathematical Models and Stability Analysis of Cholera Dynamics

Shu Liao
*Old Dominion University*

# MATHEMATICAL MODELS AND STABILITY ANALYSIS OF CHOLERA DYNAMICS

by

Shu Liao
M.S. Aug 2009, Old Dominion University

A Dissertation Submitted to the Faculty of
Old Dominion University in Partial Fulfillment of the
Requirement for the Degree of

DOCTOR OF PHILOSOPHY

COMPUTATIONAL AND APPLIED MATHEMATICS

OLD DOMINION UNIVERSITY
December 2010

Approved by:

Jin Wang (Director)

John A. Adam (Member)

Yan Peng (Member)

Holly D. Gaff (Member)

# ABSTRACT

## MATHEMATICAL MODELS AND STABILITY ANALYSIS OF CHOLERA DYNAMICS

Shu Liao
Old Dominion University, 2010
Director: Dr. Jin Wang

In this dissertation, we present a careful mathematical study of several epidemic cholera models, including the model of Codeco [11] in 2001, that of Hartley, Morris and Smith [22] in 2006, and that of Mukandavire, Liao, Wang and Gaff *et al.* [60] in 2010. We formally derive the basic reproduction number $R_0$ for each model by computing the spectral radius of the next generation matrix. We focus our attention on the stability analysis at the disease-free equilibrium which determines the short-term epidemic behavior, and the endemic equilibrium which determines the long-term disease dynamics. Particularly, we incorporate the Volterra-Lyapunov matrix theory into Lyapunov functions to facilitate the analysis of the global endemic stability. Based on the previous cholera models, we propose a new and unified deterministic model which incorporates a general incidence rate and a general formulation of the pathogen concentration, to improve our understanding of cholera dynamics. In addition, we briefly discuss the changes of the dynamics for the cholera models when several control measures are incorporated.

# ACKNOWLEDGMENTS

I wish to express the deepest thanks and gratitude to my advisor Professor Jin Wang for his numerous suggestions and patient guidance throughout the development of this dissertation. His knowledge and passion in research have motivated me to be a better student and researcher since day one. Above all, he provided me continuous support in various ways, and helped me navigate through many curveballs during the course of my study. I am indebted to him more than he knows.

I would like to thank Dr. John A. Adam, Dr. Yan Peng and Dr. Holly D. Gaff for serving on my dissertation committee. I would also like to extend my thanks to the faculty and staff of the department of mathematics and statistics at Old Dominion University for their unconditional support and collegiality. This dissertation would not have been finished without their input. Special thanks goes to Professor Dorrepaal, for providing a pleasant and stimulating environment. I extend thanks to the Department of Mathematics and Statistics for the financial support for my graduate studies. Finally, I extend gratitude to Barbara Jeffrey, Gayle Tarkelsen and Sheila Hegwood, all of whom made my experience quite enjoyable. Thank you all, now and always.

I dedicate this thesis to Weiming who is glad that I started,
and to my parents who are glad that I finished.

# TABLE OF CONTENTS

# LIST OF TABLES

# LIST OF FIGURES

# CHAPTER I

# INTRODUCTION

Cholera, a water-borne disease caused by the bacterium *Vibrio cholerae* and spread by eating or drinking contaminated food or water, remains a significant threat to public health in developing countries. For example, over 142,000 cholera cases and over 4,500 deaths were reported in 2002 by 52 nations worldwide [86]. Most of these countries are in Africa. In addition, many believe the actual infection and death numbers have been far more than those reported due to poor surveillance and incomplete records. In some parts of Africa, measurable improvements in sanitation, hygiene, and infrastructure have occurred during recent years, but the majority of the population still live in environments without safe drinking water, putting them at ongoing risk for cholera [59].

A notable example of recent cholera epidemics is the 2008-2009 cholera outbreak in Zimbabwe, which was regarded as the worst African cholera epidemic in the last 15 years. In addition to the large number of infections, this cholera outbreak was also characterized by its wide spread and high fatality rate. It began in August 2008, swept across the whole country by December 2008, and by July 2009 there had been over 98,500 reported cases and over 4,200 deaths [84; 85; 86]. The case fatality ratio (CFR) was about 4.3%, whereas the CFR in most outbreaks around the world was below 1%. In some remote areas of Zimbabwe which were outside the treatment facilities, the CFRs were as high as 40% [54; 86].

In order to fight against cholera and to design effective control strategies, we need to better understand the dynamics of cholera in its initiation, spread and evolution. Cholera dynamics is complicated by the multiple interactions between the human host, the pathogen, and the environment [62], which contribute to both direct human-to-human and indirect environment-to-human transmission pathways. Despite a large body of clinical, experimental and theoretical studies [1; 31; 57; 62; 64; 79], the fundamental mechanism of transmission for cholera is not well understood at present, which has hindered effective prevention and control strategies of the disease. The difficulty stems from the complex, multiple transmission pathways which include

This dissertation follows the style of *PLoS Medicine*.

both direct human-to-human and indirect environment-to-human transmissions, and which distinct cholera from many other infectious diseases.

Mathematical modeling, simulation and analysis provide a promising way to look into the nature of the cholera dynamics, and many efforts have been devoted to this topic. Capasso and Paveri-Fontana [7] introduced a simple deterministic model in 1979 to study a cholera epidemic in the Mediterranean. They considered a population of bacteria and a population of infected humans, with infectivity modeled under a saturation condition. Pourabbas *et al.* published an SIRS cholera model [65] in 2001, representing human-to-human transmission with a time-dependent infectivity coefficient $\beta(t)$ so that the incidence rate was given by $\beta(t)\, I$ (where $I$ denotes the infected).

In the classic SIRS model, the population is divided into three disjoint classes according to disease status: the susceptible, the infected, and the recovered populations, respectively. The susceptible class (S) contains the individuals who are not infected with the disease yet but can occur the disease. The infected class (I) contains the individuals who are currently infected, and the recovered class (R) contains the individuals who can not transmit the disease any more by recovery with immunity. For simplicity, the total population is assumed to be a constant $N$, where $N = I + S + R$, and the total population must be sufficiently large so that the size of each class can be considered as a continuous variable. Normally, the models are named by a sequence of letters which tell the flow of different classes. For example, in an SIRS model, people are first susceptible, then infectious, then recovered, and finally susceptible again after they have lost their temporary immunity. Some important parameters are used frequently in most models: such as the daily contact rate which is defined by the average number of contacts per infective per day. The death rate is defined in the model which represents the death from each class at a rate proportional to the class size. Based on the death rate, the average lifetime is 1 / (death rate). The recovery rate is defined as individuals recover and are removed from the infected class at a rate proportional to the number of infectious [24]. The incidence rate, is the rate of new cases of a disease in a specified population over a defined period.

With the progress of research, people found that toxigenic *V. cholerae* can stay in

some aquatic environments for a long time [11], suggesting that the aquatic environment may be a reservoir of toxigenic *V. cholerae*. However, the mechanism driving *V. cholerae* dynamics in water was still unknown. Codeco in 2001 published a model [11] that explicitly accounted for the environmental component, i.e., the *V. cholerae* concentration in the water supply, denoted as $B$, into a regular SIR epidemiological model. The incidence was modeled by $a\frac{B}{K+B}$ where $a$ is the contact rate with contaminated water, and $K$ is the half saturation rate (i.e., $ID_{50}$, the infectious dose in water sufficient to produce disease in 50% of those exposed). Fig 1.1 shows Codeco's model flow diagram.

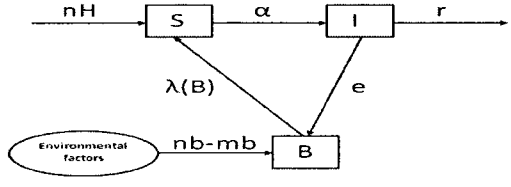


Figure 1.1: Codeco's model flow diagram. Note: $\lambda(B) = \frac{B}{\kappa+B}$.

Ghosh *et al.* in 2004 published an SIS model [20] which included both the concentration $B$ of vibrios and the density $E$ of environmental discharge that contributes to the growth of the vibrio population. The model had both human-to-human and environment-to-human transmission modes with the incidence given by $\beta I + \lambda B$, where $\beta$ and $\lambda$ are corresponding contact rates. Hartley, Morris and Smith [22] in 2006 extended Codeco's work to include a hyperinfectious state of the pathogen, representing the "explosive" infectivity of freshly shed *V. cholerae*, based on the laboratory measurements that freshly shed *V. cholerae* from human intestines outcompeted other *V. cholerae* by as much as 700-fold for the first few hours in the environment [1; 57]. Their model is a combination of SIR formulation and two environmental variables, which constitute a high-dimensional autonomous system. The article [22] provided deeper insight into cholera epidemics, though no rigorous dynamical analysis was presented in that work with its focus on medical aspects. Fig 1.2 shows Hartley's model of cholera transmission.

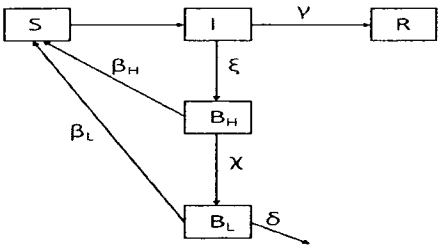


Figure 1.2: Hartley's model of cholera transmission, incorporating a HI state of *V. cholera*

.

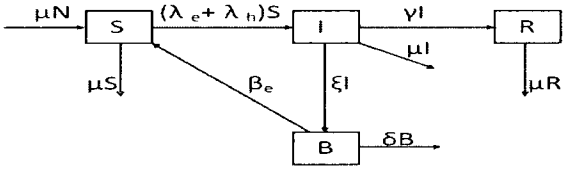


Figure 1.3: Mukandavire's model flow diagram. Susceptible individuals acquire cholera infection either by ingesting environmental vibrios from contaminated aquatic reservoirs or through human-to-human transmission resulting from the ingestion of hyperinfectious vibrios, at rates $\lambda_e = \frac{\beta_e B}{\kappa + B}$ and $\lambda_h = \beta_h I$, respectively.

Recently, Mukandavire, Liao, Wang and Gaff *et al.* [60] proposed a model to study the 2008-2009 cholera outbreak in Zimbabwe. The model considered both human-to-human and environment-to-human transmission pathways. This model treats the hyperinfectious vibrio state as a direct human-to-human transmission, considering that the lifespan of the hyperinfectious bacterium in the environment is very short. Such a simplification of the cholera model probably does not result in any loss of mathematical generality [2] and retains the model's capability to describe the explosive nature of cholera outbreaks. However, the former approach makes the interaction between humans and hyperinfectious vibrios more explicit. Fig 1.3 shows the model flow diagram.

Finally, we mention a very recent work by Tien and Earn [78] which constructed a mathematical model for general water-borne diseases where bilinear incidence rates are used to model both environment-to-human and human-to-human transmissions.

All these models have their own strength and weakness. Some of the models only track the human population dynamics directly and represent the *V. cholerae* population in a separate manner, whereas some other models tend to focus on the environmental components while neglecting direct human-to-human transmission. In addition, many of these studies lack rigorous mathematical analysis which accounts for part of the reason that cholera dynamics has not been well understood so far. In this dissertation, we focus on the following three models: Codeco [11], Hartley, Morris and Smith [22] and Mukandavire, Liao, Wang and Gaff *et al.* [60] to conduct mathematical analysis. Also, we notice that two major differences among these models are how the incidence rate is determined and how the environmental vibrio concentration is formulated. Hence, we try to propose a unified cholera model which allows general nonlinear incidence factors and general representation of the pathogen concentrations. Based on this generalized model, we will conduct a careful mathematical study to explore the complex cholera dynamics so as to improve our understanding of the fundamental disease transmission mechanism. We will particularly investigate the stability property in both the epidemic and endemic dynamics through equilibrium analysis.

This dissertation is organized into seven chapters as follows. In chapter II, we introduce necessary theoretical background of the basic reproduction number $R_0$, the definition and methods of local stability and global stability which help the reader to follow the materials in the following chapters. In chapter III, we give a discussion of the behavior of dynamical systems which allows us to derive the basic reproduction number $R_0$ by using the next-generation matrix approach. Then we conduct local asymptotic stability analysis to the three important epidemic models. Moreover, bifurcation diagram and numerical simulation results are presented. In chapter IV, we construct the generalized model based on the previous work under the necessary assumptions and conduct a careful mathematical study. In chapter V, we discuss the global asymptotical stability of three dimensional and four dimensional models. In the last part of this chapter, we will unify several existing models in the analysis and simulation. In chapter VI, we modify Codeco's model [11] and the generalized model

introduced in chapter IV by incorporating three particular controls, i.e., vaccination, antibiotic and water sanitation. Finally, some conclusions, discussion and future research work will be presented in chapter VII.

# CHAPTER II

# MATHEMATICAL BACKGROUND

## II.1 The basic reproduction number $R_0$

The basic reproduction number, commonly denoted as $R_0$, is a crucial quantity in all epidemiology models; it is defined as the average number of secondary infections that occur when one infective is introduced into a completely susceptible host population [23; 80]. Thus the number $R_0$ is considered as the key threshold that determines whether an infectious disease can invade and persist in a new host population. It is widely accepted that an epidemic will occur when $R_0 > 1$. The magnitude of $R_0$ allows public health administrators and policy makers to determine the amount of effort necessary to prevent or eliminate an epidemic. In particular, the value of $R_0$ is directly related to the minimum coverage required by various control strategies such as vaccination and chemotherapy [14]. It is thus important to have an accurate estimate of $R_0$ for any infectious disease that threatens human health.

There are two common ways to obtain the basic reproduction number for an infectious disease: one is to directly evaluate $R_0$ using available data and some statistical techniques (e.g., [14; 81]), often resulting in simple mathematical formulas, and this method has to use the initial growth rate and final size of the epidemic with the data of age-specific prevalence. The other is to determine $R_0$ based on a specific mathematical model (such as a system of differential equations) targeted at the given disease (e.g., [11; 80]). The formulas obtained from the first approach could be more general and applicable to different types of infectious diseases, but the result may be less accurate than that from the second approach when a specific epidemic is concerned. In this dissertation, we will focus our attention on the second approach and apply it to the three mathematical models we introduced in the first charter in order to investigate the cholera outbreak.

While $R_0$ can be found by computing the eigenvalues of the Jacobian at the disease free equilibrium, Diekmann [13] follows a different approach based on the next generation matrix. According to the work of van den Driessche and Watmough [80], $R_0$ is mathematically defined as the spectral radius of the next generation matrix.

Let $X = [x_1, x_2, \ldots, x_n]^T$ with the first $m$ compartments corresponding to infected individuals. If we define $X_s$ to be the set of all disease free states, that is

$$X_s = \{x \geq 0 | x_i = 0, i = 1, ...m\}.$$

Let $\mathcal{F}_i(X)$ be the rate of appearance of new infections in compartment $i$, $\mathcal{V}_i^+(x)$ be the rate of transfer of individuals into compartment $i$, $\mathcal{V}_i^-(x)$ be the rate of transfer of individuals out compartment $i$. A disease transmission model can be represented by the following system of equations:

$$\frac{dX}{dt} = \mathcal{F}_i(X) - \mathcal{V}_i(X) \tag{2.1.1}$$

where $\mathcal{V}_i = \mathcal{V}_i^- - \mathcal{V}_i^+$. Since each function represents a rate of appearance or transfer of individuals, they are all nonnegative. We have the following lemma.

**Lemma 1.** *[80] Let $x_0$ be a disease free equilibrium and $\mathcal{F}_i(x)$ satisfie the following assumptions:*
*(A1) if $x \geq 0$, then $\mathcal{F}_i \geq 0$, $\mathcal{V}_i^+ \geq 0$ and $\mathcal{V}_i^- \geq 0$ for $i = 1, ..., n$.*
*(A2) if $x_i = 0$ then $\mathcal{V}_i^- = 0$. In particular, if $x \in X_s$ then $\mathcal{V}_i^- = 0$ for $i = 1, ..., n$.*
*(A3) $\mathcal{F}_i = 0$ if $i > n$.*
*(A4) if $x \in X_s$ then $\mathcal{F}_i(x) = 0$ and $\mathcal{V}_i^+(x) = 0$ for $i = 1, ..., n$.*
*(A5) if $\mathcal{F}_i(X)$ is set to zero, then all eigenvalues of $Df(x_0)$ have negative real parts.*
*Then the derivatives $D\mathcal{F}(x_0)$ and $D\mathcal{V}(x_0)$ are partitioned as*

$$D\mathcal{F}(x_0) = \begin{bmatrix} F & 0 \\ 0 & 0 \end{bmatrix}, \qquad D\mathcal{V}(x_0) = \begin{bmatrix} V & 0 \\ J_3 & J_4 \end{bmatrix}$$

*where $F$ and $V$ are the $m \times m$ matrices defined by*

$$F = \left[\frac{\partial \mathcal{F}_i}{\partial X_j}(x_0)\right] \qquad \text{and} \qquad V = \left[\frac{\partial \mathcal{V}_i}{\partial X_j}(x_0)\right] \qquad \text{with } 1 \leq i, j \leq m.$$

*Further, $F$ is nonnegative, $V$ is a nonsingular M-matrix and all eigenvalues of $J_4$ have positive real parts.*

Since $F$ is nonnegative, $V$ is a nonsingular M-matrix, $V^{-1}$ is nonnegative [4], as is $FV^{-1}$. Following [13] and [80], we define $FV^{-1}$ the next generation matrix for our mathematical models and set

$$R_0 = \rho(FV^{-1}),$$

where $\rho(A)$ denotes the spectral radius of a matrix A. Therefore, based on our mathematical models, we will formally derive the basic reproduction number $R_0$ through the computation of the next generation matrix. Also, the stability of the disease-free equilibrium leads to the same result for $R_0$. Based on the cholera models, we will show that if $R_0 < 1$, the DFE is locally asymptotically stable; if $R_0 > 1$, the DFE is unstable, but the positive endemic equilibrium exists and is locally asymptotically stable. In other words, there is a stability exchange at $R_0 = 1$, and a transcritical bifurcation takes place.

## II.2 Local stability

An equilibrium point for a dynamical system is a point $X_0$ such that if $X(0) = X_0$, then $X(t) = X_0$ for all t. Equilibrium points represent stationary conditions for the dynamics of a system.

**Definition 1.** *[30] An equilibrium point $X^*$ of $\dot{X} = f(X)$ is*

- *stable if for each $\varepsilon > 0$ there is $\delta > 0$ (dependent on $\varepsilon$) such that*

$$\|X(0) - X^*\| < \delta \Rightarrow \|X(t) - X^*\| < \varepsilon, \forall t \geq 0;$$

- *unstable if it is not stable;*
- *asymptotically stable if it is stable and $\delta$ can be chosen such that*

$$\|X_0 - X^*\| < \delta \Rightarrow \lim_{t\to\infty} X(t) = X^*;$$

- *globally asymptotically stable if it is stable and*

$$\lim_{t\to\infty} X(t) = X^*,$$

*for all $X$.*

Now, our main concern is the stability of the dynamics of a system. In order to investigate the local asymptotic stability of the equilibrium point, we use Routh-Hurwitz stability criterion [85; 33] which provides necessary and sufficient conditions to establish the local stability of a dynamical system. We first consider the Jacobian $J(X^*)$ at the endemic equilibrium to obtain the characteristic polynomial, and set

$$det(\lambda I - J(X^*)) = 0.$$

Table 2.1: General Routh's array of coefficients

| | | | |
|---|---|---|---|
| $\lambda^n$ | $a_0$ | $a_2$ | $a_4\ a_6\ \cdots$ |
| $\lambda^{n-1}$ | $a_1$ | $a_3$ | $a_5\ a_7\ \cdots$ |
| $\lambda^{n-2}$ | $b_1$ | $b_2$ | $b_3\ b_4\ \cdots$ |
| $\lambda^{n-3}$ | $c_1$ | $c_2$ | $c_3\ c_4\ \cdots$ |
| $\vdots$ | $\vdots$ | $\vdots$ | |
| $\lambda^2$ | $e_1$ | $e_2$ | |
| $\lambda^1$ | $f_1$ | | |
| $\lambda^0$ | $g_1$ | | |

We can then to obtain a polynomial as follows:

$$a_0\lambda^n + a_1\lambda^{n-1} + \cdots + a_{n-1}\lambda + a_n = 0 \tag{2.2.1}$$

where $a_0 \neq 0$ and $a_n > 0$.

The equilibrium is locally asymptotically stable if all roots of equation (2.2.1) have negative real parts and unstable if equation (2.2.1) has at least one root with nonnegative real part. Table 2.1 shows how to compute the Routh array, after arranging the coefficients of the polynomial.

Specifically, we generate coefficients $b_i$ until all subsequent coefficients are zero:

$$b_1 = \frac{a_1a_2 - a_0a_3}{a_1}, \quad b_2 = \frac{a_1a_4 - a_0a_5}{a_1}, \quad b_3 = \frac{a_1a_6 - a_0a_7}{a_1}\cdots$$

Similarly, we can obtain the $c_i$, $d_i$, etc:

$$c_1 = \frac{b_1a_3 - a_1b_2}{b_1}, \quad c_2 = \frac{b_1a_5 - a_1b_3}{b_1}, \quad c_3 = \frac{b_1a_7 - a_1b_4}{b_1}\cdots$$

$$d_1 = \frac{c_1b_2 - b_1c_2}{c_1}, \quad d_2 = \frac{c_1b_3 - b_1c_3}{c_1}\cdots$$

This array above is called the Routh array [33]. It can be shown that a necessary and sufficient condition for all roots of the equation (2.2.1) to have negative real parts is that all the $a_i$ are positive and all of the coefficients in the first column of the Routh array are positive.

Table 2.2: Routh's array of a quadratic polynomial

| | | |
|---|---|---|
| $\lambda^2$ | $a_0$ | $a_2$ |
| $\lambda^1$ | $a_1$ | 0 |
| $\lambda^0$ | $a_2$ | |

Table 2.3: Routh's array of a cubic polynomial

| | | |
|---|---|---|
| $\lambda^3$ | $a_0$ | $a_2$ |
| $\lambda^2$ | $a_1$ | $a_3$ |
| $\lambda^1$ | $\frac{a_1 a_2 - a_0 a_3}{a_1}$ | |
| $\lambda^0$ | $a_3$ | |

We will apply Routh-Hurwitz stability criterion [85; 33] to generic quadratic polynomials, cubic polynomials and quartic polynomials as follows.

**Quadratic polynomial.**
Consider the quadratic polynomial:

$$a_0\lambda^2 + a_1\lambda + a_2 = 0,$$

where all the $a_i$ are positive. The Routh's array of coefficients becomes the table 2.2. The condition that all roots have negative real parts is:

$$a_0 > 0, \quad a_1 > 0, \quad a_2 > 0.$$

**Cubic polynomial.**
Consider the cubic polynomial:

$$a_0\lambda^3 + a_1\lambda^2 + a_2\lambda + a_3 = 0,$$

where all the $a_i$ are positive. The Routh's array of coefficients becomes the table 2.3. The condition that all roots have negative real parts is:

$$a_0 > 0, \quad a_1 > 0, \quad a_2 > 0, \quad a_3 > 0, \quad a_1 a_2 > a_0 a_3.$$

Table 2.4: Routh's array of a quartic polynomial

| | | | |
|---|---|---|---|
| $\lambda^4$ | $a_0$ | $a_2$ | $a_4$ |
| $\lambda^3$ | $a_1$ | $a_3$ | 0 |
| $\lambda^2$ | $\frac{a_1a_2-a_0a_3}{a_1}$ | $a_4$ | 0 |
| $\lambda^1$ | $a_3-\frac{a_4a_1^2}{a_1a_2-a_0a_3}$ | 0 | 0 |
| $\lambda^0$ | $a_4$ | 0 | 0 |

**Quartic polynomial.**

Consider the quartic polynomial:

$$a_0\lambda^4+a_1\lambda^3+a_2\lambda^2+a_3\lambda+a_4=0,$$

where all the $a_i$ are positive. The Routh's array of coefficients becomes the table 2.4. The condition that all roots have negative real parts is:

$$a_0>0,\quad a_1>0,\quad a_2>0,\quad a_3>0,\quad a_4>0\,,$$

$$a_1a_2-a_0a_3>0,\quad a_3>\frac{a_4a_1^2}{a_1a_2-a_0a_3}.$$

## II.3 Global stability analysis

To improve our understanding of the fundamental mechanism in the initiation and transmission of infectious diseases, careful mathematical analysis is required to study the dynamics of the model systems. In particular, an important question in epidemiology is whether an infectious disease, after possible epidemic outbreak, will persist and stay at a positive infection level over time, and whether this behavior depends on the initial size of the infection. Mathematically, this is represented by the global asymptotic stability of the endemic equilibria. An equilibrium point is globally asymptotically stable if all solutions converge to that equilibrium point, the proof of which remains open for many important epidemiological models. For two-dimensional autonomous systems, the classical Poincare-Bendixson theory [21] is a powerful tool to analyze global stability.

**Theorem 1.** *[50; 76] If a trajectory $x(t,p)$, starting from a point $p$, of the equation,*

$$X^{'}(t) = f(X(t)), \ X(t_0) = p,$$

*is bounded in $\Re^2$ for $t \geq 0$ (the corresponding results for $t \leq 0$ are also true), then one of the following three things must happen:*
*1. there exist a sequence of points on the trajectory as $t \to \infty$ that approach a critical point;*
*2. $X(t,p)$ is a periodic orbit;*
*3. $\omega(t)$ is a periodic orbit, and $X(t,p)$ approaches $\omega(t)$ spirally as $t \to \infty$, where $\omega(t)$ is the set such that each point of $\omega(t)$ is a limit of some sequence of points on the trajectory as $t \to \infty$.*

In particular, the Dulac criterion can be conveniently used to preclude the existence of non-constant periodic orbits.

**Theorem 2.** *[50; 76] Let $P(x,y)$, $Q(x,y)$, and $B(x,y)$ have continuous first partial derivatives in a simply connected domain $D \in \Re^2$ and assume that $\frac{\partial(PB)}{\partial x} + \frac{\partial(QB)}{\partial y}$ is not identically zero and does not change sign in any open set of $D$. Then the system,*

$$\begin{aligned} x^{'}(t) &= P(x(t), y(t)), \\ y^{'}(t) &= Q(x(t), y(t)), \ x, y, t \in \Re. \end{aligned}$$

*has no periodic orbit in $D$.*

Note, the Bendixson criterion is a special case when we use $B = 1$ in Theorem 2. Unfortunately, this framework is no longer valid for general dynamical systems of dimension three or higher. To partially overcome this difficulty, the concept of monotone flows [42; 44; 73; 74; 75] was introduced for a class of dynamical systems which possess monotonicity (e.g., competitive systems [27; 42]). For such high-dimensional systems, the Poincare-Bendixson property is preserved and the existence of non-constant periodic solutions is ruled out by the orbital asymptotic stability, thus establishing the global stability of the positive endemic equilibria. However, most high-dimensional epidemiological models do not possess the nice properties of monotone systems, which limits the application of this approach. Another method, the geometric approach, originally proposed by Li and Muldowney [16; 45], has gained some popularity in recent years (see, e.g. [6; 39]) as it has less constraints

on the model systems. The key part of this approach is to check a high-dimensional Bendixson criterion (derived from the Lozinskii measure [41]) which is robust under $C^1$ local perturbations, and based on which the local asymptotic stability leads to the global stability. The procedure to check this criterion, however, is highly nontrivial. Both the methods of monotone flows and geometric approach require the biologically feasible region to be bounded, convex and contains a compact absorbing set, a condition which is usually difficult to validate, and may not even be satisfied, by many epidemiological models. In addition, both methods encounter significant difficulty when dealing with four- or even higher-dimensional systems. Nonetheless, these two methods have been successfully applied to quite a few epidemiological models in the form of regular SEIR, SIRS and SEIRS formulations (see, e.g., [40; 42; 44; 45; 43; 46; 48; 74; 75; 83]).

Another approach of global stability analysis is based on Lyapunov functions [30; 52] and has been well known for many decades, though its application to biological systems has a relatively short history [36]. Lyapunov functions are functions which can be used to prove the stability of a certain fixed point in a dynamical system or autonomous differential equation. We introduce the definition of Lyapunov-candidate-functions and Lyapunov theorems below.

**Definition 2.** *[85] Let $V: \mathbb{R}^n \to \mathbb{R}$ be a scalar function. $V$ is a Lyapunov-candidate-function if it is a locally positive-definite function, i.e.*

$$\begin{aligned} V(0) &= 0, \\ V(x) &> 0, \forall x \in U \setminus \{0\}, \end{aligned}$$

*with $U$ being a neighborhood region around $x = 0$.*

**Theorem 3.** *[85] Let $X^* = 0$ be an equilibrium of the autonomous system*

$$\dot{x} = f(x),$$

*and let*

$$\dot{V}(x) = \frac{\partial V}{\partial x} \cdot \frac{dx}{dt} = \nabla V \cdot \dot{x} = \nabla V \cdot f(x)$$

*be the time derivative of the Lyapunov-candidate-function $V$.*

*• If the Lyapunov-candidate-function $V$ is locally positive definite and the time derivative of the Lyapunov-candidate-function is locally negative semidefinite:*

$$\dot{V}(x) \leq 0, \ \forall x \in \mathcal{B} \setminus \{0\}$$

*for some neighborhood $\mathcal{B}$ of 0, then the equilibrium is proven to be stable.*

• *If the Lyapunov-candidate-function $V$ is locally positive definite and the time derivative of the Lyapunov-candidate-function is locally negative definite:*

$$\dot{V}(x) < 0, \ \forall x \in \mathcal{B} \setminus \{0\}$$

*for some neighborhood $\mathcal{B}$ of 0, then the equilibrium is proven to be locally asymptotically stable.*

• *If the Lyapunov-candidate-function $V$ is globally positive definite, radially unbounded and the time derivative of the Lyapunov-candidate-function is globally negative definite:*

$$\dot{V}(x) < 0, \ \forall x \in \mathbb{R}^n \setminus \{0\}$$

*then the equilibrium is proven to be globally asymptotically stable.*

• *The Lyapunov-candidate function V(x) is radially unbounded if*

$$\|x\| \to \infty \Rightarrow V(x) \to \infty.$$

For example, if we consider the following differential equation on $\mathbb{R}$:

$$\dot{x} = -x.$$

The velocity vector points always towards the origin, so the distance from it decreases with time and is a natural candidate for a Lyapunov function. Take $V(x) = |x|$ on $\mathbb{R} \setminus \{0\}$. Then

$$\dot{V}(x) = V'(x)f(x) = sign(x) \cdot (-x) = -|x| < 0.$$

This correctly shows that the origin is asymptotically stable. This classical method requires little theoretical background and is straightforward to implement. The challenge, however, in the application of this method is that there is no systematic way to construct Lyapunov functions (particularly, the determination of the appropriate coefficients is often a matter of luck), so that its success largely depends on trial and error as well as on specific problems. Some recent developments of this method in the context of epidemiological models include the work of Beretta and Capasso [3] that derived a necessary condition for the global endemic stability using a skew-symmetry property of the Jacobian, the work of Rinaldi [69] that obtained global

stability results for SEIRS models, and the work of Lin and So [49] that investigated the global dynamics of SIRS multi-group models. We note that all these studies concentrated on epidemiological models with standard bilinear incidence rates. More recently, Korobeinikov and Maini [34] proposed a new type of Lyapunov functions to obtain global stability results for models with nonlinear incidence in the form of $\beta I^p S^q$.

In this dissertation, we improve the method of Lyapunov functions and formulate a systematic approach in global stability analysis that will effectively overcome some of the disadvantages of the existing approaches. We incorporate the Volterra-Lyapunov matrix theory [66; 67; 69] into Lyapunov functions, which completely eliminate the need of determing the coefficient values. So one of the key points to use this technique is to prove that a suitable matrix is Volterra-Lyapunov stable.

Below we introduce necessary concepts and notations that will facilitate our global stability analysis. We will also present several known results on stable matrices, which build the theoretical foundation of this work.

**Notation 1.** *We write a matrix $A > 0$ ( $< 0$ ) if $A$ is symmetric positive (negative) definite.*

The following fundamental result on matrix stability was originally proved by Lyapunov:

**Lemma 2.** *[52] Let $A$ be an $n \times n$ real matrix. Then all the eigenvalues of $A$ have negative (positive) real parts if and only if there exists a matrix $H > 0$ such that $HA + A^T H^T < 0$ $(> 0)$ .*

**Definition 3.** *We say a nonsingular $n \times n$ matrix $A$ is Volterra-Lyapunov stable if there exists a positive diagonal $n \times n$ matrix $M$ such that $MA + A^T M^T < 0$ .*

**Definition 4.** *We say a nonsingular $n \times n$ matrix $A$ is diagonally stable (or positive stable) if there exists a positive diagonal $n \times n$ matrix $M$ such that $MA + A^T M^T > 0$.*

From Definitions 3 and 4, it is clear that a matrix A is Volterra-Lyapunov stable if and only if $-A$ is diagonally stable. The following lemma determines all $2 \times 2$ Volterra-Lyapunov stable matrices.

**Lemma 3.** *[66] Let* $D = \begin{bmatrix} d_{11} & d_{12} \\ d_{21} & d_{22} \end{bmatrix}$ *be an* $2 \times 2$ *matrix. Then* $D$ *is Volterra-Lyapunov stable if and only if* $d_{11} < 0$ , $d_{22} < 0$ , *and* $det(D) = d_{11}d_{22} - d_{12}d_{21} > 0$ .

The characterization of Volterra-Lyapunov stable (or diagonally stable) matrices of higher dimensions, however, is much more difficult. Cross [12] obtained the following sufficient and necessary conditions for $3 \times 3$ diagonally stable matrices.

**Lemma 4.** *[12] Let* $P = (p_{ij})$ *be a* $3 \times 3$ *real matrix and* $\widehat{Q} = (\widehat{q}_{ij}) = det(P)Q$ *be the adjoint of* $P$ , *where* $Q = (q_{ij})$ *is the inverse of* $P$ . *Then* $P$ *is diagonally stable if and only if all the signed principal minors of* $-P$ *are positive, and the inequalities*

$$(p_{31} + zp_{13})^2 < 4p_{11}p_{33}z\,, \qquad (\widehat{q}_{31} + z\widehat{q}_{13})^2 < 4\widehat{q}_{11}\widehat{q}_{33}z$$

*are satisfied simultaneously.*

**Notation 2.** *For any* $n \times n$ *matrix* $A$, *we let* $\widetilde{A}$ *denote the* $(n-1) \times (n-1)$ *matrix obtained from* $A$ *by deleting its last row and last column.*

Based on Lemma 4, the following generalized result was obtained by Redheffer [66; 67] which will be frequently used in our global stability analysis. For simplicity, we only state the sufficient condition below.

**Lemma 5.** *[66; 67] Let* $D = [d_{ij}]$ *be a nonsingular* $n \times n$ *matrix* $(n \geq 2)$ *and* $M = diag(m_1, ..., m_n)$ *be a positive diagonal* $n \times n$ *matrix. Let* $E = D^{-1}$ . *Then, if* $d_{nn} > 0$ , $\widetilde{M}\widetilde{D} + (\widetilde{M}\widetilde{D})^T > 0$, *and* $\widetilde{M}\widetilde{E} + (\widetilde{M}\widetilde{E})^T > 0$ , *it is possible to choose* $m_n > 0$ *such that* $MD + D^TM^T > 0$.

Here we use a simple example to illustrate the global stability analysis. The system of a SEIS model is:

$$\frac{dS}{dt} = -\lambda SI + \mu - \mu S + \gamma I, \tag{2.3.1}$$

$$\frac{dE}{dt} = \lambda SI - (\varepsilon + \mu)E, \tag{2.3.2}$$

$$\frac{dI}{dt} = \varepsilon E - (\gamma + \mu)I, \tag{2.3.3}$$

where $S$ , $I$ and $E$ denote the susceptible, the infected, the exposed populations, respectively. $\mu$ is the natural human birth/death rate, $\gamma$ is the recovery rate, and

$\lambda IS$ is the incidence rate. All parameters are positive constants. Note this model does not consider immunity and there is no $R$ class.

If we write $X(t) = S(t) + E(t)$, and assume the total population is 1, this SEIS model becomes:

$$\begin{aligned} \frac{dX}{dt} &= -(\mu+\gamma)X - \varepsilon E + (\mu+\gamma), && (2.3.4)\\ \frac{dE}{dt} &= \lambda X[1-(X-E)] - (\varepsilon+\mu+\lambda)E, && (2.3.5)\\ I(t) &= 1 - X(t). && (2.3.6) \end{aligned}$$

We let $(X^*, E^*, I^*)$ be the nontrivial equilibrium point and consider the global stability in the region:

$$\Gamma = \{(X, E) \in \mathbb{R}^2_+ : 0 < X < 1, 0 < E < 1\}.$$

The components of the endemic equilibrium of system (2.3.4-2.3.5) must satisfy:

$$\begin{aligned} E^* &= \frac{\mu+\gamma}{\varepsilon(1-X^*)}, && (2.3.7)\\ X^* &= \frac{(\varepsilon+\mu+\lambda)(\mu+\gamma)}{(\lambda\varepsilon)+\lambda(\mu+\gamma)}. && (2.3.8) \end{aligned}$$

From equations (2.3.7) and (2.3.8), we can easily obtain:

$$\begin{aligned} (\mu+\gamma) &> \varepsilon E^*, && (2.3.9)\\ (\mu+\gamma)(\varepsilon+\mu) &> (\varepsilon+\mu))\varepsilon E^*\\ &> \varepsilon\lambda(X^*-E^*). && (2.3.10) \end{aligned}$$

We then translate the equilibrium points $(X^*, E^*)$ to the origin by considering $x_1 = X - X^*$ and $x_2 = E - E^*$. Then (2.3.4-2.3.5) become

$$\begin{aligned} x_1' &= -(\mu+\gamma)x_1 - \varepsilon E x_2, && (2.3.11)\\ x_2' &= \lambda x_1[1-(x_1-x_2)-(X^*-E^*)] - \lambda X^*(x_1-x_2)\\ &\quad -(\varepsilon+\mu+\lambda)x_2. && (2.3.12) \end{aligned}$$

We now construct Lyapunov function

$$V(x_1, x_2) = \sum_{i=1}^{2} w_i x_i^2$$

where $w_i > 0$ are both constants. And we have

$$\begin{aligned}\frac{dV}{dt}(x_1, x_2) &= 2w_1x_1[-(\mu+\gamma)x_1 - \varepsilon x_2] + 2w_2\lambda x_1[1-(x_1-x_2)-(X^*-E^*)]x_2 \\ &\quad -2w_2(\varepsilon+\mu+\lambda)x_2^2 - 2w_2\lambda X^*(x_1-x_2)x_2 \\ &= -2w_1(\mu+\gamma)x_1^2 - 2w_1\varepsilon x_1x_2 - 2w_2[(\varepsilon+\mu)+\lambda(1-x_1-X^*)]x_2^2 \\ &\quad +2w_2\lambda[(1-x_1-X^*)-(X^*-E^*)]x_1x_2 \\ &= Y^T(WA+A^TW)Y\end{aligned}$$

where $Y = [x_1,\ x_2]$, $W = diag(w_1,\ w_2)$, and

$$A = \begin{bmatrix} -(\mu+\gamma) & -\varepsilon \\ \lambda[(1-x_1-X^*)-(X^*-E^*)] & -[(\varepsilon+\mu)+\lambda(1-x_1-X^*)] \end{bmatrix}. \quad (2.3.13)$$

From inequality (2.3.10), it is easy to see

$$\begin{aligned} det\, A &= \left[(\mu+\gamma)(\varepsilon+\mu) - \varepsilon\lambda(X^*-E^*)\right] + (\mu+\gamma+\varepsilon)\lambda(1-x_1-X^*) \\ &> 0. \end{aligned} \quad (2.3.14)$$

Hence A is Volterra-Lyapunov stable by Lemma 3, and we obtain the global stability of the equilibrium in this example.

Because this simplified SEIS model (2.3.4-2.3.5) is two-dimensional, this conclusion can also be easily obtained based on Theorems 1 and 2 [50; 76], by setting $B(X,\ E) = 1/E$, that is:

$$\frac{\partial}{\partial X}(BP) + \frac{\partial}{\partial E}(BQ) = -\frac{\mu+\gamma}{E} - \frac{\lambda X(1-X)}{E^2} < 0,$$

where

$$\begin{aligned} P &= -(\mu+\gamma)X - \varepsilon E + (\mu+\gamma), \\ Q &= \lambda X[1-(X-E)] - (\varepsilon+\mu+\lambda)E. \end{aligned}$$

Hence, there is no periodic solution.

## II.4 Transcritical Bifurcation and diagram

Bifurcation theory [77] is concerned with how solutions of a differential equation depend on a parameter and can explain how the changes in dynamics, from a resting state to oscillations, take place. This may be a good way to test a model.

Normally, we have four different types of bifurcations: Saddle-Node bifurcation, Transcritical bifurcation, Pitchfork bifurcation and Hopf bifurcation. Moreover, the parameter values at which they occur are called bifurcation points. In this dissertation, we only consider transcritical bifurcation. Transcritical bifurcation [85; 77] is characterized by an equilibrium having an eigenvalue whose real part passes through zero. Both before and after the bifurcation, there is one unstable and one stable fixed point. However, their stability is exchanged when they collide. So the unstable fixed point becomes stable and vice versa.

The normal form of a transcritical bifurcation in one dimension is

$$\frac{dx}{dt} = rx - x^2. \tag{2.4.1}$$

The two fixed points (i.e., equilibria) are $x = 0$ and $x = r$.

To determine the stability of the fixed points, we let $f_r(x) = rx - x^2$ be the right hand side of equation (2.4.1). Since $f_r'(x) = r - 2x$, it is easy to see the fixed point at $x = 0$ is stable if $r < 0$ and is unstable if $r > 0$. Also, the fixed point at $x = r$ is stable if $r > 0$ and is unstable if $r < 0$.

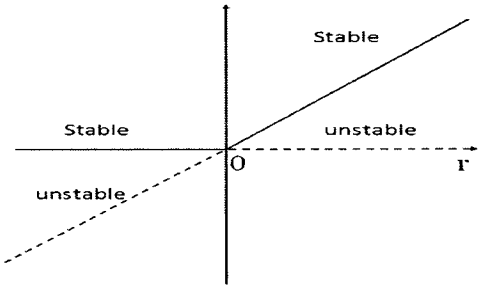


Figure 2.1: The bifurcation diagram of x vs. r which shows a transcritical bifurcation at $r = 0$. The solid lines represent the stable equilibria, and the dashed lines represent the unstable equilibria.

The bifurcation diagram corresponding to this equation is shown above. We plot values of the fixed points versus the bifurcation parameter $r$. The solid lines represent the stable equilibria, and the dashed lines represent the unstable equilibria. Clearly there is an exchange of stability at the bifurcation point $(r, x) = (0, 0)$.

# CHAPTER III

# STABILITY ANALYSIS

## III.1 The disease-free equilibrium and basic reproduction number $R_0$

In this section, we use the models of Hartley, Morris and Smith [22] and Mukandavire, Liao, Wang and Gaff *et al.* [60] to discuss the dynamics of the disease-free equilibrium.

### III.1.1 Hartley's Model

The deterministic model of Hartley, Morris and Smith [22] consists of the following ordinary differential equations (ODE)

$$\frac{dS}{dt} = bN - \beta_L S\frac{B_L}{\kappa_L + B_L} - \beta_H S\frac{B_H}{\kappa_H + B_H} - bS, \tag{3.1.1}$$

$$\frac{dI}{dt} = \beta_L S\frac{B_L}{\kappa_L + B_L} + \beta_H S\frac{B_H}{\kappa_H + B_H} - (\gamma + b)I, \tag{3.1.2}$$

$$\frac{dR}{dt} = \gamma I - bR, \tag{3.1.3}$$

$$\frac{dB_H}{dt} = \xi I - \chi B_H, \tag{3.1.4}$$

$$\frac{dB_L}{dt} = \chi B_H - \delta_L B_L, \tag{3.1.5}$$

where $B_H$ and $B_L$ denote the concentrations of the hyperinfectious (HI) and lessinfectious (LI) vibrios. The parameters $\beta_H$ and $\beta_L$ represent the HI and LI ingestion rates, $\kappa_H$ and $\kappa_L$ the HI and LI half saturation rates, $b$ the natural human birth/death rate, $\chi$ the bacterial transition rate, $\xi$ the shedding rate, $\delta_L$ the bacterial death rate, and $\gamma$ the recovery rate.

Written in a vector form, the above equations become

$$\frac{d}{dt}X = \mathbf{F}(X), \tag{3.1.6}$$

with

$$X = \left(S,\ I,\ R,\ B_H,\ B_L\right)^T. \tag{3.1.7}$$

It is straightforward to see that equations (3.1.1-3.1.5) have a unique disease-free equilibrium (DFE)

$$X_0 = \big(N,\ 0,\ 0,\ 0,\ 0\big)^T. \tag{3.1.8}$$

The local stability of the DFE, which is directly related to the disease epidemics [11; 23], is analyzed as follows.

The Jacobian of the ODE system (3.1.1-3.1.5) is

$$\begin{bmatrix} -\beta_L\frac{B_L}{\kappa_L+B_L} - \beta_H\frac{B_H}{\kappa_H+B_H} - b & 0 & 0 & -\beta_H S\frac{\kappa_H}{(\kappa_H+B_H)^2} & -\beta_L S\frac{\kappa_L}{(\kappa_L+B_L)^2} \\ \beta_L\frac{B_L}{\kappa_L+B_L} + \beta_H\frac{B_H}{\kappa_H+B_H} & -(\gamma+b) & 0 & \beta_H S\frac{\kappa_H}{(\kappa_H+B_H)^2} & \beta_L S\frac{\kappa_L}{(\kappa_L+B_L)^2} \\ 0 & \gamma & -b & 0 & 0 \\ 0 & \xi & 0 & -\chi & 0 \\ 0 & 0 & 0 & \chi & -\delta_L \end{bmatrix}. \tag{3.1.9}$$

After substituting the values for the DFE: $S = N$, $I = R = B_H = B_L = 0$, the above matrix becomes

$$J_B = \begin{bmatrix} -b & 0 & 0 & -\beta_H N\frac{1}{\kappa_H} & -\beta_L N\frac{1}{\kappa_L} \\ 0 & -(\gamma+b) & 0 & \beta_H N\frac{1}{\kappa_H} & \beta_L N\frac{1}{\kappa_L} \\ 0 & \gamma & -b & 0 & 0 \\ 0 & \xi & 0 & -\chi & 0 \\ 0 & 0 & 0 & \chi & -\delta_L \end{bmatrix}.$$

The characteristic polynomial of the matrix $J_B$ is found as

$$\begin{aligned} \mathrm{Det}\,(\lambda I - J_B) \;=\; & \Big[\lambda^3 + \lambda^2(\delta_L+\chi+\gamma+b) + \lambda\big(\chi\delta_L + \gamma\delta_L + \gamma\chi + b\delta_L + b\chi - \frac{\beta_H N\xi}{\kappa_H}\big) \\ & + \big(\gamma\chi\delta_L + b\chi\delta_L - \frac{\beta_H N\xi\delta_L}{\kappa_H} - \frac{\beta_L N\xi\chi}{\kappa_L}\big)\Big](\lambda+b)^2. \end{aligned}$$

The equilibrium (3.1.8) is locally asymptotically stable if and only if all roots of the above equation have negative real parts. Obviously $\lambda = -b$ is a negative root of multiplicity 2. To analyze the three roots of the cubic polynomial inside the square brackets, we set

$$\begin{aligned} b_1 &= \delta_L + \chi + \gamma + b, \\ b_2 &= \chi\delta_L + \gamma\delta_L + \gamma\chi + b\delta_L + b\chi - \frac{\beta_H N\xi}{\kappa_H}, \\ b_3 &= \chi\gamma\delta_L + b\chi\delta_L - \frac{\beta_H N\xi\delta_L}{\kappa_H} - \frac{\beta_L N\xi\chi}{\kappa_L}. \end{aligned}$$

Based on the Routh-Hurwitz criterion [33; 63], the sufficient and necessary condition for stability is

$$b_1 > 0\,, \qquad b_3 > 0\,, \qquad b_1\, b_2 - b_3 > 0. \tag{3.1.10}$$

Note that the first inequality is automatically satisfied since all the model parameters are positive. The second inequality, $b_3 > 0$, holds if and only if

$$\big[-\chi(\gamma + b) + \frac{\beta_H N\xi}{\kappa_H}\big] + \frac{\beta_L N\xi\chi}{\kappa_L\delta_L} < 0 \tag{3.1.11}$$

which yields

$$N < \frac{(\gamma + b)\chi\kappa_H\kappa_L\delta_L}{\xi(\beta_H\kappa_L\delta_L + \beta_L\chi\kappa_H)}. \tag{3.1.12}$$

In addition, we have

$$\begin{aligned} b_1b_2 - b_3 &= (\delta_L + \chi + \gamma + b)\big[\delta_L(\chi + \gamma + b) + \chi(\gamma + b) - \frac{\beta_H N\xi}{\kappa_H}\big] \\ &\quad - \gamma\chi\delta_L - b\chi\delta_L + \frac{\beta_H N\xi\delta_L}{\kappa_H} + \frac{\beta_L N\xi\chi}{\kappa_L} \\ &= (\chi + \gamma + b)[\delta_L(\delta_L + \chi + \gamma + b) + \chi(\gamma + b) - \frac{\beta_H N\xi}{\kappa_H}] + \frac{\beta_L N\xi\chi}{\kappa_L}. \end{aligned}$$

It is thus clear to see that $b_1b_2 - b_3 > 0$ as long as the inequality (3.1.11) or, equivalently, (3.1.12), holds. The condition (3.1.12) provides a threshold for the total population (which is assumed to be completely susceptible initially):

$$S_c = \frac{(\gamma + b)\chi\kappa_H\kappa_L\delta_L}{\xi(\beta_H\kappa_L\delta_L + \beta_L\chi\kappa_H)}. \tag{3.1.13}$$

When $N$ is below $S_c$, the DFE is stable and no epidemicity would occur. In contrast, if $N$ is above this critical value, the DFE becomes unstable and any infection entering the population would persist and lead to an epidemic.

We define the basic reproduction number, $R_0$, of this model by

$$R_0 = \frac{N}{S_c} = \frac{\xi(\beta_H \kappa_L \delta_L + \beta_L \chi \kappa_H)}{(\gamma + b)\chi \kappa_H \kappa_L \delta_L} N. \tag{3.1.14}$$

The condition (3.1.12) is then equivalent to

$$R_0 < 1.$$

Thus, we have established the result below

**Theorem 4.** *The disease-free equilibrium of the model (3.1.6) is locally asymptotically stable if* $R_0 < 1$, *and unstable if* $R_0 > 1$.

This is one common method to obtain the basic reproduction number. For comparsion, we derive the basic reproduction number, given in equation (3.1.14), using the next generation matrix analysis [80].

According to the work of van den Driessche and Watmough [80], $R_0$ is mathematically defined as the spectral radius of the next generation matrix. Following their theoretical framework, we assemble the unknowns in equations (3.1.1-3.1.5) into a vector

$$X = \left( I,\ B_H,\ B_L,\ S,\ R \right)^T,$$

where we have arranged the order of the unknowns so that the first three entries of $X$ are directly related to the infection. We then rewrite the ODE system as

$$\frac{dX}{dt} = \mathcal{F}(X) - \mathcal{V}(X) \tag{3.1.15}$$

where $\mathcal{F}$ denotes the rate of appearance of new infections, and $\mathcal{V}$ denotes the rate of transfer of individuals into or out of each population set. (For details, see Lemma 1.) These two vectors are given by

$$\mathcal{F} = \begin{bmatrix} \beta_L S \frac{B_L}{\kappa_L + B_L} + \beta_H S \frac{B_H}{\kappa_H + B_H} \\ 0 \\ 0 \\ 0 \\ 0 \end{bmatrix},$$

and

$$\mathcal{V} = \begin{bmatrix} (\gamma + b)I \\ \chi B_H - \xi I \\ \delta_L B_L - \chi B_H \\ \beta_L S\frac{B_L}{\kappa_L + B_L} + \beta_H S\frac{B_H}{\kappa_H + B_H} + bS - bN \\ bR - \gamma I \end{bmatrix}.$$

The next generation matrix is defined as $FV^{-1}$, where $F$ and $V$ are $3 \times 3$ Jacobian matrices given by

$$F = \left[\frac{\partial \mathcal{F}_i}{\partial X_j}(X_0)\right] \qquad \text{and} \qquad V = \left[\frac{\partial \mathcal{V}_i}{\partial X_j}(X_0)\right] \qquad \text{with } 1 \leq i, j \leq 3.$$

Here $X_0$ is the disease-free equilibrium (DFE), and

$$X_0 = \big(0,\ 0,\ 0,\ N,\ 0\big)^T \tag{3.1.16}$$

for the cholera model. After some algebra, it is found that

$$F = \begin{bmatrix} 0 & \frac{\beta_H N}{\kappa_H} & \frac{\beta_L N}{\kappa_L} \\ 0 & 0 & 0 \\ 0 & 0 & 0 \end{bmatrix} \qquad \text{and} \qquad V = \begin{bmatrix} \gamma + b & 0 & 0 \\ -\xi & \chi & 0 \\ 0 & -\chi & \delta_L \end{bmatrix}.$$

Hence, the next generation matrix is

$$FV^{-1} = \begin{bmatrix} \frac{\beta_H N\xi}{\kappa_H(\gamma+b)\chi} + \frac{\beta_L N\xi}{\kappa_L(\gamma+b)\delta_L} & \frac{\beta_H N}{\kappa_H \chi} + \frac{\beta_L N}{\kappa_L \delta_L} & \frac{\beta_L N}{\kappa_L \delta_L} \\ 0 & 0 & 0 \\ 0 & 0 & 0 \end{bmatrix},$$

whose spectral radius can be easily found by $\rho\big(FV^{-1}\big) = \max\limits_{1 \leq i \leq 3} |\lambda_i|$ where $\lambda_i$ denote the eigenvalues of the next generation matrix. Therefore, we obtain

$$R_0 = \frac{N\xi}{\gamma + b}\Big(\frac{\beta_H}{\kappa_H \chi} + \frac{\beta_L}{\kappa_L \delta_L}\Big), \tag{3.1.17}$$

which exactly matches equation (3.1.14). Hartley *et al.* [22] obtained the same result using the next-generation matrix approach, though no derivation was provided in their work.

To study the global asymptotic stability of the DFE, one common approach is to construct an appropriate Lyapunov function [36; 42]. We have found, however, that it is simpler to apply the following result introduced by Castillo-Chavez *et al.* [9].

**Lemma 6.** *[9] Consider a model system written in the form*

$$\begin{aligned} \frac{dX_1}{dt} &= F(X_1, X_2)\,, \\ \frac{dX_2}{dt} &= G(X_1, X_2)\,, \qquad G(X_1, 0) = 0 \end{aligned} \tag{3.1.18}$$

*where $X_1 \in \mathbb{R}^m$ denotes (its components) the number of uninfected individuals and $X_2 \in \mathbb{R}^n$ denotes (its components) the number of infected individuals including latent, infectious, etc; $X_0 = (X_1^*, 0)$ denotes the disease-free equilibrium of the system.*

*Also assume the conditions $(H1)$ and $(H2)$ below:*
*(H1) For $\frac{dX_1}{dt} = F(X_1, 0)$, $X_1^*$ is globally asymptotically stable;*
*(H2) $G(X_1, X_2) = A X_2 - \hat{G}(X_1, X_2)$, $\hat{G}(X_1, X_2) \geq 0$ for $(X_1, X_2) \in \Omega$, where the Jacobian $A = \frac{\partial G}{\partial X_2}(X_1^*, 0)$ is an M-matrix (the off diagonal elements of $A$ are nonnegative) and $\Omega$ is the region where the model makes biological sense.*

*Then the DFE $X_0 = (X_1^*, 0)$ is globally asymptotically stable provided that $R_0 < 1$.*

**Theorem 5.** *The disease-free equilibrium of the model (3.1.6) is globally asymptotic stable if $R_0 < 1$.*

*Proof.* We only need to show that the conditions $(H1)$ and $(H2)$ hold when $R_0 < 1$. In our ODE system (3.1.1-3.1.5), $X_1 = (S, R)$, $X_2 = (I, B_H, B_L)$, and $X_1^* = (N, 0)$. We note that the system

$$\frac{dX_1}{dt} = F(X_1, 0) = \begin{bmatrix} bN - bS \\ \\ -bR \end{bmatrix}$$

is linear and its solution can be easily found as

$$R(t) = R(0)e^{-bt} \qquad \text{and} \qquad S(t) = N - \big(N - S(0)\big)\, e^{-bt}.$$

Clearly, $R(t) \to 0$ and $S(t) \to N$ as $t \to \infty$, regardless of the values of $R(0)$ and $S(0)$. Thus $X_1^* = (N, 0)$ is globally asymptotically stable.

Next, we have

$$G(X_1, X_2) = \begin{bmatrix} \beta_L S\frac{B_L}{K_L+B_L} + \beta_H S\frac{B_H}{k_H+B_H} - (\gamma+b)I \\ \\ \xi I - \chi B_H \\ \\ \chi B_H - \delta_L B_L \end{bmatrix}.$$

We can then obtain

$$A = \begin{bmatrix} -\gamma+b & \beta_H N\frac{1}{\kappa_H} & \beta_L N\frac{1}{\kappa_L} \\ \\ \xi & -\chi & 0 \\ \\ 0 & \chi & -\delta_L \end{bmatrix}$$

which is clearly an $M$-matrix. Meanwhile, we find

$$\hat{G}(X_1, X_2) = \left[\frac{\beta_H B_H \kappa_H (N-S) + \beta_H N B_H^2}{\kappa_H(\kappa_H+B_H)} + \frac{\beta_L B_L \kappa_L (N-S) + \beta_L N B_L^2}{\kappa_L(\kappa_L+B_L)},\quad 0,\quad 0\right]^T.$$

Since $0 \le S \le N$, it is obvious that $\hat{G}(X_1, X_2) \ge 0$. □

### III.1.2 Mukandavire's Model

Here we introduce Mukandavire's Model which is proposed by Mukandavire, Liao, Wang and Gaff *et al.* [60]. In this section, we use very similar methods as presented in Section III.1.1 to derive the basic reproduction number $R_0$, and analyze the stability of DFE.

This model considered both human-to-human and environment-to-human transmission pathways. The model takes the form:

$$\frac{dS}{dt} = \mu N - \beta_e S\frac{B}{\kappa+B} - \beta_h SI - \mu S, \tag{3.1.19}$$

$$\frac{dI}{dt} = \beta_e S\frac{B}{\kappa+B} + \beta_h SI - (\gamma+\mu)I, \tag{3.1.20}$$

$$\frac{dR}{dt} = \gamma I - \mu R, \tag{3.1.21}$$

$$\frac{dB}{dt} = \xi I - \delta B, \tag{3.1.22}$$

where $B$ denotes the concentration of vibrios in contaminated water. The parameters $\beta_e$ and $\beta_h$ represent the rates of ingesting vibrios from the contaminated environment and through human-to-human interaction respectively. $\mu$ is the natural human birth/death rate, $\kappa$ the concentration of *V. cholerae* in contaminated water, $\xi$ the shedding rate, $\delta$ the net death rate of the vibrios, and $\gamma$ the recovery rate.

The disease-free equilibrium for Mukandavire's model is given by,

$$X_0 = \left(N,\ 0,\ 0,\ 0\right)^T. \tag{3.1.23}$$

We compute the basic reproductive number for the cholera model using the next generation matrix method. Here, the associated next generation matrices are given by

$$F = \begin{bmatrix} N\beta_h & \frac{N\beta_e}{\kappa} \\ 0 & 0 \end{bmatrix}, \qquad V = \begin{bmatrix} \gamma+\mu & 0 \\ -\xi & \delta \end{bmatrix}, \qquad FV^{-1} = \begin{bmatrix} \frac{N\beta_h}{\gamma+\mu} + \frac{N\beta_e\xi}{\delta\kappa(\gamma+\mu)} & \frac{N\beta_e}{\delta\kappa} \\ 0 & 0 \end{bmatrix}.$$

The expression of the basic reproductive number, is given by

$$R_0 = \frac{N}{\delta\kappa(\gamma+\mu)}\left[\xi\beta_e + \delta\kappa\beta_h\right] = R_e + R_h, \tag{3.1.24}$$

where, $R_e$ and $R_h$ are partial reproductive numbers due to environment-to-human transmission and human-to-human transmission respectively. We note that when $\beta_e = 0$, $R_0 = R_h$ and when $R_h = 0$, $R_0 = R_h$, suggesting that the two modes of cholera transmission can independently or together start an epidemic as long as conditions are conducive. Thus we can improve the understanding of $R_0$ that measures the number of secondary cholera infections generated in a wholly susceptible community, when a sufficient concentration of vibrios contaminates the aquatic environment and/or when a cholera infected individual is introduced into the community. In $R_e$, $\frac{1}{\gamma+\mu}$ is the expected time humans will be infected, $\frac{\xi}{\gamma+\mu}$ is the average amount of *V. cholerae* shed per infected individual, $\frac{1}{\delta}$ is the life time of the vibrios in the environment and $\frac{\beta_e}{\kappa}$ is the number of new cases generated in terms of vibrios per unit time as measured by the number of $ID_{50}$ concentration. In $R_h$, $\frac{\beta_h}{\gamma+\mu}$ is the average amount of hyperinfectious *V. cholerae* ingested by an infected individual [60].

## III.2 Endemic dynamics

The stability at the DFE determines the short-term epidemics of the disease, whereas its dynamics over a longer period of time is characterized by the stability at the endemic equilibrium. We find long term behavior has some important epidemiological implications such as whether an outbreak of a disease may result in an endemic situation or the infection will die out. In this section we shall conduct the endemic analysis.

### III.2.1 Hartley's Model

Let us denote the endemic equilibrium of system (3.1.6) by

$$X^* = \left(S^*, I^*, R^*, B_H^*, B_L^*\right)^T. \tag{3.2.1}$$

Its components must satisfy

$$I^* = \frac{S^*}{\gamma + b}\left(\frac{\beta_L \xi I^*}{\delta_L \kappa_L + \xi I^*} + \frac{\beta_H \xi I^*}{\chi \kappa_H + \xi I^*}\right), \tag{3.2.2}$$

$$S^* = N - \frac{(\gamma + b)I^*}{b}, \tag{3.2.3}$$

$$R^* = \frac{\gamma I^*}{b}, \tag{3.2.4}$$

$$B_L^* = \frac{\xi I^*}{\delta_L}, \tag{3.2.5}$$

$$B_H^* = \frac{\xi I^*}{\chi}. \tag{3.2.6}$$

We first show the following theorem

**Theorem 6.** *The positive endemic equilibrium exists and is unique if and only if* $R_0 > 1$.

*Proof.* By manipulating equations (3.2.2-3.2.6), we obtain a cubic equation for $I^*$:

$$I^*\left[A(I^*)^2 + BI^* + C\right] = 0 \tag{3.2.7}$$

where

$$\begin{aligned} A &= -\xi^2(\gamma + b)(\beta_L + \beta_H + b), \\ B &= \xi^2 bN(\beta_L + \beta_H) - \xi(\gamma + b)(\beta_L \chi \kappa_H + \beta_H \delta_L \kappa_L + b\delta_L \kappa_L + b\chi \kappa_H), \\ C &= \xi(\beta_L \chi \kappa_H + \beta_H \kappa_L \delta_L)(bN - bS_c), \end{aligned}$$

and where $S_c$ is defined in equation (3.1.13). The zero root of equation (3.2.7) corresponds to the DFE. The other two (non-zero) roots, $I_1$ and $I_2$, of the equation must satisfy:

$$I_1 I_2 = \frac{C}{A}, \tag{3.2.8}$$

$$I_1 + I_2 = -\frac{B}{A}. \tag{3.2.9}$$

It is obvious that $A < 0$ since all parameters are positive. When $R_0 > 1$, we have $N > S_c$ and $C > 0$, so that the right-hand side of equation (3.2.8) is negative. Hence, there is one and only one positive real root for equation (3.2.7).

On the other hand, if $R_0 < 1$, then $N < S_c$ and $C < 0$, so that the right-hand side of equation (3.2.8) is positive. Next we show $B < 0$. We have

$$\xi^2 bN(\beta_L + \beta_H) < \frac{\xi b(\beta_L + \beta_H)(\gamma + b)\chi\kappa_H\kappa_L\delta_L}{\beta_H\kappa_L\delta_L + \beta_L\chi\kappa_H} \tag{3.2.10}$$

when $N < S_c$ (see equation 3.1.13). Meanwhile,

$$b(\beta_L + \beta_H)(\gamma + b)\chi\kappa_H\kappa_L\delta_L < (\gamma + b)(\beta_L\chi\kappa_H + \beta_H\delta_L\kappa_L + b\delta_L\kappa_L + b\chi\kappa_H)(\beta_H\kappa_L\delta_L + \beta_L)$$

which yields

$$\frac{\xi b(\beta_L + \beta_H)(\gamma + b)\chi\kappa_H\kappa_L\delta_L}{\beta_H\kappa_L\delta_L + \beta_L\chi\kappa_H} < \xi(\gamma + b)(\beta_L\chi\kappa_H + \beta_H\delta_L\kappa_L + b\delta_L\kappa_L + b\chi\kappa_H). \tag{3.2.11}$$

Combining (3.2.10) and (3.2.11), we obtain $B < 0$. Hence, the right-hand side of equation (3.2.9) is negative. In this case we either have two negative real roots, or two complex conjugate roots with negative real parts, for $A(I^*)^2 + BI^* + C = 0$. There is no positive endemic equilibrium.

Finally, if $R_0 = 1$, then $C = 0$ and equation (3.2.7) has only one nonzero root, $-\frac{B}{A}$, which is negative. □

We have the following result regarding the local stability of the endemic equilibrium.

**Theorem 7.** *When $R_0 > 1$, the positive endemic equilibrium of system (3.1.6) is locally asymptotically stable.*

*Proof.* Consider the Jacobian (3.1.9) at the endemic equilibrium. To make the algebraic manipulation simpler, we set

$$P = \beta_L \frac{B_L^*}{\kappa_L + B_L^*} + \beta_H \frac{B_H^*}{\kappa_H + B_H^*}, \quad Q = \beta_H S^* \frac{\kappa_H}{(\kappa_H + B_H^*)^2}, \quad T = \beta_L S^* \frac{\kappa_L}{(\kappa_L + B_L^*)^2}. \tag{3.2.12}$$

Note that $P$, $Q$ and $T$ are all positive. The Jacobian matrix (3.1.9) then becomes

$$J_B^* = \begin{bmatrix} -P-b & 0 & 0 & -Q & -T \\ P & -(\gamma+b) & 0 & Q & T \\ 0 & \gamma & -b & 0 & 0 \\ 0 & \xi & 0 & -\chi & 0 \\ 0 & 0 & 0 & \chi & -\delta_L \end{bmatrix}.$$

The characteristic polynomial of $J_B^*$ is

$$\begin{aligned} \mathrm{Det}\,(\lambda I - J_B^*) &= (\lambda+b)\big[(\lambda+\delta_L)(\lambda+P+b)(\lambda+\gamma+b)(\lambda+\chi) \\ &\quad -\xi Q(\lambda+b)(\lambda+\delta_L) - T\xi\chi(\lambda+b)\big]. \end{aligned}$$

Obviously, this equation has a negative root $\lambda = -b$. we expand the expression in the square brackets to obtain

$$a_4\lambda^4 + a_3\lambda^3 + a_2\lambda^2 + a_1\lambda^1 + a_0 = 0 \tag{3.2.13}$$

where

$$\begin{aligned} a_4 &= 1, \\ a_3 &= 2b + \chi + \delta_L + \gamma + P, \\ a_2 &= b^2 + \gamma P + 2b\chi + 2b\delta_L + \chi\delta_L + b\gamma + \chi\gamma - Q\xi + \delta_L\gamma + bP + \chi P + \delta_L P, \\ a_1 &= b^2\chi + b^2\delta_L + b\chi P + b\delta_L P + \chi\delta_L P + \chi\gamma P + \delta_L\gamma P + 2b\chi\delta_L + b\chi\gamma - Qb\xi \\ &\quad + b\delta_L\gamma + \chi\delta_L\gamma - Q\delta_L\xi - T\chi\xi, \\ a_0 &= b^2\chi\delta_L + b\chi\delta_L\gamma - Qb\delta_L\xi - Tb\chi\xi + b\chi\delta_L P + \chi\delta_L\gamma P. \end{aligned}$$

To ensure that all roots of equation (3.2.13) have negative real parts, the Routh-Hurwitz stability criterion (see Section II.2) requires

$$a_3 > 0, \qquad a_1 > 0, \qquad a_0 > 0, \qquad a_1(a_2a_3 - a_1) > a_0a_3^2. \tag{3.2.14}$$

Among these $a_3 > 0$ is obvious. The other three inequalities in (3.2.14) hold when $R_0 > 1$; the details are provided below.

First we rewrite $a_0$ as

$$a_0 = P(\gamma + b)\chi\delta_L + b(\gamma + b)\chi\delta_L - b\xi(\chi T + \delta_L Q). \tag{3.2.15}$$

Substituting equations (3.2.5) and (3.2.6) into (3.2.2) and (3.2.3), we obtain

$$\gamma + b = \xi S^*(\frac{\beta_L}{\kappa_L\delta_L + \xi I^*} + \frac{\beta_H}{\chi\kappa_H + \xi I^*}). \tag{3.2.16}$$

Using equations (3.2.12) and (3.2.16), we have

$$\begin{aligned} a_0 &= P(\gamma + b)\chi\delta_L + b\xi\chi\delta_L S^*[\frac{\beta_L}{\kappa_L\delta_L + \xi I^*} + \frac{\beta_H}{\chi\kappa_H + \xi I^*}] \\ &\quad - b\xi\chi\delta_L S^*[\frac{\beta_L\delta_L\kappa_L}{(\kappa_L\delta_L + \xi I^*)^2} + \frac{\beta_H\chi\kappa_H}{(\chi\kappa_H + \xi I^*)^2}] \\ &= P(\gamma + b)\chi\delta_L + b\xi\chi\delta_L S^*[\frac{\beta_L\xi I^*}{(\kappa_L\delta_L + \xi I^*)^2} + \frac{\beta_H\xi I^*}{(\chi\kappa_H + \xi I^*)^2}] \\ &> 0. \end{aligned}$$

Next, we rewrite $a_1$ into the sum of three parts:

$$\begin{aligned} a_1 &= (b^2\chi + b\gamma\chi - Qb\xi) + (\delta_L\chi\gamma + \delta_L\chi b - Q\delta_L\xi - T\chi\xi) \\ &\quad + (b\chi P + b\delta_L P + \chi\delta_L P + \chi\gamma P + \delta_L\gamma P + b\chi\delta_L + b\delta_L\gamma). \end{aligned} \tag{3.2.17}$$

Note that the last part in equation (3.2.17) is positive. After substitution of equations (3.2.12) and (3.2.16), the first two parts of $a_1$ become

$$\begin{aligned} b^2\chi + b\gamma\chi - Qb\xi &= \xi b\chi S^*(\frac{\beta_L}{\kappa_L\delta_L + \xi I^*} + \frac{\beta_H}{\chi\kappa_H + \xi I^*}) - \xi b\beta_H S^*\frac{\kappa_H}{(\kappa_H + \frac{\xi I^*}{\chi})^2} \\ &= \xi b\chi S^*[\frac{\beta_L}{\kappa_L\delta_L + \xi I^*} + \frac{\beta_H}{\chi\kappa_H + \xi I^*} - \frac{\beta_H\kappa_H\chi}{(\kappa_H\chi + \xi I^*)^2}] \\ &= \xi b\chi S^*[\frac{\beta_L}{\kappa_L\delta_L + \xi I^*} + \frac{\beta_H\xi I^*}{(\kappa_H\chi + \xi I^*)^2}] \\ &> 0, \end{aligned}$$

and

$$\begin{aligned}
& \delta_L\chi\gamma + \delta_L\chi b - Q\delta_L\xi - T\chi\xi \\
= \; & \xi\delta_L\chi S^*(\frac{\beta_L}{\kappa_L\delta_L + \xi I^*} + \frac{\beta_H}{\chi\kappa_H + \xi I^*}) - \xi[\chi\beta_L S^* \frac{\kappa_L}{(\kappa_L + \frac{\xi I^*}{\delta_L})^2} + \delta_L\beta_H S^* \frac{\kappa_H}{(\kappa_H + \frac{\xi I^*}{\chi})^2}] \\
= \; & \xi\delta_L\chi S^*[\frac{\beta_L}{\kappa_L\delta_L + \xi I^*} + \frac{\beta_H}{\chi\kappa_H + \xi I^*} - \frac{\beta_L\kappa_L\delta_L}{(\kappa_L\delta_L + \xi I^*)^2} - \frac{\beta_H\kappa_H\chi}{(\kappa_H\chi + \xi I^*)^2}] \\
= \; & \xi\delta_L\chi S^*[\frac{\beta_L\xi I^*}{(\kappa_L\delta_L + \xi I^*)^2} + \frac{\beta_H\xi I^*}{(\kappa_H\chi + \xi I^*)^2}] \\
> \; & 0.
\end{aligned}$$

Thus $a_1 > 0$ holds.

To prove the last inequality in (3.2.14), i.e., $a_1a_2a_3 - a_1^2 > a_0a_3^2$, it is sufficient to establish the following two inequalities:

$$a_1a_2a_3 > 2a_1^2, \tag{3.2.18}$$

$$a_1a_2a_3 > 2a_0a_3^2. \tag{3.2.19}$$

To show (3.2.18), we write $a_2a_3 - 2a_1$ into the sum of four parts:

$$\begin{aligned}
a_2a_3 - 2a_1 = \; & (P\chi b + P\chi\gamma - PQ\xi) + (\chi^2 b + \chi^2\gamma - Q\chi\xi) + (\chi b^2 + \chi\gamma^2 + 2b\gamma\chi - Q\gamma\xi) \\
& + \big(3Pb^2 + P^2b + P\chi^2 + P^2\chi + P\delta_L^2 + P^2\delta_L + P\gamma^2 + P^2\gamma + b\chi^2 + 2b^2\chi \\
& + 2b\delta_L^2 + 3b^2\delta_L + \chi\delta_L^2 + \chi^2\delta_L + b\gamma^2 + 3b^2\gamma + \delta_L\gamma^2 + \delta_L^2\gamma + 2b^3 + 2Pb\chi \\
& + 3Pb\delta_L + P\chi\delta_L + 4Pb\gamma + P\delta_L\gamma + 2b\chi\delta_L + b\chi\gamma + 3b\delta_L\gamma + \chi\delta_L\gamma \\
& + Q\delta_L\xi + 2T\chi\xi\big).
\end{aligned}$$

Note again that the last part in the above expression is positive. After substitution of equations (3.2.12) and (3.2.16), the first part becomes

$$\begin{aligned}
P\chi b + P\chi\gamma - PQ\xi = \; & P\Big[\xi\chi S^*(\frac{\beta_L}{\kappa_L\delta_L + \xi I^*} + \frac{\beta_H}{\chi\kappa_H + \xi I^*}) - \xi\beta_H S^* \frac{\kappa_H}{(\kappa_H + B_H)^2}\Big] \\
= \; & P\xi\chi S^*\Big[\frac{\beta_L}{\kappa_L\delta_L + \xi I^*} + \frac{\beta_H}{\chi\kappa_H + \xi I^*} - \frac{\beta_H\kappa_H\chi}{(\kappa_H\chi + \xi I^*)^2}\Big] \\
= \; & P\xi\chi S^*\Big[\frac{\beta_L}{\kappa_L\delta_L + \xi I^*} + \frac{\beta_H\xi I^*}{(\kappa_H\chi + \xi I^*)^2}\Big] \\
> \; & 0.
\end{aligned} \tag{3.2.20}$$

In a similar way, we can prove $\chi^2 b + \chi^2\gamma - Q\chi\xi > 0$ and $\chi b^2 + \chi\gamma^2 + 2b\gamma\chi - Q\gamma\xi > 0$. Thus (3.2.18) holds.

Finally, to show (3.2.19), we write $a_1a_2 - 2a_0a_3$ into the sum of many parts as follows:

$$\begin{aligned}
a_1a_2 - 2a_0a_3 \;=\; & (Pb\chi\delta_L^2 + P\chi\delta_L^2\gamma - TP\chi\delta_L\xi - PQ\delta_L^2\xi) + (\chi\delta_L^2\gamma^2 + b\chi\delta_L^2\gamma - T\chi\delta_L\gamma\xi - Q\delta_L^2\gamma\xi) \\
& +(P^2\chi^2\delta_L - T\chi^2\gamma\xi - Q\chi\delta_L\gamma\xi) + (b^4\chi + b^3\chi\gamma - Qb^3\xi) \\
& +(b^3\chi\gamma + b^2\chi\delta_L\gamma + b^2\chi\gamma^2 + b\chi\delta_L\gamma^2 - Qb^2\gamma\xi - Qb\delta_L\gamma\xi) \\
& +(Pb^3\chi + Pb\chi\gamma^2 + 2Pb^2\chi\gamma - PQb^2\xi - PQb\gamma\xi) \\
& +(3b^2\chi^2\delta_L + 3b\chi^2\delta_L\gamma - 3Qb\chi\delta_L\xi) + (2Pb^2\chi^2 + 2Pb\chi^2\gamma - 2PQb\chi\xi) \\
& +(P\chi^2\delta_L^2 + P\chi^2\gamma^2 + P\chi^2\delta_Lb - PQ\chi\delta_L\xi) + (Pb^2\chi^2 + 2b^3\chi^2 + 3b^2\chi^2\gamma - 3Qb^2\chi\xi) \\
& +(P\chi^2\delta_L\gamma + P\chi^2\delta_Lb - TP\chi^2\xi - PQ\chi\delta_L\xi) + (2Pb\chi^2\gamma - 2Qb\chi\gamma\xi) \\
& +(P\chi\gamma^2\delta_L + P\chi b\delta_L\gamma - TP\chi\gamma\xi - PQ\delta_L\gamma\xi) + (P^2\chi^2\gamma - PQ\chi\gamma\xi) \\
& +(Pb^2\chi\delta_L + Pb\chi\delta_L\gamma - PQb\delta_L\xi) + (\delta_L^2\chi^2\gamma + \delta_L^2\chi^2b - T\chi^2\delta_L\xi - Q\chi\delta_L^2\xi) \\
& +(\chi^2\delta_L\gamma^2 + \chi^2\delta_L^2b + \chi^2b\gamma^2 - Q\chi\delta_L\gamma\xi) + (P^2\chi\gamma\delta_L - PQ\delta_L\gamma\xi) \\
& +P^2b^2\chi + P^2b^2\delta_L + P^2b\chi^2 + P^2b\chi\delta_L + 2P^2b\chi\gamma + P^2b\delta_L^2 + 2P^2b\delta_L\gamma \\
& +P^2\chi\delta_L^2 + P^2\chi\gamma^2 + P^2\delta_L^2\gamma + P^2\delta_L\gamma^2 + Pb^3\chi + 2Pb^3\delta_L + 2Pb^2\chi\delta_L \\
& +2Pb^2\chi\gamma + 3Pb^2\delta_L^2 + 4Pb^2\delta_L\gamma + Pb\chi^2\delta_L + 2Pb\chi\delta_L^2 + 2Pb\chi\delta_L\gamma + Pb\chi\gamma^2 \\
& +TPb\chi\xi + 4Pb\delta_L^2\gamma + 2Pb\delta_L\gamma^2 + P\delta_L^2\gamma^2 + Q^2b\xi^2 + Q^2\delta_L\xi^2 + TQ\chi\xi^2 + b^4\delta_L \\
& +2b^3\chi\delta_L + 2b^3\delta_L^2 + 2b^3\delta_L\gamma + 3b^2\chi\delta_L^2 + 2b^2\chi\delta_L\gamma + 3Tb^2\chi\xi \\
& +3b^2\delta_L^2\gamma + b^2\delta_L\gamma^2 + 2b\chi\delta_L^2\gamma + Tb\chi\gamma\xi + b\delta_L^2\gamma^2.
\end{aligned}$$

Now we prove $a_1a_2 - 2a_0a_3 > 0$ term by term by using some results from (3.2.18), (3.2.19), and (3.2.20). Some of them can be obtained immediately, while others require some basic algebra. We have:

$$Pb\chi\delta_L^2 + P\chi\delta_L^2\gamma > TP\chi\delta_L\xi + PQ\delta_L^2\xi,$$

$$\chi\delta_L^2\gamma^2 + b\chi\delta_L^2\gamma > T\chi\delta_L\gamma\xi + Q\delta_L^2\gamma\xi,$$

$$P^2\chi^2\delta_L > P\chi^2\delta_L(\gamma + b) > T\chi^2\gamma\xi + Q\chi\delta_L\gamma\xi,$$

$$b^4\chi + b^3\chi\gamma > Qb^3\xi,$$

$$b^3\chi\gamma + b^2\chi\delta_L\gamma + b^2\chi\gamma^2 + b\chi\delta_L\gamma^2 > Qb^2\gamma\xi > Qb\delta_L\gamma\xi,$$

$$Pb^3\chi + Pb\chi\gamma^2 + 2Pb^2\chi\gamma > PQb^2\xi + PQb\gamma\xi,$$

$$3b^2\chi^2\delta_L + 3b\chi^2\delta_L\gamma > 3Qb\chi\delta_L\xi,$$

$$2Pb^2\chi^2 + 2Pb\chi^2\gamma > 2PQb\chi\xi,$$

$$P\chi^2\delta_L^2 + P\chi^2\gamma^2 + P\chi^2\delta_L b > PQ\chi\delta_L\xi,$$

$$Pb^2\chi^2 + 2b^3\chi^2 + 3b^2\chi^2\gamma > 3b^3\chi^2 + 3b^2\chi^2\gamma > 3Qb^2\chi\xi,$$

$$P\chi^2\delta_L\gamma + P\chi^2\delta_L b > TP\chi^2\xi + PQ\chi\delta_L\xi,$$

$$P^2\chi^2\gamma > 2\chi^2b^2\gamma + 2\chi^2\gamma^2 b > PQ\chi\gamma\xi,$$

$$Pb^2\chi\delta_L + Pb\chi\delta_L\gamma > PQb\delta_L\xi,$$

$$P\chi\gamma^2\delta_L + P\chi b\delta_L\gamma > TP\chi\gamma\xi + PQ\delta_L\gamma\xi,$$

$$P^2\chi^2\gamma > PQ\chi\gamma\xi,$$

$$Pb^2\chi\delta_L + Pb\chi\delta_L\gamma > PQb\delta_L\xi,$$

$$\delta_L^2\chi^2\gamma + \delta_L^2\chi^2 b > T\chi^2\delta_L\xi + Q\chi\delta_L^2\xi,$$

$$\chi^2\delta_L\gamma^2 + \chi^2\delta_L^2 b + \chi^2 b\gamma^2 > \chi^2\delta_L\gamma^2 + \gamma b\chi^2\delta_L > Q\chi\delta_L\gamma\xi,$$

$$P^2\chi\gamma\delta_L > PQ\delta_L\gamma\xi.$$

These yield $a_1a_2 - 2a_0a_3 > 0$. □

### III.2.2 Mukandavire's Model

The endemic equilibrium of this cholera model (3.1.19-3.1.22) is given by $X^* = (S^*, I^*, R^*, B^*)$ where

$$S^* = N - \frac{(\gamma+\mu)I^*}{\mu}, \tag{3.2.21}$$

$$I^* = \frac{\beta_e S^*}{\gamma+\mu-\beta_h S^*} - \frac{\delta\kappa}{\xi}, \tag{3.2.22}$$

$$R^* = \frac{\gamma I^*}{\mu}, \tag{3.2.23}$$

$$B^* = \frac{\xi I^*}{\delta}. \tag{3.2.24}$$

We establish the following theorem.

**Theorem 8.** *If $R_0 > 1$, a unique endemic equilibrium exists and is locally asymptotically stable.*

*Proof.* By solving equations (3.2.21-3.2.24), we obtain

$$I^*(AI^{*2} + BI^* + C) = 0 \tag{3.2.25}$$

where

$$\begin{aligned} A &= -\beta_h(\gamma+\mu)\xi, \\ B &= \beta_h N\mu\xi - (\gamma+\mu)(\beta_e\xi + \beta_h\delta\kappa + \mu\xi), \\ C &= \beta_e\xi\mu N - (\gamma+\mu)\mu\delta\kappa + \beta_h N\mu\delta\kappa. \end{aligned}$$

From (3.2.25), we have $I^* = 0$ which corresponds to the disease-free equilibrium and a quadratic equation given by

$$AI^{*2} + BI^* + C = 0. \tag{3.2.26}$$

The roots of this quadratic equation must satisfy,

$$I_1^* I_2^* = \frac{C}{A} \tag{3.2.27}$$

$$I_1^* + I_2^* = -\frac{B}{A}. \tag{3.2.28}$$

Having,

$$R_0 = \frac{N(\xi\beta_e + \delta\kappa\beta_h)}{\delta\kappa(\gamma + \mu)} \tag{3.2.29}$$

and defining

$$S_c = \frac{\delta\kappa(\gamma + \mu)}{\xi\beta_e + \delta\kappa\beta_h} \tag{3.2.30}$$

gives $N > S_c$ when $R_0 > 1$, and it follows that $A < 0$ and $C > 0$, and the right-hand side of the equation (3.2.27) is less than zero. Thus the quadratic equation (3.2.26) has a unique positive root $I^*$. On the other hand, if $R_0 < 1$ which yields $N < S_c$, we can obtain $C < 0$ so that the right-hand side of equation (3.2.27) $> 0$ and the right-hand side of equation (3.2.28) $< 0$ if $B < 0$.

We have $(\gamma + \mu) > N\beta_h$ for $N < S_c$, thus we obtain $(\gamma + \mu)\mu\xi > N\beta_h\mu\xi$ which gives $B < 0$. In this case, the equation (3.2.26) has two negative roots and the positive endemic equilibrium does not exist. Hence it's not biologically feasible.

In order to deduce the local stability of the endemic equilibrium, we use the Jacobian of the cholera model system (3.1.19-3.1.22). For simplicity we set $P = \frac{\beta_e B^*}{\kappa + B^*} + \beta_h I^*$, $Q = \frac{\beta_e S^* \kappa}{(\kappa + B^*)^2}$, and the Jacobian matrix becomes

$$J_B^* = \begin{bmatrix} -P - \mu & -\beta_h S & 0 & -Q \\ P & \beta_h S - (\gamma + \mu) & 0 & Q \\ 0 & \gamma & -\mu & 0 \\ 0 & \xi & 0 & \delta \end{bmatrix}.$$

The characteristic polynomial of the matrix $J_B^*$ is given by

$$\begin{aligned} \mathrm{Det}\,(\lambda I - J_B^*) &= (\lambda + \mu)[(\lambda + \mu)(\lambda - \beta_h S^* + \gamma + \mu)(\lambda + \delta) \\ &\quad + P(\lambda + \gamma + \mu)(\lambda + \delta) - Q\xi(\lambda + \mu)] = 0. \end{aligned} \tag{3.2.31}$$

Clearly, equation (3.2.31) has a negative root $\lambda = -\mu$.

Expanding equation (3.2.31) gives,

$$(\lambda + \mu)(\lambda - \beta_h S^* + \gamma + \mu)(\lambda + \delta) + P(\lambda + \gamma + \mu)(\lambda + \delta) - Q\xi(\lambda + \mu)$$

which we write as,

$$a_0\lambda^3 + a_1\lambda^2 + a_2\lambda + a_3 = 0, \tag{3.2.32}$$

where

$$\begin{aligned} a_0 &= 1, \\ a_1 &= P + \delta + \gamma + 2\mu - \beta_h S^*, \\ a_2 &= \mu^2 + P\delta + P\gamma + P\mu - Q\xi + \delta\gamma + 2\delta\mu + \gamma\mu - \beta_h S^*\delta - \beta_h S^*\mu, \\ a_3 &= \delta\mu^2 + P\delta\gamma + P\delta\mu - Q\mu\xi + \delta\gamma\mu - S^*\beta_h\delta\mu. \end{aligned}$$

The Routh-Hurwitz stability criterion (see Section II.2) requires,

$$a_1 > 0, a_2 > 0, a_3 > 0, \qquad \text{and} \qquad a_1a_2 - a_0a_3 > 0$$

as the necessary and sufficient conditions for the local stability.

From equation (3.2.22), we have the expression of $(\gamma+\mu)$ at the positive endemic equilibrium,

$$\gamma + \mu = \frac{S^*\beta_e\xi\delta\kappa + S^*\beta_e\xi^2 I^*}{(\delta\kappa + \xi I^*)^2} + \beta_h S^*.$$

Note that $Q\xi = \frac{\delta^2\beta_e S^*\kappa\xi}{(\kappa\delta+\xi I^*)^2}$, and we have two conditions that we use to prove the necessary and sufficient conditions which are,

$$\gamma + \mu > \beta_h S^*, \tag{3.2.33}$$

$$\delta(\gamma + \mu) > Q\xi + \beta_h S^*\delta. \tag{3.2.34}$$

First, we prove that $a_1 > 0$ using condition (3.2.33) and $P > 0$. We have

$$a_1 = P + \delta + \mu + (\gamma + \mu) - \beta_h S^* > 0. \tag{3.2.35}$$

Second, using the two inequalities $\delta(\gamma+\mu) > Q\xi + \beta_h S^*\delta$ and $\mu(\gamma+\mu) > \beta_h S^*\mu$, it can be shown that $a_2 > 0$. In addition, it can also be shown that $a_3 > 0$ by using $\delta\mu(\gamma+\mu) > Q\xi\mu + \beta_h S^*\delta\mu$.

We show $a_1a_2 - a_0a_3 > 0$ in the following.

$$\begin{aligned} a_2(\mu+\delta) - a_3 &= (\delta^2\gamma + \delta^2\mu - Q\delta\xi - S^*\beta_h\delta^2) \\ &\quad +(\gamma\mu^2 + \mu^3 + \delta\gamma\mu + \delta\mu^2 - S^*\beta_h\mu^2 - S^*\beta_h\delta\mu) \\ &\quad +P\delta^2 + P\mu^2 + \delta\mu^2 + \delta^2\mu + P\delta\mu + P\gamma\mu. \end{aligned}$$

Using conditions (3.2.33) and (3.2.34), we have

$$\begin{aligned} \delta^2\gamma + \delta^2\mu > Q\delta\xi + S^*\beta_h\delta^2 \text{ and} \\ \gamma\mu^2 + \mu^3 + \delta\gamma\mu + \delta\mu^2 > S^*\beta_h\mu^2 + S^*\beta_h\delta\mu. \end{aligned}$$

Thus $a_2(\mu+\delta) > a_3$ holds. Since $a_1 > (\mu+\delta)$, based on equation (3.2.35), we obtain $a_1a_2 > a_3$.

Thus, we have shown that when $R_0 > 1$, a unique endemic equilibrium is locally asymptotically stable. □

### III.2.3 Bifurcation diagram

In this section, we use a bifurcation diagram to illustrate the stability exchange at $R_0 = 1$ in Hartley's model. (If we use Mukandavire's Model, we have the same bifurcation point and similar bifurcation diagram). Summarizing our stability analysis results, we have established the following theorem:

**Theorem 9.** *The dynamical system (3.1.1-3.1.5) has a forward transcritical bifurcation at* $R_0 = 1$ .

A bifurcation diagram [77] of $I$ vs. $R_0$ for system (3.1.1-3.1.5) is given in Figure 3.1. In sketching the endemic branch of the bifurcation, we write the endemic quadratic equation $A(I^*)^2 + BI^* + C = 0$ (see equation (3.2.7)) as

$$A(I^*)^2 + (DR_0 - E)I^* + F(R_0 - 1) = 0 \tag{3.2.36}$$

where the constant coefficients $D$, $E$ and $F$ are given by

$$\begin{aligned} D &= \xi^2 bS_c(\beta_L + \beta_h), \\ E &= \xi(\gamma+b)(\beta_L\chi\kappa_H + \beta_H\delta_L\kappa_L) + b\xi(\gamma+b)(\delta_L\kappa_L + \chi\kappa_H), \\ F &= bS_c\xi(\beta_L\chi\kappa_H + \beta_H\kappa_L\delta_L). \end{aligned}$$

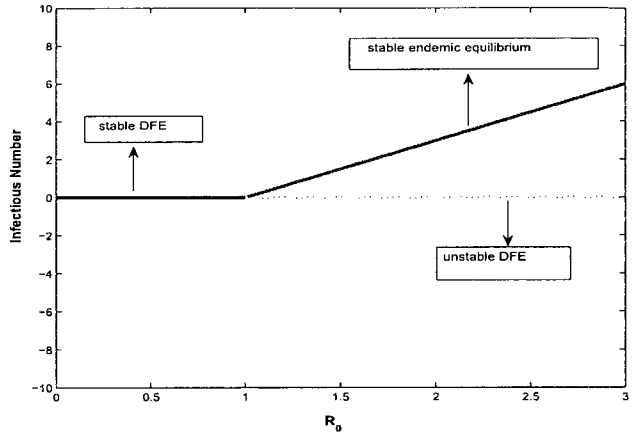


Figure 3.1: The bifurcation diagram of $I$ vs. $R_0$. There is a transcritical bifurcation at $R_0 = 1$.

We then obtain

$$R_0 = 1 + \frac{-A(I^*)^2 + (E - D)I^*}{DI^* + F}. \tag{3.2.37}$$

When $I^*$ is small or moderate, equation (3.2.37) represents approximately a straight line passing the bifurcation point $R_0 = 1$, $I^* = 0$.

### III.3 A case study: the Zimbabwean cholera outbreak

From the introduction in chapter I, we already have some background about Zimbabwean cholera. The 2008-2009 cholera outbreak in Zimbabwe was regarded as the worst African cholera epidemic in the last 15 years and received worldwide media attention [54; 84; 85; 86]. In order to improve our understanding of the development of this serious cholera outbreak, as well as for possible prediction and control of future cholera epidemics, we apply the mathematical model (3.1.1-3.1.5) to study the Zimbabwean cholera dynamics.

The values of those parameters are listed in the Table 3.1. Note, $b = (35\,\mathrm{yr})^{-1}$ in this paper based on the life expectancy in Zimbabwe [85; 86]. However, the values of $\beta_L$ and $\beta_H$ are less well known. The authors of [22] took $\beta_L = 1.5/\mathrm{wk}$ and $\beta_H$ as a variable; they also stated that these two parameters are particularly "difficult to estimate". This suggests that $\beta_L$ and $\beta_H$ are sensitive in the ODE model (3.1.1-3.1.5).

Table 3.1: Model Parameters and Values in Zimbabwe

| Model Parameter | Symbol | Value |
|---|---|---|
| HI ingestion rate | $\beta_H$ | Variable |
| LI ingestion rate | $\beta_L$ | Variable |
| LI half saturation rate | $\kappa_L$ | $10^6$ cells/ml |
| HI half saturation rate | $\kappa_H$ | 1428.6 cells/ml |
| Natural human birth / death rate | b | $(35\ yr)^{-1}$ |
| Bacterial transition rate | $\chi$ | $(5\ h)^{-1}$ |
| Shedding rate | $\xi$ | 10 cells/ml-day |
| Bacterial death rate | $\delta_L$ | $(30\ d)^{-1}$ |
| Recovery rate | $\gamma$ | $(5\ d)^{-1}$ |

Table 3.2: LHS sensitivity analysis

| Parameters | Minimum | Maximum | PRCC values |
|---|---|---|---|
| $\beta_L$ | 0.01 | 3 | 0.245957 |
| $\beta_H$ | 0.01 | 3 | -0.912184 |

LHS sensitivity analysis for $\beta_L$ and $\beta_H$ with respect to the infection number $I$. The sample size is $n = 400$. Results show that the infection is especially sensitive to $\beta_H$.

To verify it, we have carried out a sensitivity analysis for these two parameters using the Latin Hypercube Sampling (LHS) method [5; 53]. The LHS method, which is one of the most efficient ways to analyze sensitivity and uncertainty, calculates the Partial Rank Correlation Coefficients (PRCC) in the range of $[-1, 1]$ for the model parameters with respect to outcome measurements. A small PRCC value (close to 0) indicates that changes in the input parameter have little impact on the outcome, whereas a bigger PRCC value suggests that the outcome is significantly influenced by, thus sensitive to, the changes of the input parameter. In this study we pick the total infection, $I$, as the outcome and present the results in Table 3.2 with a sample size $n = 400$; similar patterns are observed for differing samples sizes. The results

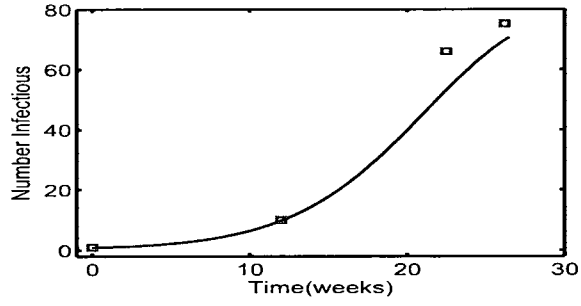


Figure 3.2: The data fitting for the infected population $I$, where the curve represents the model prediction and the squares mark the reported Zimbabwean data (normalized by a factor of 1,200).

confirm the sensitivity of the two parameters $\beta_L$ and $\beta_H$; in particular, we observe that the number of the infected people is very sensitive to $\beta_H$.

In the work of [22], the ODE model (3.1.1-3.1.5) was introduced and discussed for a hypothetical community with a total population of $N = 10,000$. In order to assess the applicability of this model to the Zimbabwean cholera outbreak, we will first need to ensure the available Zimbabwean data can be reasonably fitted by the model results, which necessitates the adjustment of parameter values. The discussion in [22] and our sensitivity analysis indicate that the parameters $\beta_L$ and $\beta_H$ are sensitive and possibly vary from country to country. Hence, in what follows we adjust these two parameters to match the reported infections in Zimbabwe.

According to the published data by WHO [85; 86], the cholera outbreak started in the end of August 2008, with 11,735 cases reported by December 1, 2008, 79,613 cases by February 18, 2009 and 91,164 cases by March 17, 2009; afterwards the situation had improved significantly due to various control measures and international aids. Since the total population in Zimbabwe is about 12 million [86], we scale down this number by a factor of 1,200 to match the hypothetical population of $N = 10,000$ in [22]. Accordingly, we now have 10, 66 and 76 (normalized) cholera infections after 12 weeks, 22.5 weeks and 26.5 weeks, respectively, from the beginning of the outbreak. By varying the two parameters, we find that when $\beta_L = 0.126$ and $\beta_H = 0.0995$, the model prediction for the infected population, $I$, can well fit these data (see Figure 3.2).

By substituting the values of $\beta_L$, $\beta_H$ and other parameters into equations (3.1.13)

and (3.1.14), we find the basic reproduction number

$$R_0 \approx 1.222, \tag{3.3.1}$$

and the population threshold

$$S_c \approx 8183.$$

Thus, the model predicts that the infection would spread and an epidemic would develop, which is consistent with the reality in Zimbabwe. The fact that $R_0 > 1$ justifies the development of the cholera epidemics. Since the values of $\beta_L$ and $\beta_H$ are much lower in the Zimbabwean cholera outbreak than those used in [22], the value of $R_0 \approx 1.22$ is much smaller than that obtained in [22] (about 18.2). The relatively low value of $R_0$ for the Zimbabwean cholera outbreak is attributed to the fact that although nearly 0.1 million cases have been reported, the overall percentage of infection with respect to the total population is still pretty low (less than 0.8%). The $R_0$ estimated here is regarded as a nationally averaged reproduction rate.

The basic reproduction number found in (3.3.1) provides useful guidelines for the prevention and control strategies on cholera epidemics in Zimbabwe. For example, consider the use of chemotherapy (including antibiotics) to treat the cholera infection. Based on the work of Dietz [14], the chemotherapy program has to achieve a minimum proportional reduction of the susceptible population by

$$a \geq 1 - \frac{1}{R_0} \tag{3.3.2}$$

for eliminating an epidemic, where a homogeneous population is assumed. Substituting (3.3.1) into (3.3.2), we obtain

$$a \geq 0.1816.$$

This result can possibly explain that, although the medical resources were very limited in Zimbabwe and many rural areas were outside the treatment facilities, the 2008-2009 cholera outbreak was still under control and terminated in July 2009. In contrast, should the value of $R_0$ be much higher than that in (3.3.1), say 12.22 instead of 1.222, we would need $a \geq 0.9182$ which would be impossible to achieve in Zimbabwe. In addition, if we use vaccination as a preventive measure against the cholera outbreak, the minimal vaccination coverage would have to be [14]:

$$c \geq \frac{1 - R_0^{-1}}{1 - (1-r)(1-s)}, \tag{3.3.3}$$

where $r$ is the fraction of the vaccinated population who are completely immunized (i.e., with zero susceptibility), and $s$ is the proportional reduction of the susceptibility for those partially immunized. For a homogeneous population, we may assume $r = 0$. Meanwhile, $s = 0.5$ would be a reasonable estimate for Zimbabwean people. Substituting these numbers and $R_0 = 1.222$ into (3.3.3), we find

$$c \geq 0.3633,$$

which requires at least 36.33% of the total population to receive vaccination in order to prevent future cholera outbreaks. Clearly, this standard has not been met in Zimbabwe due to collapsed economics, broken health system and severe shortage of primary care facilities [54]. This provides a possible explanation to the fact that cholera has remained endemic in Zimbabwe for many years [54; 86].

As a means to check the validity of our study, we compare the value of $R_0$ in (3.3.1), which is calculated from equation (3.1.17), to those that do not require specific mathematical models.

One simple and general formula to estimate $R_0$ was given in [81] based on the final size of the epidemic:

$$R_0 = \frac{N-1}{C} \sum_{i=S_f+1}^{S_0} \frac{1}{i}, \tag{3.3.4}$$

where $S_0$ and $S_f$ are the numbers of the susceptible at the start and end of the epidemic, respectively, and $C = S_0 - S_f$ is the total number of infections. Since

$$\sum_{i=1}^{n} \frac{1}{i} \approx \ln n,$$

when $n$ is large, equation (3.3.4) yields

$$R_0 \approx \frac{N-1}{S_0 - S_f} \left[\ln S_0 - \ln S_f\right] \approx \frac{1 - 1/N}{S_0/N - S_f/N} \left[\ln\left(S_0/N\right) - \ln\left(S_f/N\right)\right].$$

Let $u_0 = S_0/N$ and $u_\infty = S_f/N$ denote the initial and final proportions of the susceptible, respectively, in the duration of the epidemic. We then obtain

$$R_0 = \frac{1}{u_0 - u_\infty} \left[\ln u_0 - \ln u_\infty\right]. \tag{3.3.5}$$

which is asymptotically equivalent to the formula (3.3.4) for large population $N$. Equation (3.3.5) was also presented in the work of Dietz [14].

Based on [85; 86], we take July 2009 as the termination for the Zimbabwean cholera outbreak, with a total of 98,592 reported cases. Assuming the total population is completely susceptible (i.e., $u_0 = 100\%$), the formula (3.3.5) yields

$$R_0 \approx 1.004 \tag{3.3.6}$$

for this cholera epidemic.

In addition, another method of estimating $R_0$ was provided in [14], using the initial growth rate of the epidemic:

$$R_0 = 1 + \frac{D \ln 2}{t_d}, \tag{3.3.7}$$

where $D$ is the duration of the epidemic and $t_d$ is the initial doubling time. The value of $t_d$ can be approximated by

$$t_d \approx \frac{\ln 2}{\ln(1 + r/100)},$$

where $r$ is the initial growth rate for the infection. Substitute the Zimbabwean data into equation (3.3.7) and we obtain

$$R_0 \approx 1.226. \tag{3.3.8}$$

The results in (3.3.6) and (3.3.8) are qualitatively consistent with (3.3.1), the value obtained from the ODE model.

Meanwhile, we substitute these parameter values into equations (3.2.7) and (3.2.3-3.2.6), and find the unique positive endemic equilibrium:

$$S^* \doteq 7666, \qquad I^* \doteq 0.9157, \qquad R^* \doteq 2333, \qquad B_H^* \doteq 1.908, \qquad B_L^* \doteq 274.7.$$

Note again that we have scaled down the total population in Zimbabwe by a factor of $1,200$ to match the hypothetical population $N = 10,000$. Thus, the model predicts that the realistic endemic infection number in Zimbabwe is about $1,099$.

To verify the model prediction, we run the numerical simulation for a much longer period of time (up to 7,000 weeks) and present the results for $I$, $S$ and $R$ in Figures 3.3 and 3.4. The first peak of the infection curve in Figure 3.3 represents the 2008-2009 cholera outbreak. The infection number ($I$) starts to decline once the susceptible population ($S$) falls below the threshold, $S_c \doteq 8183$. After this

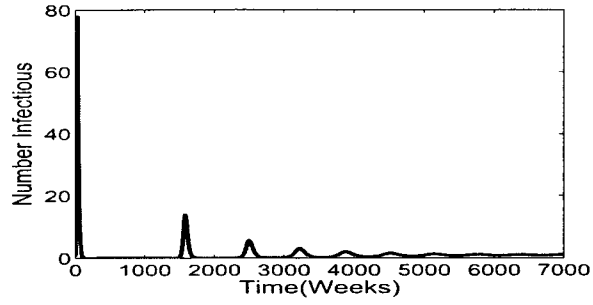


Figure 3.3: The infected population vs. time with the initial setting: $I(0) = 1$, $S(0) = 9999$, $R(0) = B_H(0) = B_L(0) = 0$. The curve exhibits several epidemic oscillations (outbreaks), then approaches the endemic equilibrium $I^* \doteq 0.9157$ after about 5,000 weeks.

outbreak $I$ drops to almost zero, meaning that the majority of the infected people have recovered and entered the $R$ class, so that we see a significant increase of $R$ in Figure 3.4. Then $I$ stays at the zero level for the next 1,500 weeks or so (about 30 years). During this period $R$ gradually decreases due to natural death of recovered people, and $S$ increases due to natural birth of new susceptibles. Once the susceptible population exceeds the threshold $S_c$, another cholera outbreak is triggered but with much lower magnitude. This pattern continues for a few more outbreaks with decaying magnitudes. After about 5,000 weeks, the infection curve rests at the endemic value, $I^* \doteq 0.9157$; the $S$ and $R$ curves also converge to their endemic values,

Figures 3.5 and 3.6 show the results of another numerical run with different initial conditions: $I(0) = 500$, $S(0) = 8500$, $R(0) = 1000$, $B_H(0) = B_L(0) = 0$. We observe very similar pattern. In particular, the $I$, $S$ and $R$ curves all approach their endemic equilibrium values after about 5,000 weeks. This pattern is also observed with various other initial conditions, which demonstrates the global asymptotic stability of the endemic equilibrium when $R_0 > 1$. Meanwhile, these results also justify the instability of the disease-free equilibrium, as cholera outbreaks occur whenever the susceptible population $S$ exceeds the critical value $S_c$. $S^* \doteq 7666$ and $R^* \doteq 2333$, respectively.

Finally, to validate the global asymptotical stability of the disease-free equilibrium when $R_0 < 1$, we have conducted many numerical runs with differing population $N$ and initial conditions, and the results agree with the model prediction. A typical

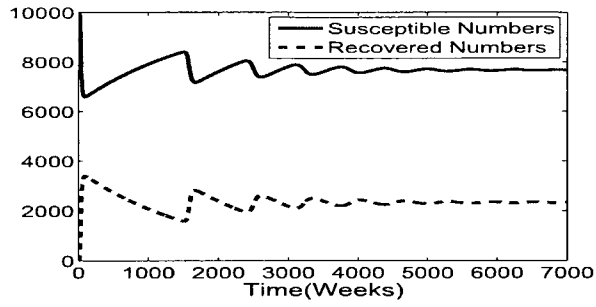


Figure 3.4: The susceptible and recovered populations vs. time with the initial setting: $I(0) = 1$, $S(0) = 9999$, $R(0) = B_H(0) = B_L(0) = 0$. Both curves exhibit several epidemic oscillations before approaching the endemic equilibrium: $S^* \doteq 7666$, $R^* \doteq 2333$.

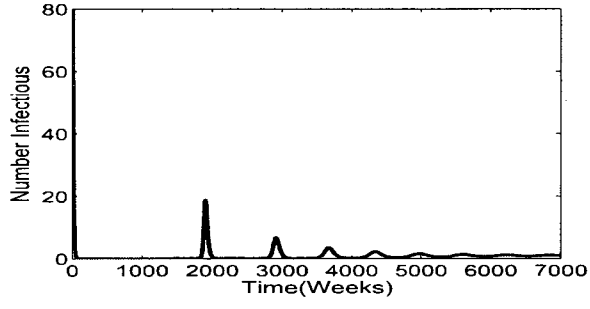


Figure 3.5: The infected population vs. time with the initial setting: $I(0) = 500$, $S(0) = 8500$, $R(0) = 1000$, $B_H(0) = B_L(0) = 0$. The curve exhibits several epidemic oscillations and then approaches the endemic equilibrium over time.

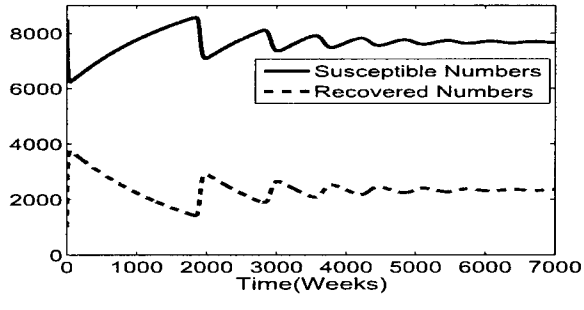


Figure 3.6: The susceptible and recovered populations vs. time with the initial setting: $I(0) = 500$, $S(0) = 8500$, $R(0) = 1000$, $B_H(0) = B_L(0) = 0$. Both curves exhibit several epidemic oscillations and then approach the endemic equilibrium over time.

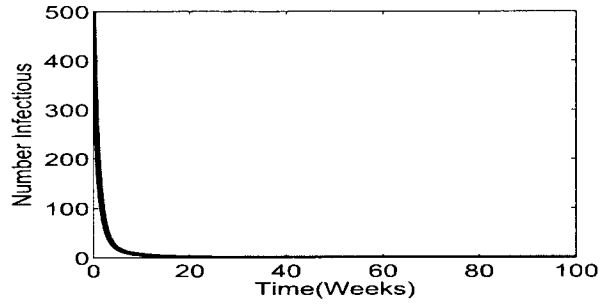


Figure 3.7: The infected population vs. time with the initial setting: $I(0) = 500$, $S(0) = 4500$, $R(0) = B_H(0) = B_L(0) = 0$. In this case $R_0 \doteq 0.611$ and the disease quickly dies out ($I = 0$).

numerical result is presented in Figure 3.7, where the total hypothetical population is set as $N = 5,000$ (i.e., halving the current Zimbabwean population) so that $R_0 \doteq 0.611$. Initially $I$ is 500; then the infection number quickly drops to zero and stays at zero for all time afterwards.

# CHAPTER IV

# GENERALIZED CHOLERA MODEL

Two major differences among all models we mentioned in the first three chapters (for example, the model of Codeco [11], the model of Hartley [22] and the model of Mukandavire [60]), are how the incidence rate is determined and how the environmental vibrio concentration is formulated. Hence, a goal of this chapter is to propose a unified cholera model which allows general nonlinear incidence factor and general representation of the pathogen concentrations.

## IV.1 Model and notations

We construct the following differential equations for the cholera dynamics, based on the combination of a regular SIR model and an environmental component:

$$\frac{dS}{dt} = bN - Sf(I,B) - bS, \tag{4.1.1}$$

$$\frac{dI}{dt} = Sf(I,B) - (\gamma + b)I, \tag{4.1.2}$$

$$\frac{dR}{dt} = \gamma I - bR, \tag{4.1.3}$$

$$\frac{dB}{dt} = h(I,B), \tag{4.1.4}$$

where, as usual, $S$, $I$ and $R$ denote the susceptible, the infected, and the recovered populations, respectively, and $B$ denotes the concentration of the vibrios in the contaminated water. The total population $N = S + I + R$ is assumed to be a constant. The parameter $b$ represents the natural human birth/death rate, and $\gamma$ represents the rate of recovery from cholera. In this generalized model, $f(I,B)$ is the incidence function which determines the rate of new infection, and the function $h(I,B)$ describes the rate of change for the pathogen in the environment.

If we set

$$X = \big(S,\ I,\ R,\ B\big)^T, \tag{4.1.5}$$

then the above equations can be put in a vector form as

$$\frac{d}{dt}X = \mathbf{F}(X). \tag{4.1.6}$$

**Remark 1.** *We allow $B$ to be either a scalar or a vector in this system, to facilitate more general formulation. For example, if we consider both the hyper-infectious (HI) and less-infectious (LI) states of the vibrios, then we may write $B = [B_H, B_L]$. In such a case it is understood that*

$$\frac{dB}{dt} = \begin{bmatrix} \frac{dB_H}{dt} \\ \\ \frac{dB_L}{dt} \end{bmatrix}, \qquad h(I,B) = \begin{bmatrix} h_H(I,B) \\ \\ h_L(I,B) \end{bmatrix}$$

*and*

$$\frac{\partial f}{\partial B} = \begin{bmatrix} \frac{\partial f}{\partial B_H} \\ \\ \frac{\partial f}{\partial B_L} \end{bmatrix}, \qquad \frac{\partial^2 f}{\partial B^2} = \begin{bmatrix} \frac{\partial^2 f}{\partial B_H^2} & \frac{\partial^2 f}{\partial B_H \partial B_L} \\ \\ \frac{\partial^2 f}{\partial B_L \partial B_H} & \frac{\partial^2 f}{\partial B_L^2} \end{bmatrix}, \qquad \frac{\partial h}{\partial B} = \begin{bmatrix} \frac{\partial h_H}{\partial B_H} & \frac{\partial h_H}{\partial B_L} \\ \\ \frac{\partial h_L}{\partial B_H} & \frac{\partial h_L}{\partial B_L} \end{bmatrix}, \quad \text{etc.}$$

**Remark 2.** *We write a vector $V \geq 0$ $(\leq 0)$ if each component of $V$ is $\geq 0$ $(\leq 0)$. We write a matrix $A \geq 0$ $(\leq 0)$ if $A$ is positive (negative) semidefinite.*

To make biological sense for our model, we assume the two functions $f$ and $h$ satisfy the following conditions for $I \geq 0$, $B \geq 0$:

**(a)** $f(0,0) = 0$, $\quad h(0,0) = 0$,

**(b)** $f(I,B) \geq 0$,

**(c)** $\dfrac{\partial f}{\partial I}(I,B) \geq 0$, $\quad \dfrac{\partial f}{\partial B}(I,B) \geq 0$, $\quad \dfrac{\partial h}{\partial I}(I,B) \geq 0$, $\quad \dfrac{\partial h}{\partial B}(I,B) \leq 0$,

**(d)** $f(I,B)$ is concave; i.e., the matrix $D^2 f \triangleq \begin{bmatrix} \frac{\partial^2 f}{\partial I^2} & \frac{\partial^2 f}{\partial I \partial B} \\ \\ \frac{\partial^2 f}{\partial B \partial I} & \frac{\partial^2 f}{\partial B^2} \end{bmatrix}$ is negative semidefinite everywhere.

**(d')** $h(I,B)$ is concave; i.e., the matrix $D^2 h$ is negative semidefinite.

The assumption **(a)** ensures the existence of a unique disease-free equilibrium (DFE) for system (4.1.6), i.e.,

$$X_0 = (N,\, 0,\, 0,\, 0)^T. \tag{4.1.7}$$

The assumption (**b**) ensures a positive incidence rate. The first two inequalities in assumption (**c**) state that increased infection and pathogen concentration lead to higher incidence rate (due to higher level of transmission), whereas the third inequality states that increased infection results in higher growth rate for the pathogen in the environment (due to higher shedding rate). The last inequality in assumption (**c**) indicates a positive net death rate of the vibrios. The condition (**d**) is a common assumption for nonlinear incidence [25; 35; 58]. In our model, this condition regulates $f(I, B)$ as a biologically realistic incidence based on a consequence of saturation effects: when the number of the infective, or the environmental pathogen concentration, is high, the incidence rate will respond more slowly than linearly to the increase in $I$ and $B$. The condition (**d'**) is an additional assumption we introduce for the regulation of the function $h(I, B)$; it states that at an equilibrium level, the response of the pathogen growth rate will be slower than linear. Furthermore, we assume the equation $h(I, B) = 0$ implicitly defines a function $B = g(I)$, which satisfies the following condition:

(**e**) $g'(I) \geq 0, \quad g''(I) \leq 0, \quad$ for $I \geq 0$.

This assumption states that the pathogen concentration increases with the number of the infected, while the rate of increase will be below linear when the infected population is high, due to saturation effects.

Based on the assumption (**b**), it is straightforward to see that if any component of ($S$, $I$, $R$) becomes 0, then the derivative of this component will be non-negative. Meanwhile, since $\frac{d}{dt}(S + I + R) = 0$, $S(t) + I(t) + R(t)$ will remain a constant (i.e., $N$) for all $t \geq 0$. Hence, the following result can be easily established.

**Lemma 7.** *If $S(0) \geq 0$, $I(0) \geq 0$, $R(0) \geq 0$, and $S(0) + I(0) + R(0) = N$, then $S(t) \geq 0$, $I(t) \geq 0$, $R(t) \geq 0$, and $S(t) + I(t) + R(t) = N$, for all $t \geq 0$.*

**Remark 3.** *Lemma 7 ensures that the solution of the model system (4.1.1-4.1.4) is biologically feasible for all times. Mathematically speaking, the solution domain*

$$\bar{D} = \{(S, I, R) \,|\, S \geq 0,\ I \geq 0,\ R \geq 0,\ S + I + R = N\}$$

*is a positively invariant set in $\mathbb{R}^3$.*

**Remark 4.** *[85] A positive invariant set is a set with the following properties: Given a system $\dot{x} = f(x)$ and trajectory $x(t) = x_0$ where $x_0$ is the initial point. Let*

$\mathcal{O} \triangleq \{x \in \mathbb{R}^n \mid \phi(x) = 0\}$ *where* $\phi$ *is a real valued function that characterizes* $\mathcal{O}$. *The set* $\mathcal{O}$ *is said to be positively invariant if* $x_0 \in \mathcal{O}$ *implies that* $x(t, x_0) \in \mathcal{O}\ \forall t \geq 0$.

## IV.2 Next-generation matrix analysis

We start our analysis by determining the basic reproduction number, $R_0$, of our proposed model. Based on the work of van den Driessche and Watmough [80], and our work in chapter III, let's recall that $R_0$ is mathematically defined as the spectral radius of the next generation matrix. In our system (4.1.1)-(4.1.4), only $I$ and $B$ are directly related to the infection. Following the approach in [80], we write

$$\begin{bmatrix} \frac{dI}{dt} \\ \\ \frac{dB}{dt} \end{bmatrix} = \begin{bmatrix} Sf(I,B) \\ \\ 0 \end{bmatrix} - \begin{bmatrix} (\gamma+b)I \\ \\ -h(I,B) \end{bmatrix} = \mathcal{F} - \mathcal{V} \tag{4.2.1}$$

where again, $\mathcal{F}$ denotes the rate of appearance of new infections, and $\mathcal{V}$ denotes the rate of transfer of individuals into or out of each population set.

The next generation matrix is defined as $FV^{-1}$, where $F$ and $V$ are $2\times 2$ Jacobian matrixes given by

$$F = D\mathcal{F}(X_0) = \begin{bmatrix} N\frac{\partial f}{\partial I}(0,0) & N\frac{\partial f}{\partial B}(0,0) \\ \\ 0 & 0 \end{bmatrix}, \qquad V = D\mathcal{V}(X_0) = \begin{bmatrix} \gamma+b & 0 \\ \\ -\frac{\partial h}{\partial I}(0,0) & -\frac{\partial h}{\partial B}(0,0) \end{bmatrix}$$

where $X_0$ is the DFE defined in equation (4.1.7). After some algebra, we obtain

$$V^{-1} = \frac{-1}{\gamma+b}\begin{bmatrix} -1 & 0 \\ \\ \left(\frac{\partial h}{\partial B}(0,0)\right)^{-1}\frac{\partial h}{\partial I}(0,0) & \left(\frac{\partial h}{\partial B}(0,0)\right)^{-1}(\gamma+b) \end{bmatrix}.$$

Hence, the next generation matrix is

$$FV^{-1} = \frac{-1}{\gamma+b}\begin{bmatrix} -N\left[\frac{\partial f}{\partial I}(0,0) - \frac{\partial f}{\partial B}(0,0)\left(\frac{\partial h}{\partial B}(0,0)\right)^{-1}\frac{\partial h}{\partial I}(0,0)\right] & N(\gamma+b)\left(\frac{\partial h}{\partial B}(0,0)\right)^{-1}\frac{\partial f}{\partial B}(0,0) \\ \\ 0 & 0 \end{bmatrix}.$$

Its spectral radius $\rho(FV^{-1}) = \max_{1\le i\le 2}|\lambda_i|$, where $\lambda_i$ denotes the $i$th eigenvalue, can be easily found. Therefore, we obtain the basic reproduction number as

$$R_0 = \frac{N}{\gamma+b}\Big[\frac{\partial f}{\partial I}(0,0) - \frac{\partial f}{\partial B}(0,0)\Big(\frac{\partial h}{\partial B}(0,0)\Big)^{-1}\frac{\partial h}{\partial I}(0,0)\Big]. \tag{4.2.2}$$

By our assumption, $h(I,B)=0$ defines an implicit function $B=g(I)$. Using implicit differentiation, we obtain $\dfrac{\partial h}{\partial I} + \dfrac{\partial h}{\partial B}\,g'(I) = 0$, which yields

$$g'(I) = -\Big(\frac{\partial h}{\partial B}\Big)^{-1}\frac{\partial h}{\partial I} \tag{4.2.3}$$

for $I \ge 0$. Substituting equation (4.2.3) into equation (4.2.2), we obtain

$$R_0 = \frac{N}{\gamma+b}\frac{\partial f}{\partial I}(0,0) + \frac{N}{\gamma+b}\frac{\partial f}{\partial B}(0,0)\,g'(0) \triangleq R_0^{hh} + R_0^{eh}. \tag{4.2.4}$$

Equation (4.2.4) clearly shows that $R_0$ depends on two factors: one is due to human-to-human transmission ($R_0^{hh}$) and the other is due to environment-to-human transmission ($R_0^{eh}$). If $\frac{\partial f}{\partial I}(0,0)=0$, then $R_0 = R_0^{eh}$; if $\frac{\partial f}{\partial B}(0,0)=0$, then $R_0 = R_0^{hh}$. In general, both $R_0^{hh}$ and $R_0^{eh}$ contribute to the basic reproduction rate. Biologically speaking, $R_0$ measures the average number of secondary infections that occur when one infective is introduced into a completely susceptible host population [23; 80; 81]. In equation (4.2.4), the term $\frac{1}{\gamma+b}$ represents the expected time of the infection, $\frac{\partial f}{\partial I}(0,0)$ represents the unit human-to-human transmission rate, and $\frac{N}{\gamma+b}\frac{\partial f}{\partial I}(0,0)$ measures the total number of secondary infections caused by the human-to-human transmission. Similarly, the product $\frac{\partial f}{\partial B}(0,0)\,g'(0)$ represents the unit environment-to-human transmission rate, and $\frac{N}{\gamma+b}\frac{\partial f}{\partial B}(0,0)\,g'(0)$ measures the total number of secondary infections caused by the environment-to-human transmission.

**Remark 5.** *It can be easily verified that this derivation of $R_0$ holds true no matter $B$ is a scalar or vector. In case $B$ is a vector, $\frac{\partial h}{\partial B}(0,0)$ is a matrix (see Remark 1) and $\big(\frac{\partial h}{\partial B}(0,0)\big)^{-1}$ represents its inverse.*

Based on the framework in [80], we immediately obtain the result below regarding the local asymptotical stability of the DFE.

**Theorem 10.** *Let $R_0$ be defined in equation (4.2.4). The disease-free equilibrium of the system (4.1.1)-(4.1.4) is locally asymptotically stable if $R_0 < 1$, and unstable if $R_0 > 1$.*

## IV.3 DFE global stability

To study the global asymptotic stability of the DFE, we need Lemma 6 introduced by Castillo-Chavez *et al.* [9] which we applied in chapter III, Section III.1 to show the DFE global stability of Hartley's model [22].

**Theorem 11.** *The disease-free equilibrium of the model (4.1.1)-(4.1.4) is globally asymptotic stable if* $R_0 < 1$ .

*Proof.* We adopt the notations in Lemma 6 and verify the conditions (H1) and (H2) in Lemma 6. In our model, $X_1 = (S,\, R)^T$ , $X_2 = (I,\, B)^T$ , and $X_1^* = (N,\, 0)^T$ . The uninfected subsystem is

$$\frac{d}{dt}\begin{bmatrix} S \\ R \end{bmatrix} = F = \begin{bmatrix} bN - bS - Sf(I,B) \\ \gamma I - bR \end{bmatrix}, \tag{4.3.1}$$

and the infected subsystem is

$$\frac{d}{dt}\begin{bmatrix} I \\ B \end{bmatrix} = G = \begin{bmatrix} Sf(I,B) - (\gamma + b)I \\ h(I,B) \end{bmatrix}. \tag{4.3.2}$$

When $I = B = 0$ (i.e., $X_2 = 0$), the uninfected subsystem (4.3.1) becomes

$$\frac{d}{dt}\begin{bmatrix} S \\ \\ R \end{bmatrix} = \begin{bmatrix} bN - bS \\ \\ -bR \end{bmatrix}, \tag{4.3.3}$$

and its solution is

$$R(t) = R(0)e^{-bt}, \qquad S(t) = N - \big(N - S(0)\big)\, e^{-bt}.$$

Clearly, $R(t) \to 0$ and $S(t) \to N$ as $t \to \infty$, regardless of the values of $R(0)$ and $S(0)$. Hence, $X_1^* = (N,\, 0)$ is globally asymptotically stable for the subsystem $\dfrac{dX_1}{dt} = F(X_1,\, 0)$.

Next, we have

$$
\begin{aligned}
G &= \frac{\partial G}{\partial X_2}(N,0,0,0)\,X_2 - \hat{G} \\
&= \begin{bmatrix} N\frac{\partial f}{\partial I}(0,0) - (\gamma+b) & N\frac{\partial f}{\partial B}(0,0) \\ \\ \frac{\partial h}{\partial I}(0,0) & \frac{\partial h}{\partial B}(0,0) \end{bmatrix} \begin{bmatrix} I \\ \\ B \end{bmatrix} \\
&- \begin{bmatrix} N\frac{\partial f}{\partial I}(0,0)I + N\frac{\partial f}{\partial B}(0,0)B - Sf(I,B) \\ \\ \frac{\partial h}{\partial I}(0,0)I + \frac{\partial h}{\partial B}(0,0)B - h(I,B) \end{bmatrix}.
\end{aligned}
$$

Obviously $A = \frac{\partial G}{\partial X_2}(N,0,0,0)$ is an M-matrix based on the assumption (**c**). It remains to show $\hat{G} \geq 0$. The assumption (**d**) implies that the surface $f = f(I,B)$ is below its tangent plane at any point $(I_0, B_0) \geq 0$; that is,

$$
f(I,B) \leq f(I_0,B_0) + \frac{\partial f}{\partial I}(I_0,B_0)(I-I_0) + \frac{\partial f}{\partial B}(I_0,B_0)(B-B_0). \tag{4.3.4}
$$

Particularly, setting $(I_0, B_0) = (0,0)$ and using the assumption (**a**), we obtain

$$
f(I,B) \leq \frac{\partial f}{\partial I}(0,0)I + \frac{\partial f}{\partial B}(0,0)B \tag{4.3.5}
$$

for all $(I,\ B) \geq 0$. A similar argument leads to, according to the assumption (**d'**),

$$
h(I,B) \leq \frac{\partial h}{\partial I}(0,0)I + \frac{\partial h}{\partial B}(0,0)B. \tag{4.3.6}
$$

Hence, $\hat{G} \geq 0$ for $I \geq 0$, $B \geq 0$.

Based on Lemma 6, the DFE $X_0 = (N,\ 0,\ 0,\ 0)$ is globally asymptotically stable when $R_0 < 1$. □

**Corollary 1.** *If $R_0 < 1$, then $\lim_{t\to\infty} X(t) = X_0$ for any solution $X(t)$ of the system (4.1.1)-(4.1.4).*

### IV.4 The endemic equilibrium

Theorem 11 completely determines the global dynamics of our model when $R_0 < 1$. The epidemiological consequence is that the number of the infected, no matter how

large initially, will vanish in time so that the disease dies out. In contrast, the disease will persist when $R_0 > 1$. To investigate the resulted long-term dynamics, we turn to the endemic analysis in what follows.

The theorem below shows the existence and uniqueness of the endemic equilibrium.

**Theorem 12.** *For the model system (4.1.1)-(4.1.4), there exists a unique positive endemic equilibrium if $R_0 > 1$, and there is no positive endemic equilibrium if $R_0 < 1$.*

*Proof.* By our assumption, $h(I, B) = 0$ defines an implicit function $B = g(I)$. Meanwhile, by setting the right-hand sides of equations (4.1.1) and (4.1.2) to zero, we obtain

$$S = \frac{bN}{b + f(I, g(I))}, \qquad I = \frac{Sf(I, g(I))}{(\gamma + b)} \tag{4.4.1}$$

which yields

$$I = \tilde{H}(I) \triangleq \frac{bNf(I, g(I))}{(\gamma + b)[b + f(I, g(I))]}. \tag{4.4.2}$$

Now the question is whether $\tilde{H}(I)$ has a nontrivial fixed point on $(0, \infty)$.

Clearly, $\tilde{H}(I) \geq 0$ for $I \geq 0$, and $\tilde{H}(0) = 0$. Let us denote $P(I) = f(I, g(I))$. Then

$$\begin{aligned} \tilde{H}'(I) &= \frac{bN}{\gamma + b} \frac{(b + P(I))P'(I) - P(I)P'(I)}{[b + P(I)]^2} \\ &= \frac{bN}{\gamma + b} \frac{bP'(I)}{[b + P(I)]^2} \end{aligned} \tag{4.4.3}$$

where

$$P'(I) = \frac{\partial f}{\partial I} + \frac{\partial f}{\partial B} g'(I) \geq 0, \tag{4.4.4}$$

due to assumptions (**c**) and (**e**). Thus $\tilde{H}'(I) \geq 0$ for $I \geq 0$. In particular,

$$\tilde{H}'(0) = \frac{N}{\gamma + b} P'(0) = R_0. \tag{4.4.5}$$

Next, we have

$$\tilde{H}''(I) = \frac{b^2 N}{(\gamma + b)[b + P(I)]^3} \left[ \big(b + P(I)\big) P''(I) - 2\big(P'(I)\big)^2 \right] \tag{4.4.6}$$

where

$$P''(I) = \frac{\partial^2 f}{\partial I^2} + 2g'(I)\frac{\partial^2 f}{\partial I \partial B} + \left(g'(I)\right)^2 \frac{\partial^2 f}{\partial B^2} + \frac{\partial f}{\partial B} g''(I)$$

$$= \begin{bmatrix} 1, & g'(I) \end{bmatrix} \begin{bmatrix} \frac{\partial^2 f}{\partial I^2} & \frac{\partial^2 f}{\partial I \partial B} \\ \frac{\partial^2 f}{\partial I \partial B} & \frac{\partial^2 f}{\partial B^2} \end{bmatrix} \begin{bmatrix} 1 \\ g'(I) \end{bmatrix} + \frac{\partial f}{\partial B} g''(I). \qquad (4.4.7)$$

Based on the assumption (**d**), the matrix $\begin{bmatrix} \frac{\partial^2 f}{\partial I^2} & \frac{\partial^2 f}{\partial I \partial B} \\ \frac{\partial^2 f}{\partial I \partial B} & \frac{\partial^2 f}{\partial B^2} \end{bmatrix}$ is negative semidefinite. Meanwhile, $g''(I) \leq 0$ due to the assumption (**e**). Thus $P''(I) \leq 0$. Consequently, $\tilde{H}''(I) \leq 0$ for all $I \geq 0$. Therefore, $\tilde{H}(I)$ is increasing and concave on $(0, \infty)$ with $\tilde{H}(0) = 0$.

Clearly, if $\tilde{H}'(0) = R_0 > 1$, there is a unique positive fixed point $I^*$ for $\tilde{H}$ (see Figure 4.1-a). If $\tilde{H}'(0) = R_0 < 1$, there is no positive fixed point for $\tilde{H}$ (see Figure 4.1-b). □

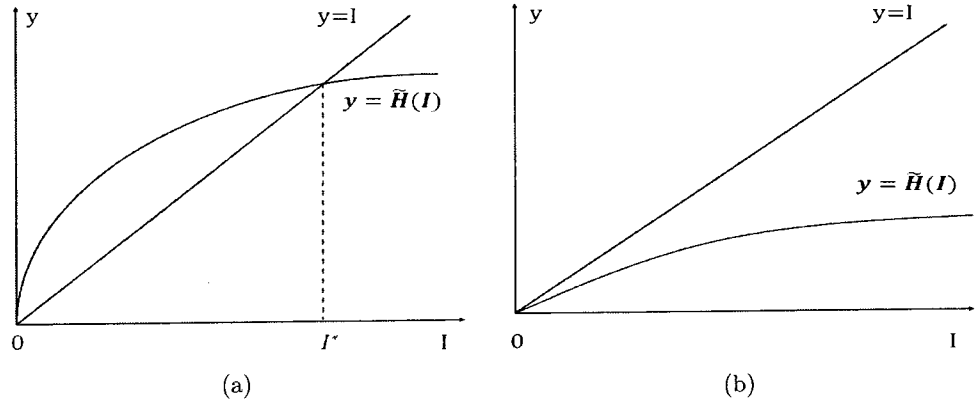


Figure 4.1: Two typical scenarios for the function $\tilde{H}(I)$ defined in equation (4.4.2): (a) when $\tilde{H}'(0) > 1$, the curve $y = \tilde{H}(I)$ has a unique intersection with the line $y = I$ for $I > 0$; and (b) when $\tilde{H}'(0) < 1$, the curve $y = \tilde{H}(I)$ has no intersection with the line $y = I$ for $I > 0$.

**Remark 6.** *The same result holds in case $B$ is a vector, say, $B = [B_H, B_L]$. In fact, we can write $g(I) = [g_H(I), g_L(I)]^T$ and $g'(I) = [g'_H(I), g'_L(I)]^T$. It is then*

*straightforward to verify that*

$$P'(I) = \frac{\partial f}{\partial I} + \left[ \frac{\partial f}{\partial B_H}, \frac{\partial f}{\partial B_L} \right] \begin{bmatrix} g'_H \\ \\ g'_L \end{bmatrix} = \frac{\partial f}{\partial I} + \frac{\partial f}{\partial B} g'(I) \geq 0$$

*which takes the same form as (4.4.4). Meanwhile,*

$$\begin{aligned} P''(I) &= \frac{\partial^2 f}{\partial I^2} + 2 \left[ \frac{\partial^2 f}{\partial I \partial B_H}, \frac{\partial^2 f}{\partial I \partial B_L} \right] \begin{bmatrix} g'_H \\ \\ g'_L \end{bmatrix} \\ &\quad + \left[ g'_H, g'_L \right] \begin{bmatrix} \frac{\partial^2 f}{\partial B_H^2} & \frac{\partial^2 f}{\partial B_H \partial B_L} \\ \\ \frac{\partial^2 f}{\partial B_L \partial B_H} & \frac{\partial^2 f}{\partial B_L^2} \end{bmatrix} \begin{bmatrix} g'_H \\ \\ g'_L \end{bmatrix} + \left[ \frac{\partial f}{\partial B_H}, \frac{\partial f}{\partial B_L} \right] \begin{bmatrix} g''_H \\ \\ g''_L \end{bmatrix} \\ &= \left[ 1, g'_H, g'_L \right] \begin{bmatrix} \frac{\partial^2 f}{\partial I^2} & \frac{\partial^2 f}{\partial I \partial B_H} & \frac{\partial^2 f}{\partial I \partial B_L} \\ \\ \frac{\partial^2 f}{\partial I \partial B_H} & \frac{\partial^2 f}{\partial B_H^2} & \frac{\partial^2 f}{\partial B_H \partial B_L} \\ \\ \frac{\partial^2 f}{\partial I \partial B_L} & \frac{\partial^2 f}{\partial B_H \partial B_L} & \frac{\partial^2 f}{\partial B_L^2} \end{bmatrix} \begin{bmatrix} 1 \\ \\ g'_H \\ \\ g'_L \end{bmatrix} + \left[ \frac{\partial f}{\partial B_H}, \frac{\partial f}{\partial B_L} \right] \begin{bmatrix} g''_H \\ \\ g''_L \end{bmatrix} \end{aligned}$$

*which matches equation (4.4.7).*

## IV.5 Stability of the endemic equilibrium

### IV.5.1 Local stability

Now that we have established the existence of the unique positive endemic equilibrium $X^*$, we proceed to show $X^*$ is locally asymptotically stable.

The Jacobian matrix of the model system (4.1.1)-(4.1.4) is

$$J_B = \begin{bmatrix} -b - f(I,B) & -S\frac{\partial f}{\partial I}(I,B) & 0 & -S\frac{\partial f}{\partial B}(I,B) \\ \\ f(I,B) & S\frac{\partial f}{\partial I}(I,B) - (\gamma + b) & 0 & S\frac{\partial f}{\partial B}(I,B) \\ \\ 0 & \gamma & -b & 0 \\ \\ 0 & \frac{\partial h}{\partial I}(I,B) & 0 & \frac{\partial h}{\partial B}(I,B) \end{bmatrix}. \qquad (4.5.1)$$

At the endemic equilibrium $X^* = (S^*, I^*, R^*, B^*)$, the components satisfy

$$I^* = \frac{1}{(\gamma+b)}\frac{bNf(I^*,B^*)}{b+f(I^*,B^*)}, \tag{4.5.2}$$

$$S^* = \frac{bN}{b+f(I^*,B^*)}, \tag{4.5.3}$$

$$R^* = \frac{\gamma}{b}I^*, \tag{4.5.4}$$

$$0 = h(I^*,B^*). \tag{4.5.5}$$

For the convenience of algebraic manipulation, we denote

$$F = f(I^*,B^*), \quad E = \frac{\partial f}{\partial I}(I^*,B^*), \quad P = \frac{\partial f}{\partial B}(I^*,B^*),$$

$$Q = \frac{\partial h}{\partial B}(I^*,B^*), \quad T = \frac{\partial h}{\partial I}(I^*,B^*).$$

From the assumptions (**b**) and (**c**), $F \geq 0,\ E \geq 0,\ P \geq 0,\ T \geq 0$, whereas $Q \leq 0$. Evaluated at $X^*$, the Jacobian matrix (4.5.1) becomes

$$J_B^* = \begin{bmatrix} -F-b & -S^*E & 0 & -S^*P \\ F & S^*E-(\gamma+b) & 0 & S^*P \\ 0 & \gamma & -b & 0 \\ 0 & T & 0 & Q \end{bmatrix}.$$

The characteristic polynomial of $J_B^*$ is

$$\begin{aligned} \mathrm{Det}\,(\lambda I - J_B^*) &= (\lambda+b)\big[(\lambda+b)(\lambda-S^*E+\gamma+b)(\lambda-Q) \\ &\quad +F(\lambda+\gamma+b)(\lambda-Q)-(\lambda+b)S^*PT\big]. \end{aligned}$$

The equilibrium $X^*$ is locally asymptotically stable if and only if all roots of the above polynomial have negative real parts. Obviously $\lambda = -b$ is a negative root. To investigate the other three roots, we expand the expression in the square brackets to obtain a cubic equation

$$a_0\lambda^3 + a_1\lambda^2 + a_2\lambda^1 + a_3 = 0 \tag{4.5.6}$$

with

$$\begin{aligned} a_0 &= 1, && (4.5.7)\\ a_1 &= F - Q + 2b + \gamma - ES^*, && (4.5.8)\\ a_2 &= b^2 - FQ + Fb + F\gamma - 2Qb - Q\gamma + b\gamma && (4.5.9)\\ &\quad +EQS^* - PS^*T - ES^*b, \\ a_3 &= -Qb^2 - FQb - FQ\gamma - Qb\gamma + EQS^*b - PS^*Tb. && (4.5.10) \end{aligned}$$

To ensure that all roots of equation (4.5.6) have negative real parts, the Routh-Hurwitz stability criterion requires

$$a_1 > 0\,, \qquad a_2 > 0\,, \qquad a_3 > 0\,, \qquad a_1 a_2 > a_0 a_3. \tag{4.5.11}$$

We shall prove all the four inequalities in (4.5.11). To that end we first establish the following lemma:

**Lemma 8.** *At the endemic equilibrium $X^*$, we have*

$$\begin{aligned} b + \gamma - ES^* &\geq 0, && (4.5.12)\\ -Q(b+\gamma) &\geq PTS^* - EQS^*. && (4.5.13) \end{aligned}$$

*Proof.* Based on our assumption (**d**), we have known that the inequality (4.3.4) holds at any given point $(I_0,\, B_0) \geq 0$. In particular, if we set $(I_0,\, B_0) = (I^*,\, B^*)$, i.e., the positive endemic equilibrium, we obtain

$$f(I,B) \leq f(I^*,B^*) + \frac{\partial f}{\partial I}(I^*,B^*)(I - I^*) + \frac{\partial f}{\partial B}(I^*,B^*)(B - B^*) \tag{4.5.14}$$

which holds for all $(I,\, B) \geq 0$. Substitute $B = B^*$, $I = 0$ and (4.5.14) becomes

$$0 \leq f(0,\, B^*) \leq f(I^*,\, B^*) - \frac{\partial f}{\partial I}(I^*,\, B^*)\, I^*. \tag{4.5.15}$$

Using equations (4.5.2)(4.5.3) and inequality (4.5.15), we obtain

$$\begin{aligned} b + \gamma - ES^* &= (b+\gamma) - \frac{\partial f}{\partial I}(I^*,B^*)S^* \\ &= \frac{bNf(I^*,B^*)}{[b + f(I^*,B^*)]I^*} - \frac{\partial f}{\partial I}(I^*,B^*)\frac{bN}{b + f(I^*,B^*)} \\ &= \frac{bN}{[b + f(I^*,B^*)]I^*}\Big[ f(I^*,B^*) - \frac{\partial f}{\partial I}(I^*,B^*)I^* \Big] \\ &\geq 0 && (4.5.16) \end{aligned}$$

which establishes the result in (4.5.12).

Next, based on the assumption (**e**), the function $h(I, B)$ is concave at the point $(I^*, B^*)$. Thus

$$h(I,B) \leq h(I^*,B^*) + \frac{\partial h}{\partial I}(I^*,B^*)(I-I^*) + \frac{\partial h}{\partial B}(I^*,B^*)(B-B^*). \quad (4.5.17)$$

Note that $h(I^*, B^*) = 0$, $h(0, 0) = 0$. Substitute $I = B = 0$ into equation (4.5.17) to obtain

$$\frac{\partial h}{\partial I}(I^*,B^*)I^* + \frac{\partial h}{\partial B}(I^*,B^*)B^* \leq 0. \quad (4.5.18)$$

Since $\frac{\partial h}{\partial B}(I^*, B^*) \leq 0$ due to the assumption (**c**), the inequality (4.5.18) yields

$$\overline{B} \triangleq B^* + \frac{\frac{\partial h}{\partial I}(I^*,B^*)}{\frac{\partial h}{\partial B}(I^*,B^*)} I^* \geq 0. \quad (4.5.19)$$

Now, substitute the point $(I, B) = \left(0, \overline{B}\right)$, which is in the biologically feasible domain of our model, into the inequality (4.5.14) to obtain

$$0 \leq f(0,\overline{B}) \leq f(I^*,B^*) - \frac{\partial f}{\partial I}(I^*,B^*)I^* + \frac{\partial f}{\partial B}(I^*,B^*)\frac{\frac{\partial h}{\partial I}(I^*,B^*)}{\frac{\partial h}{\partial B}(I^*,B^*)} I^*. \quad (4.5.20)$$

Combining the inequality (4.5.20) and the facts: $S^* f(I^*, B^*) = (\gamma + b)I^*$, $\frac{\partial h}{\partial B}(I^*, B^*) \leq 0$, we obtain

$$\begin{aligned} -Q(b+\gamma) &= -\frac{\partial h}{\partial B}(I^*,B^*)(b+\gamma) \\ &\geq \frac{\partial f}{\partial B}(I^*,B^*)\frac{\partial h}{\partial I}(I^*,B^*)S^* - \frac{\partial f}{\partial I}(I^*,B^*)\frac{\partial h}{\partial B}(I^*,B^*)S^* \\ &= PTS^* - EQS^*, \end{aligned} \quad (4.5.21)$$

which establishes the result in (4.5.13). □

Based on Lemma 8, we are now ready to proceed to (4.5.11).

**Lemma 9.** *At the endemic equilibrium $X^*$, all the four inequalities in (4.5.11) hold.*

*Proof.* First, using the inequality (4.5.12), we obtain

$$\begin{aligned} a_1 &= F - Q + 2b + \gamma - ES^* \\ &= f(I^*,B^*) - \frac{\partial h}{\partial B}(I^*,B^*) + 2b + \gamma - \frac{\partial f}{\partial I}(I^*,B^*)S^* \\ &> (b+\gamma) - \frac{\partial f}{\partial I}(I^*,B^*)S^* \\ &> 0. \end{aligned} \quad (4.5.22)$$

Next, using both results in (4.5.12) and (4.5.13), we obtain

$$\begin{aligned} a_2 &= b^2 - FQ + Fb + F\gamma - 2Qb - Q\gamma + b\gamma + EQS^* - PS^*T - ES^*b \\ &= b(b + \gamma - ES^*) + (-Qb - Q\gamma - PS^*T + EQS^*) + (Fb + F\gamma - FQ - Qb) \\ &> 0. \end{aligned} \tag{4.5.23}$$

Similarly, we have

$$\begin{aligned} a_3 &= -Qb^2 - FQb - FQ\gamma - Qb\gamma + EQS^*b - PS^*Tb \\ &= b(-Qb - Q\gamma + EQS^* - PS^*T) + (-FQb - FQ\gamma) \\ &> 0. \end{aligned} \tag{4.5.24}$$

Finally, note that $a_1 = F - Q + 2b + \gamma - ES^* > -Q > 0$ and that

$$(-Q)a_2 - a_0a_3 = \left(Q^2b + Q^2\gamma - EQ^2S^* + PTQS^*\right) + (FQ^2 + Q^2b + PS^*Tb) > 0. \tag{4.5.25}$$

It is thus clear to see $a_1a_2 > a_0a_3$ holds. □

Therefore, based on the Routh-Hurwitz stability criterion, we have established the following result:

**Theorem 13.** *When $R_0 > 1$, the endemic equilibrium of system (4.1.1)-(4.1.4) is locally asymptotically stable.*

### IV.5.2 Bifurcation diagram

Our stability analysis of the DFE and the endemic equilibrium shows a forward bifurcation with respect to the parameter $R_0$. The results are summarized by the following theorem:

**Theorem 14.** *Under the assumptions* (**a**)-(**e**), *the model system (4.1.1)-(4.1.4) has a forward transcritical bifurcation at $R_0 = 1$.*

**Remark 7.** *Theorem 14 states that for biologically feasible incidence and pathogen functions, our cholera model does not exhibit backward (or subcritical) bifurcation [10; 15; 68; 72] and the endemic level is continuously depending on $R_0$. A value of $R_0$ slightly above one will, regarding long-term dynamics, only lead to a low endemic*

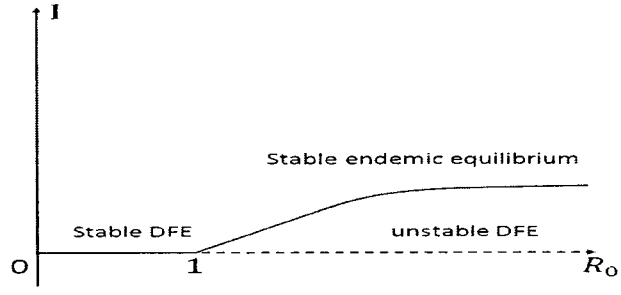


Figure 4.2: The bifurcation diagram of $I$ vs. $R_0$ which shows a transcritical bifurcation at $R_0 = 1$.

*state. This has important implication on the prevention and intervention strategies for cholera, as reducing, and keeping, $R_0$ below one would be sufficient to eradicate the disease in the long run.*

A bifurcation diagram for $I$ vs. $R_0$ is sketched in Figure 4.2. At the DFE, $I = 0$ is stable for $R_0 < 1$ and unstable for $R_0 > 1$. At the endemic equilibrium,

$$I = \tilde{H}(I) = \tilde{H}(0) + \tilde{H}'(0)I + Q(I) \tag{4.5.26}$$

where $\tilde{H}(I)$ is defined in equation (4.4.2) and where

$$Q(I) = \sum_{m=2}^{\infty} \frac{\tilde{H}^m(0)}{m!} I^m. \tag{4.5.27}$$

Since $\tilde{H}(0) = 0$, $\tilde{H}'(0) = R_0$, we obtain

$$I = R_0 I + Q(I), \qquad \text{or} \qquad R_0 = 1 - \frac{Q(I)}{I}. \tag{4.5.28}$$

Based on equation (4.5.28), when $I$ is small, $R_0 \approx 1 - \frac{\tilde{H}''(0)}{2} I$ (notice $\tilde{H}''(0) \leq 0$), which is approximately a straight line passing the bifurcation point $(R_0, I) = (1, 0)$. When $I \to \infty$, $\frac{dR_0}{dI} \to \infty$ so that the endemic equilibrium curve becomes more and more horizontal.

## IV.6 Examples

Our generalized model (4.1.1)-(4.1.4) can unify many existing cholera models (e.g., [11; 20; 22; 60; 65]), so that these different models can be studied and applied

through a single unified framework. Below we briefly discuss three representative models. (These three models we discussed a lot in the chapter III.)

**The model of Codeco [11]**

Codeco's model [11] consists of the following ordinary differential equations:

$$\frac{dS}{dt} = n(H-S) - a\frac{B}{\kappa+B}S, \tag{4.6.1}$$

$$\frac{dI}{dt} = a\frac{B}{\kappa+B}S - rI, \tag{4.6.2}$$

$$\frac{dB}{dt} = eI - (mb-nb)B. \tag{4.6.3}$$

The parameter $n$ denotes the natural human birth/death rate, $a$ the rate of exposure to contaminated water, $\kappa$ the concentration of *V. cholerae* in water that yields 50% chance of catching cholera, $r$ the recovery rate, $nb/mb$ the growth/loss rate of *V. cholerae* in the aquatic environment, $e$ the rate of each infected person contributing to the population of *V. cholerae* in the aquatic environment. In this model, the incidence is $f(I,B) = a\frac{B}{\kappa+B}$ and the pathogen function is $h(I,B) = eI-(mb-nb)B$. Only the environment-to-human transmission mode is considered in this formulation.

It can be easily verified that the assumptions (**a**)-(**e**) all hold for the system (4.6.1-4.6.3). Hence, all the analytical results presented so far can be applied to this model. In particular, the basic reproduction number $R_0$ is determined by equation (4.2.4):

$$\begin{aligned} R_0 &= \frac{N}{\gamma+b}\Big[\frac{\partial f}{\partial I}(0,0) + \frac{\partial f}{\partial B}(0,0)\,g'(0)\Big] \\ &= \frac{Nae}{\kappa(\gamma+b)(mb-nb)}, \end{aligned} \tag{4.6.4}$$

which agrees with the result obtained in [11].

**The model of Mukandavire *et al.* [60]**

This model has been discussed and the model is given by (3.1.19-3.1.19). The incidence is $f(I,B) = \beta_e\frac{B}{\kappa+B}+\beta_h I$, and $h(I,B) = \xi I-\delta B$. Both environment-to-human

and human-to-human transmission modes are included in this model. It is straightforward to verify the assumptions (**a**)-(**e**); in particular,

$$D^2 f = \begin{bmatrix} 0 & 0 \\ 0 & \frac{-2\kappa\beta_e}{(\kappa+B)^3} \end{bmatrix} \quad \text{and} \quad D^2 h = \begin{bmatrix} 0 & 0 \\ 0 & 0 \end{bmatrix}$$

are both negative semidefinite for all $I,\ B \geq 0$. Based on equation (4.2.4), the basic reproduction number is

$$R_0 \ = \ \frac{N}{\gamma + b}\Big[\beta_h + \frac{\beta_e}{\kappa}\frac{\xi}{\delta}\Big] \ = \ \frac{N}{\delta\kappa(\gamma+b)}\big(\kappa\delta\beta_h + \xi\beta_e\big).$$

The same result was obtained in (3.1.24).

**The model of Hartley** *et al.* **[22]**

The model is given in equations (3.1.1-3.1.5).

Here $B = [B_H,\ B_L]$, $f(I,B) = \beta_L\frac{B_L}{\kappa_L+B_L} + \beta_H S\frac{B_H}{\kappa_H+B_H}$,

and $h(I,B) = \begin{bmatrix} \xi I - \chi B_H \\ \chi B_H - \delta_L B_L \end{bmatrix}$.

The assumptions (**a**)-(**e**) can be similarly verified. For instance,

$$\frac{\partial f}{\partial B} = \Big[\frac{\beta_H\kappa_H}{(\kappa_H+B_H)^2},\ \frac{\beta_L\kappa_L}{(\kappa_L+B_L)^2}\Big] > 0,$$

and

$$\frac{\partial h}{\partial B} = \begin{bmatrix} -\chi & 0 \\ \chi & -\delta_L \end{bmatrix} < 0 \quad \text{(negative definite)}.$$

Meanwhile,

$$D^2 f = \begin{bmatrix} 0 & 0 & 0 \\ 0 & \frac{-2\beta_H\kappa_H}{(\kappa_H+B_H)^3} & 0 \\ 0 & 0 & \frac{-2\beta_L\kappa_L}{(\kappa_L+B_L)^3} \end{bmatrix},$$

and $D^2 h = 0$ are both negative semidefinite for all $I \geq 0,\ B \geq 0$. The basic

reproduction number for this model is

$$\begin{aligned} R_0 &= \frac{N}{\gamma+b}\Big[\frac{\partial f}{\partial I}(0,0)+\frac{\partial f}{\partial B}(0,0)\,g'(0)\Big] \\ &= \frac{N}{\gamma+b}\Big[0+\Big(\frac{\beta_H}{\kappa_H},\ \frac{\beta_L}{\kappa_L}\Big)\begin{pmatrix}\xi/\chi\\ \\ \xi/\delta_L\end{pmatrix}\Big] \\ &= \frac{N\xi}{\gamma+b}\Big(\frac{\beta_H}{\kappa_H\chi}+\frac{\beta_L}{\kappa_L\delta_L}\Big), \end{aligned}$$

which exactly matches the result given in (3.1.17).

A quantitative comparison of these three models is made by applying each of them to study the epidemic and endemic cholera dynamics in a hypothetical community with a total population of $N = 10,000$. The initial condition is set as $I(0) = 1$, $S(0) = N - 1$, $R = B = 0$; i.e., one infective initially enters the wholly susceptible community. The parameter values are based on the published cholera data in Zimbabwe [54; 60; 84; 85; 86]. Figure 4.3 shows the simulation results of the infection curves for the three models. The first peak in each curve represents the cholera outbreak triggered by the initial infection. Among the three, the model of Hartley *et al.* shows the highest infection number due to its explicit incorporation of the hyper-infectious state of the vibrios, whereas the model of Codeco exhibits the lowest epidemic value since it only considered the environment-to-human transmission pathway with a less-infectious state of the pathogen. After the first cholera peak, all the three infection curves decline and show several outbreaks with decaying magnitudes, before they finally rest at their endemic equilibria. The model of Mukandavire *et al.* exhibits a few more epidemic oscillations than the other two models due to its explicit inclusion of both the environment-to-human and human-to-human transmission modes which lead to longer epidemic dynamics. We found the endemic infection equilibria are $I^* \doteq 0.88,\ 0.75,\ 0.92$ for the model of Codeco, that of Mukandavire *et al.*, and that of Hartley *et al.*, respectively, implying relatively low endemicity. If we scale up these numbers using the realistic population size in Zimbabwe (about 12 million), we obtain that the endemic infection numbers would be about 1056, 900, and 1104, respectively, based on these models predictions.

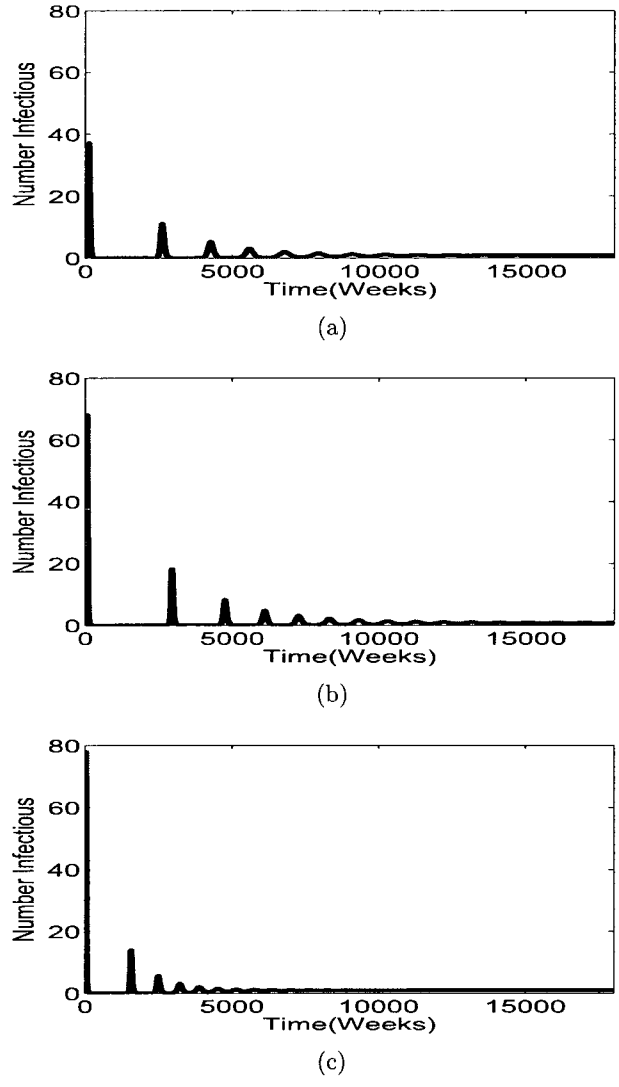


Figure 4.3: Simulation results for a hypothetical community with a total population of $N = 10,000$, using three different cholera models: (a) the model of Codeco [11]; (b) the model of Mukandavire *et al.* [60]; and (c) the model of Hartley *et al.* [22]. The initial condition is $I(0) = 1$, $S(0) = N - 1$, $R = B = 0$. After the major cholera outbreak (i.e., the first peak) caused by the initial infection, each infection curve exhibits several small-scale epidemic oscillations and finally converges to the endemic equilibrium over time. The endemic values are $I^* \doteq 0.88,\ 0.75,\ 0.92$ for the three models, respectively.

# CHAPTER V

# GLOBAL ENDEMIC STABILITY

## V.1 Global stability in two simplified cases

To prove the global asymptotic stability of the endemic equilibrium, the key is to show the non-existence of periodic orbits. This is generally difficult for high-dimensional model systems, as the classical Poincaré-Bendixson framework [21] is no longer valid in high dimensions. For some special cases, however, our general model (4.1.1)-(4.1.4) can be reduced to a two-dimensional autonomous system in $S$ and $I$, and classical dynamical system theory can be applied. We present two simple examples below.

First, we assume that the incidence $f(I, B) = C$, where $C > 0$ is a constant. Our model is then reduced to a two-dimensional linear system

$$\frac{dS}{dt} = bN - (C + b)S, \tag{5.1.1}$$

$$\frac{dI}{dt} = CS - (\gamma + b)I. \tag{5.1.2}$$

In such a case, our assumption (**a**) is not valid so that there is no disease-free equilibrium. The epidemiological implication is that the pathogen concentrations and/or the infected numbers are at such a high level that the infection is certain to those exposed. There is a unique positive endemic equilibrium of the system (5.1.1)(5.1.2):

$$S^* = \frac{bN}{C + b} \qquad \text{and} \qquad I^* = \frac{bCN}{(C + b)(\gamma + b)}. \tag{5.1.3}$$

It is straightforward to observe that

$$\frac{\partial}{\partial S}\big(bN - (C + b)S\big) + \frac{\partial}{\partial I}\big(CS - (\gamma + b)I\big) = -(\gamma + 2b + C) < 0$$

holds everywhere in the region

$$D = \{(S, I) \,|\, S > 0,\ I > 0,\ S + I < N\}, \tag{5.1.4}$$

so that no periodic orbit can exist based on Theorem 2 (with $B = 1$).

Indeed, since the system (5.1.1-5.1.2) is linear, its exact solution can be easily

found as

$$\begin{aligned} S(t) &= \frac{bN}{C+b} + \Big(S(0) - \frac{bN}{C+b}\Big)\, e^{-(C+b)t}, \\ I(t) &= \frac{bCN}{(C+b)(\gamma+b)} + k_1\, e^{-(C+b)t} + k_2\, e^{-(\gamma+b)t}, \end{aligned}$$

with

$$k_1 = \frac{C}{\gamma - C}\big(S(0) - \frac{bN}{C+b}\big), \qquad k_2 = I(0) - \frac{bCN}{(C+b)(\gamma+b)} - \frac{C}{\gamma - C}\big(S(0) - \frac{bN}{C+b}\big).$$

It is clear to see that $S(t) \to S^*$ and $I \to I^*$ as $t \to \infty$, regardless of the initial values of $S$ and $I$. Hence, the endemic equilibrium $(S^*,\ I^*)$ is globally asymptotically stable.

In the second case, we assume $f(I,\, B) = CI$, where $C > 0$ is a constant. The original system (4.1.1)-(4.1.4) is then reduced to

$$\frac{dS}{dt} = b(N - S) - CIS, \tag{5.1.5}$$

$$\frac{dI}{dt} = CIS - (\gamma + b)I, \tag{5.1.6}$$

which represents a regular SI model with a normal bilinear incidence. The endemic equilibrium of this simplified model is

$$(S^*,\ I^*) = \big(\frac{\gamma + b}{C},\ \frac{bN}{\gamma + b} - \frac{b}{C}\big). \tag{5.1.7}$$

Applying Theorem 2 and setting $P(S, I) = 1/I$ , we obtain

$$\frac{\partial}{\partial S}(PF_1) + \frac{\partial}{\partial I}(PF_2) = -(C + \frac{b}{I}) < 0$$

holds everywhere in $D$. Hence, there is no periodic solution and the endemic equilibrium $(S^*,\ I^*)$ is globally asymptotically stable.

## V.2 A combined model

Let us consider a combined human-environment epidemiological model with an environmental component, denoted by $B$, incorporated into an SIR system. We will

denoted such a model by SIR-B. Specifically, we study a system of differential equations in the following form:

$$\frac{dS}{dt} = \mu - \beta_1 S\frac{B}{1+\alpha_1 B} - \beta_2 S\frac{I}{1+\alpha_2 I} - \mu S, \tag{5.2.1}$$

$$\frac{dI}{dt} = \beta_1 S\frac{B}{1+\alpha_1 B} + \beta_2 S\frac{I}{1+\alpha_2 I} - (\gamma+\mu)I, \tag{5.2.2}$$

$$\frac{dB}{dt} = \xi I - \delta B, \tag{5.2.3}$$

together with the equation for R:

$$\frac{dR}{dt} = \gamma I - \mu R. \tag{5.2.4}$$

Here the total population $S + I + R = 1$ is assumed to be fixed. The environmental component B refers to the population density or concentration of the pathogen. We note that equation (5.2.4) is not needed in the model analysis, and equations (5.2.1-5.2.3) constitute a three-dimensional autonomous system.

In this system, the parameter $\mu$ denotes the natural human birth or death rate, $\gamma$ denotes the rate of recovery from the disease, $\xi$ represents the rate of human contribution to the growth of the pathogen, and $\delta$ represents the net death rate of the pathogen in the environment. The coefficients $\beta_1$ and $\beta_2$ represent the contact rates for the human-environment and human-human interactions, respectively. If $\beta_1 = 0$, then direct environment-to-human transmission mode is not present and the model is reduced to a regular SIR form; i.e., $B$ is separated. If, instead, $\beta_2 = 0$, then direct human-to-human transmission pathway is eliminated, though the model is still a coupled system with both human and environmental components. Finally, the constants $\alpha_1$ and $\alpha_2$ adjust the appropriate form of the incidence which determines the rate of new infection. If $\alpha_2 = 0$, the corresponding incidence is reduced to the standard bilinear form based on the mass action law, which is most common in epidemiological models. If $\alpha_2 > 0$, then the corresponding incidence represents a consequence of saturation effects: when the infected number is high, the incidence rate will respond more slowly than linearly to the increase in $I$. Similar meanings stand for $\alpha_1$. With differing values of $\alpha_1$, $\alpha_2$ and $\beta_1$, $\beta_2$, various forms of incidence rates can be represented in modeling those environment-originated diseases, particularly in the study of cholera. For example, Capasso and Serio [7] introduced an incidence rate in the form of $\frac{kSI}{1+\alpha I}$ (with human-to-human transmission mode only) in modeling the cholera outbreak in the Mediterranean in 1973 [7; 8]. Codeco [11]

proposed an incidence form of $\frac{aSB}{\kappa+B}$ (with environment-to-human transmission mode only). In addition, Mukandavire et al. [60] included both transmission pathways in the form of $\beta_e \frac{SB}{\kappa+B} + \beta_h SI$.

A study of an epidemiological model more general than system (5.2.1-5.2.3) is performed in chapter IV, based on which the following result can be directly derived:

**Theorem 15.** *The basic reproduction number of the model (5.2.1-5.2.3) is*

$$R_0 = \frac{N}{\gamma+\mu}(\beta_2 + \beta_1 \frac{\xi}{\delta}). \tag{5.2.5}$$

*When $R_0 < 1$, there is a unique disease-free equilibrium (DFE) $X_0 = (1, 0, 0)$ which is both locally and globally asymptotically stable; when $R_0 > 1$, the DFE becomes unstable, and there is a unique positive endemic equilibrium $X^* = (S^*, I^*, B^*)$ which is locally asymptotically stable.*

The global stability of the endemic equilibrium, however, has not been resolved for the system (5.2.1-5.2.3). Below we will combine the method of Lyapunov functions and Volterra-Lyapunov stable matrices to answer this question.

The feasible domain of the model (5.2.1-5.2.3) is

$$\Delta = \{(S, I, B) \,|\, S \geq 0,\ I \geq 0,\ S + I \leq 1,\ B \geq 0\}.$$

It can be easily verified that $\Delta$ is positively invariant for this system.

Note that we do not need the domain to be bounded and convex, as required by the methods of monotone flows and geometric approach. We denote the interior of $\Delta$ by $\Delta^o$.

At the endemic equilibrium $X^* = (S^*, I^*, B^*)$, we have

$$\mu - \beta_1 S^* \frac{B^*}{1+\alpha_1 B^*} - \beta_2 S^* \frac{I^*}{1+\alpha_2 I^*} - \mu S^* = 0, \tag{5.2.6}$$

$$\beta_1 S^* \frac{B^*}{1+\alpha_1 B^*} + \beta_2 S^* \frac{I^*}{1+\alpha_2 I^*} - (\gamma+\mu) I^* = 0, \tag{5.2.7}$$

$$\xi I^* - \delta B^* = 0. \tag{5.2.8}$$

From equation (5.2.7-5.2.8), we can easily obtain

$$\begin{aligned} (\gamma+\mu)\delta &= \frac{\beta_1 S^* \xi}{1+\alpha_1 B^*} + \frac{\beta_2 S^* \delta}{1+\alpha_2 I^*} \\ &> \frac{\beta_1 S^* \xi}{(1+\alpha_1 B)(1+\alpha_1 B^*)} + \frac{\beta_2 S^* \delta}{(1+\alpha_2 I)(1+\alpha_2 I^*)}. \end{aligned} \tag{5.2.9}$$

Now we construct a Lyapunov function in the usual form of square sums:

$$V = w_1(S - S^*)^2 + w_2(I - I^*)^2 + w_3(B - B^*)^2, \tag{5.2.10}$$

where $w_1$, $w_2$ and $w_3$ are positive constants. Then

$$\frac{dV}{dt} = 2w_1(S - S^*)\frac{dS}{dt} + 2w_2(I - I^*)\frac{dI}{dt} + 2w_3(B - B^*)\frac{dB}{dt}. \tag{5.2.11}$$

Obviously, when $X = X^*$, $\frac{dV}{dt} = 0$. We aim to show that when $X \neq X^*$, $\frac{dV}{dt} < 0$ holds everywhere in $\Delta^o$.

Substituting equations (5.2.1-5.2.3) and (5.2.6-5.2.7) into (5.2.11), we obtain

$$\begin{aligned}
\frac{dV}{dt} &= 2w_1(S - S^*)[-\frac{\beta_1}{1 + \alpha_1 B}SB - \frac{\beta_2}{1 + \alpha_2 I}SI - \mu S + \frac{\beta_1}{1 + \alpha_1 B^*}S^*B^* \\
&\quad + \frac{\beta_2}{1 + \alpha_2 I^*}S^*I^* + \mu S^*] \\
&\quad + 2w_2(I - I^*)[\frac{\beta_1}{1 + \alpha_1 B}SB + \frac{\beta_2}{1 + \alpha_2 I}SI - (\gamma + \mu)I - \frac{\beta_1}{1 + \alpha_1 B^*}S^*B^* \\
&\quad - \frac{\beta_2}{1 + \alpha_2 I^*}S^*I^* + (\gamma + \mu)I^*] + 2w_3(B - B^*)[\xi I - \delta B - \xi I^* + \delta B^*].
\end{aligned}$$

To manipulate the algebra, we add (and then subtract) the expression $\frac{S^*B}{1+\alpha_1 B} + \frac{S^*I}{1+\alpha_2 B}$ into the first bracket, so that all those terms can be factored out. Similarly, we insert and compensate the same expression in the second bracket. As a result, we

obtain

$$\begin{aligned}
\frac{dV}{dt} &= 2w_1(S-S^*)\Big[-\beta_1(\frac{SB}{1+\alpha_1 B}-\frac{S^*B^*}{1+\alpha_1 B^*}-\frac{S^*B}{1+\alpha_1 B}+\frac{S^*B}{1+\alpha_1 B}) \\
&\quad -\beta_2(\frac{SI}{1+\alpha_2 I}-\frac{S^*I^*}{1+\alpha_2 I^*}-\frac{S^*I}{1+\alpha_2 I}+\frac{S^*I}{1+\alpha_2 I})-\mu(S-S^*)\Big] \\
&\quad +2w_2(I-I^*)\Big[\beta_1(\frac{SB}{1+\alpha_1 B}-\frac{S^*B^*}{1+\alpha_1 B^*}-\frac{S^*B}{1+\alpha_1 B}+\frac{S^*B}{1+\alpha_1 B}) \\
&\quad +\beta_2(\frac{SI}{1+\alpha_2 I}-\frac{S^*I^*}{1+\alpha_2 I^*}-\frac{S^*I}{1+\alpha_2 I}+\frac{S^*I}{1+\alpha_2 I})-(\gamma+\mu)(S-S^*)\Big] \\
&\quad +2w_3(B-B^*)[\xi(I-I^*)-\delta(B-B^*)] \\
&= -2w_1(\frac{\beta_1 B}{1+\alpha_1 B}+\frac{\beta_2 I}{1+\alpha_2 I}+\mu)(S-S^*)^2-2w_1\frac{\beta_2 S^*}{(1+\alpha_2 I)(1+\alpha_2 I^*)} \\
&\quad (S-S^*)(I-I^*)-2w_1\frac{\beta_1 S^*}{(1+\alpha_1 B)(1+\alpha_1 B^*)}(S-S^*)(B-B^*) \\
&\quad +2w_2(\frac{\beta_1 B}{1+\alpha_1 B}+\frac{\beta_2 I}{1+\alpha_2 I})(I-I^*)(S-S^*)+2w_2[\frac{\beta_2 S^*}{(1+\alpha_2 I)(1+\alpha_2 I^*)} \\
&\quad -(\gamma+\mu)](I-I^*)^2+2w_2\frac{\beta_1 S^*}{(1+\alpha_1 B)(1+\alpha_1 B^*)}(I-I^*)(B-B^*) \\
&\quad +2w_3\xi(I-I^*)(B-B^*)-2w_3\delta(B-B^*)^2 \\
&= Y(WA+A^TW^T)Y^T,
\end{aligned}$$

where $Y=[S-S^*,\ I-I^*,\ B-B^*]$, $W=diag(w_1,\ w_2,\ w_3)$, and

$$A=\begin{bmatrix}
-\frac{\beta_1 B}{1+\alpha_1 B}-\frac{\beta_2 I}{1+\alpha_2 I}-\mu & -\frac{\beta_2 S^*}{(1+\alpha_2 I)(1+\alpha_2 I^*)} & -\frac{\beta_1 S^*}{(1+\alpha_1 B)(1+\alpha_1 B^*)} \\
\frac{\beta_1 B}{1+\alpha_1 B}+\frac{\beta_2 I}{1+\alpha_2 I} & \frac{\beta_2 S^*}{(1+\alpha_2 I)(1+\alpha_2 I^*)}-(\gamma+\mu) & \frac{\beta_1 S^*}{(1+\alpha_1 B)(1+\alpha_1 B^*)} \\
0 & \xi & -\delta
\end{bmatrix}. \tag{5.2.12}$$

The global asymptotic stability of $X^*$ will be established if we can show the matrix A defined in equation (5.2.12) is Volterra-Lyapunov stable (see Definition 3) in $\Delta^o\backslash\{X^*\}$. To this end, we will make use of Lemma 3 and 5.

From the equation (5.2.12), we can obtain

$$A^{-1} = \frac{1}{detA}\begin{bmatrix} (\gamma+\mu)\delta - \frac{\beta_1 S^*\xi}{(1+\alpha_1 B)(1+\alpha_1 B^*)} & & \\ -\frac{\beta_2 S^*\delta}{(1+\alpha_2 I)(1+\alpha_2 I^*)} & -\frac{\beta_1 S^*\xi}{(1+\alpha_1 B)(1+\alpha_1 B^*)} - \frac{\beta_2 S^*\delta}{(1+\alpha_2 I)(1+\alpha_2 I^*)} & -\frac{\beta_1 S^*(\gamma+\mu)}{(1+\alpha_1 B)(1+\alpha_1 B^*)} \\ (\frac{\beta_1 B}{1+\alpha_1 B} + \frac{\beta_2 I}{1+\alpha_2 I})\delta & (\frac{\beta_1 B}{1+\alpha_1 B} + \frac{\beta_2 I}{1+\alpha_2 I} + \mu)\delta & \frac{\beta_1 S^*\mu}{(1+\alpha_1 B)(1+\alpha_1 B^*)} \\ (\frac{\beta_1 B}{1+\alpha_1 B} + \frac{\beta_2 I}{1+\alpha_2 I})\xi & (\frac{\beta_1 B}{1+\alpha_1 B} + \frac{\beta_2 I}{1+\alpha_2 I} + \mu)\xi & (\frac{\beta_1 B}{1+\alpha_1 B} + \frac{\beta_2 I}{1+\alpha_2 I} + \mu)(\gamma+\mu) \\ & & -\frac{\beta_2 S^*\delta}{(1+\alpha_2 I)(1+\alpha_2 I^*)} \end{bmatrix}$$

where

$$\begin{aligned} detA &= -\Big(\frac{\beta_1 B}{1+\alpha_1 B} + \frac{\beta_2 I}{1+\alpha_2 I} + \mu\Big)\Big[(\gamma+\mu)\delta - \frac{\beta_1 S^*\xi}{(1+\alpha_1 B)(1+\alpha_1 B^*)} \\ &\quad -\frac{\beta_2 S^*\delta}{(1+\alpha_2 I)(1+\alpha_2 I^*)}\Big] - \Big(\frac{\beta_1 B}{1+\alpha_1 B} + \frac{\beta_2 I}{1+\alpha_2 I}\Big) \\ &\quad \Big[\frac{\beta_1 S^*\xi}{(1+\alpha_1 B)(1+\alpha_1 B^*)} + \frac{\beta_2 S^*\delta}{(1+\alpha_2 I)(1+\alpha_2 I^*)}\Big]. \end{aligned}$$

Using the inequality (5.2.9), it is straightforward to see $det\, A < 0$. Now we prove the following lemma.

**Lemma 10.** *Let $D = -A$ and $E = (-A)^{-1}$, where $A$ is defined in equation (5.2.12). Then there exists a positive $2 \times 2$ diagonal matrix $\widetilde{W} = diag(w_1, w_2)$ such that $\widetilde{W}\widetilde{D} + (\widetilde{W}\widetilde{D})^T > 0$ and $\widetilde{W}\widetilde{E} + (\widetilde{W}\widetilde{E})^T > 0$.*

*Proof.* Using the inequality (5.2.9) and the fact $detA < 0$, we clearly see that the (1, 1), (2, 2) and (2, 1) entries of $A^{-1}$ are all negative, whereas its (1, 2) entry is positive. Based on Lemma 3, $\widetilde{A^{-1}}$ is Volterra-Lyapunov stable. Hence, there exists a $2\times 2$ positive diagonal matrix $\widetilde{W} = diag(w_1, w_2)$ such that $\widetilde{W}(\widetilde{A^{-1}}) + (\widetilde{A^{-1}})^T\widetilde{W}^T < 0$. Since $E = (-A)^{-1}$, we obtain $\widetilde{W}\widetilde{E} + (\widetilde{W}\widetilde{E})^T > 0$. Specifically, we have

$$\widetilde{W}\widetilde{E} + (\widetilde{W}\widetilde{E})^T = \frac{1}{-detA}Q,$$

where the $2 \times 2$ positive definite matrix Q is given by

$$Q = \begin{bmatrix} 2w_1[(\gamma+\mu)\delta - \frac{\beta_1 S^*\xi}{(1+\alpha_1 B)(1+\alpha_1 B^*)} - \frac{\beta_2 S^*\delta}{(1+\alpha_2 I)(1+\alpha_2 I^*)}] & w_2\delta(\frac{\beta_1 B}{1+\alpha_1 B} + \frac{\beta_2 I}{1+\alpha_2 I}) - \\ & w_1[\frac{\beta_1 S^*\xi}{(1+\alpha_1 B)(1+\alpha_1 B^*)} + \frac{\beta_2 S^*\delta}{(1+\alpha_2 I)(1+\alpha_2 I^*)}] \\ w_2\delta(\frac{\beta_1 B}{1+\alpha_1 B} + \frac{\beta_2 I}{1+\alpha_2 I}) - & \\ w_1[\frac{\beta_1 S^*\xi}{(1+\alpha_1 B)(1+\alpha_1 B^*)} + \frac{\beta_2 S^*\delta}{(1+\alpha_2 I)(1+\alpha_2 I^*)}] & 2w_2\delta(\frac{\beta_1 B}{1+\alpha_1 B} + \frac{\beta_2 I}{1+\alpha_2 I} + \mu) \end{bmatrix}$$

Meanwhile, we have

$$\widetilde{W}\widetilde{D} + (\widetilde{W}\widetilde{D})^T = P,$$

where the $2 \times 2$ matrix P is given by

$$P = \begin{bmatrix} 2w_1(\frac{\beta_1 B}{1+\alpha_1 B} + \frac{\beta_2 I}{1+\alpha_2 I} + \mu) & w_1 \frac{\beta_2 S^*}{(1+\alpha_2 I)(1+\alpha_2 I^*)} - w_2(\frac{\beta_1 B}{1+\alpha_1 B} + \frac{\beta_2 I}{1+\alpha_2 I}) \\ w_1 \frac{\beta_2 S^*}{(1+\alpha_2 I)(1+\alpha_2 I^*)} - w_2(\frac{\beta_1 B}{1+\alpha_1 B} + \frac{\beta_2 I}{1+\alpha_2 I}) & 2w_2[(\gamma+\mu) - \frac{\beta_2 S^*}{(1+\alpha_2 I)(1+\alpha_2 I^*)}] \end{bmatrix}.$$

Below we show $P > 0$. In fact, since $Q > 0$, we have $\det Q > 0$. Specifically,

$$\begin{aligned} det\, Q &= \delta^2 \Big\{ 4w_1 w_2(\gamma+\mu)[\frac{\beta_2 S^*}{(1+\alpha_2 I)(1+\alpha_2 I^*)} + \mu] \\ &- 2w_1 w_2(\frac{\beta_1 B}{1+\alpha_1 B} + \frac{\beta_2 I}{1+\alpha_2 I})\frac{\beta_2 S^*}{(1+\alpha_2 I)(1+\alpha_2 I^*)} - 4w_1 w_2 \frac{\beta_2 S^* \mu}{(1+\alpha_2 I)(1+\alpha_2 I^*)} \\ &- w_1^2[\frac{\beta_2 S^*}{(1+\alpha_2 I)(1+\alpha_2 I^*)}]^2 - w_2^2(\frac{\beta_1 B}{1+\alpha_1 B} + \frac{\beta_2 I}{1+\alpha_2 I})^2 \Big\} \\ &- \Big\{ 2w_1 w_2 \delta(\frac{\beta_1 B}{1+\alpha_1 B} + \frac{\beta_2 I}{1+\alpha_2 I})\frac{\beta_1 S^* \xi}{(1+\alpha_1 B)(1+\alpha_1 B^*)} + 4w_1 w_2 \delta\mu \frac{\beta_1 S^* \xi}{(1+\alpha_1 B)(1+\alpha_1 B^*)} \\ &+ w_1^2[\frac{\beta_1 S^* \xi}{(1+\alpha_1 B)(1+\alpha_1 B^*)}]^2 + 2w_1^2 \frac{\beta_1 S^* \xi}{(1+\alpha_1 B)(1+\alpha_1 B^*)} \frac{\beta_2 S^* \delta}{(1+\alpha_2 I)(1+\alpha_2 I^*)} \Big\} \\ &= \delta^2 (det\, P) - T, \end{aligned}$$

where $T$ is obviously positive, and where

$$\begin{aligned} det\, P &= 4w_1 w_2(\gamma+\mu)(\frac{\beta_2 S^*}{(1+\alpha_2 I)(1+\alpha_2 I^*)} + \mu) \\ &- 2w_1 w_2(\frac{\beta_1 B}{1+\alpha_1 B} + \frac{\beta_2 I}{1+\alpha_2 I})\frac{\beta_2 S^*}{(1+\alpha_2 I)(1+\alpha_2 I^*)} - 4w_1 w_2 \frac{\beta_2 S^* \mu}{(1+\alpha_2 I)(1+\alpha_2 I^*)} \\ &- w_1^2[\frac{\beta_2 S^*}{(1+\alpha_2 I)(1+\alpha_2 I^*)}]^2 - w_2^2(\frac{\beta_1 B}{1+\alpha_1 B} + \frac{\beta_2 I}{1+\alpha_2 I})^2. \end{aligned}$$

Hence, the fact $\det Q > 0$ clearly indicates $\det P > 0$. Note also that the $(1,1)$ entry of $P$ is positive. We thus obtain $P > 0$. □

**Lemma 11.** *The matrix A defined in equation (5.2.12) is Volterra-Lyapunov stable.*

*Proof.* Based on Lemmas 5 and 10, there exists a positive $3 \times 3$ diagonal matrix W such that $W(-A) + (-A)^T W^T > 0$. Therefore, $WA + A^T W^T < 0$. □

Thus we have established the following theorem:

**Theorem 16.** *When $R_0 > 1$, the endemic equilibrium of system (5.2.1-5.2.3) is globally asymptotically stable in $\Delta^o$.*

**Theorem 17.** *The endemic equilibrium $X^*$ of Mukandavire's Model (3.1.19-3.1.22) is globally asymptotically stable when $R_0 > 1$.*

## V.3 Hartley's Model

The model (5.2.1-5.2.3) is a three-dimensional system. We now consider a modification of the model (5.2.1-5.2.3) to allow the environmental component $B$ to be a vector. A representative example is the model proposed by Hartley *et al.* [22], presented in (3.1.1-3.1.5). In this section, we will focus our attention on the model of Hartley *et al.* [22] to illustrate the global stability analysis in four-dimensional systems. Similar to Theorem 15, the following theorem summarizes the dynamics already known for system (3.1.1-3.1.5).

**Theorem 18.** *(see chapter III) The basic reproduction number of the model (3.1.1-3.1.5) is*

$$R_0 = \frac{N\xi}{\gamma + b}\Big(\frac{\beta_H}{\kappa_H \chi} + \frac{\beta_L}{\kappa_L \delta_L}\Big). \tag{5.3.1}$$

*When $R_0 < 1$, there is a unique disease-free equilibrium (DFE) $X_0 = (1, 0, 0)$ which is both locally and globally asymptotically stable; when $R_0 > 1$ , the DFE becomes unstable, and there is a unique positive endemic equilibrium $X^* = (S^*, I^*, B^*)$ which is locally asymptotically stable.*

Below we will concentrate on the global stability analysis of the endemic equilibrium. It can be easily seen that the following feasible domain is positively invariant for system (3.1.1-3.1.5):

$$\Delta = \{(S, I, B) \,|\, S \geq 0, I \geq 0, S + I \leq 1, B_H \geq 0, B_L \geq 0\}.$$

At the endemic equilibrium $X^* = (S^*, I^*, B^*)$, we have

$$b - \beta_L S^* \frac{B_L^*}{\kappa_L + B_L^*} - \beta_H S^* \frac{B_H^*}{\kappa_H + B_H^*} - bS^* = 0, \tag{5.3.2}$$

$$\beta_L S^* \frac{B_L^*}{\kappa_L + B_L^*} + \beta_H S^* \frac{B_H^*}{\kappa_H + B_H^*} - (\gamma + b)I^* = 0, \tag{5.3.3}$$

$$\xi I^* - \chi B_H^* = 0, \tag{5.3.4}$$

$$\chi B_H^* - \delta_L B_L^* = 0, \tag{5.3.5}$$

from which we can obtain

$$(\gamma + b)\chi\delta_L = \frac{\beta_L S^* \xi\chi}{\kappa_L + B_L^*} + \frac{\beta_H S^* \xi\delta_L}{\kappa_H + B_H^*} > \frac{\xi\delta_L}{P} + \frac{\xi\chi}{Q}, \tag{5.3.6}$$

where P and Q are defined by

$$\frac{\beta_H S^* \kappa_H}{(\kappa_H + B_H^*)(\kappa_H + B_H)} = \frac{1}{P}, \qquad \frac{\beta_L S^* \kappa_L}{(\kappa_L + B_L^*)(\kappa_L + B_L)} = \frac{1}{Q}.$$

Now we construct the following Lyapunov function:

$$V = w_1(S - S^*)^2 + w_2(I - I^*)^2 + w_3(B_H - B_H^*)^2 + w_4(B_L - B_L^*)^2, \tag{5.3.7}$$

with positive constants $w_1$ , $w_2$ , $w_3$ and $w_4$. Performing similar algebra as before,

we obtain

$$
\begin{aligned}
\frac{dV}{dt} &= 2w_1(S-S^*)\frac{dS}{dt} + 2w_2(I-I^*)\frac{dI}{dt} + 2w_3(B_H-B_H^*)\frac{dB_H}{dt} + 2w_4(B_L-B_L^*)\frac{dB_L}{dt} \\
&= 2w_1(S-S^*)[-\beta_L(\frac{SB_L}{\kappa_L+B_L} - \frac{S^*B_L^*}{\kappa_L+B_L^*} - \frac{S^*B_L}{\kappa_L+B_L} + \frac{S^*B_L}{\kappa_L+B_L}) \\
&\quad -\beta_H[\frac{SB_H}{\kappa_H+B_H} - \frac{S^*B_H^*}{\kappa_H+B_H^*} - \frac{S^*B_H}{\kappa_H+B_H} + \frac{S^*B_H}{\kappa_H+B_H}) - b(S-S^*)] \\
&\quad +2w_2(I-I^*)[\beta_L(\frac{SB_L}{\kappa_L+B_L} - \frac{S^*B_L^*}{\kappa_L+B_L^*} - \frac{S^*B_L}{\kappa_L+B_L} + \frac{S^*B_L}{\kappa_L+B_L}) \\
&\quad +\beta_H(\frac{SB_H}{\kappa_H+B_H} - \frac{S^*B_H^*}{\kappa_H+B_H^*} - \frac{S^*B_H}{\kappa_H+B_H} + \frac{S^*B_H}{\kappa_H+B_H}) - (\gamma+b)(I-I^*)] \\
&\quad +2w_3(B_H-B_H^*)[\xi(I-I^*) - \chi(B_H-B_H^*)] \\
&\quad +2w_4(B_L-B_L^*)[\chi(B_H-B_H^*) - \delta_L(B_L-B_L^*)] \\
&= 2w_1(S-S^*)\{-\beta_L[\frac{B_L}{\kappa_L+B_L}(S-S^*) - \frac{S^*\kappa_L}{(\kappa_L+B_L^*)(\kappa_L+B_L)}(B_L^*-B_L)] \\
&\quad -\beta_H[\frac{B_H}{\kappa_H+B_H}(S-S^*) - \frac{S^*\kappa_H}{(\kappa_H+B_H^*)(\kappa_H+B_H)}(B_H^*-B_H)] - b(S-S^*)\} \\
&\quad +2w_2(I-I^*)\{\beta_L[\frac{B_L}{\kappa_L+B_L}(S-S^*) - \frac{S^*\kappa_L}{(\kappa_L+B_L^*)(\kappa_L+B_L)}(B_L^*-B_L)] \\
&\quad +\beta_H[\frac{B_H}{\kappa_H+B_H}(S-S^*) - \frac{S^*\kappa_H}{(\kappa_H+B_H^*)(\kappa_H+B_H)}(B_H^*-B_H)] - (\gamma+b)(I-I^*)\} \\
&\quad +2w_3\xi(I-I^*)(B_H-B_H^*) - 2w_3\chi(B_H-B_H^*)^2 \\
&\quad +2w_4\chi(B_L-B_L^*)(B_H-B_H^*) - 2w_4\delta_L(B_L-B_L^*)^2 \\
&= -2w_1\frac{\beta_L B_L}{\kappa_L+B_L}(S-S^*)^2 - 2w_1\frac{\beta_L S^*\kappa_L}{(\kappa_L+B_L^*)(\kappa_L+B_L)}(S-S^*)(B_L-B_L^*) \\
&\quad -2w_1\frac{\beta_H B_H}{\kappa_H+B_H}(S-S^*)^2 - 2w_1\frac{\beta_H S^*\kappa_H}{(\kappa_H+B_H^*)(\kappa_H+B_H)}(S-S^*)(B_H-B_H^*) \\
&\quad -2w_1 b(S-S^*)^2 \\
&\quad +2w_2\frac{\beta_L B_L}{\kappa_L+B_L}(I-I^*)(S-S^*) + 2w_2\frac{\beta_L S^*\kappa_L}{(\kappa_L+B_L^*)(\kappa_L+B_L)}(I-I^*)(B_L-B_L^*) \\
&\quad +2w_2\frac{\beta_H B_H}{\kappa_H+B_H}(I-I^*)(S-S^*) + 2w_2\frac{\beta_H S^*\kappa_H}{(\kappa_H+B_H^*)(\kappa_H+B_H)}(I-I^*)(B_H-B_H^*) \\
&\quad -2w_2(\gamma+b)(I-I^*)^2 + 2w_3\xi(I-I^*)(B_H-B_H^*) - 2w_3\chi(B_H-B_H^*)^2 \\
&\quad +2w_4\chi(B_L-B_L^*)(B_H-B_H^*) - 2w_4\delta_L(B_L-B_L^*)^2 \\
&= Y(WA + A^TW^T)Y^T, \qquad (5.3.8)
\end{aligned}
$$

where $Y = [S - S^*,\ I - I^*,\ B_H - B_H^*,\ B_L - B_L^*]$, $W = diag(w_1,\ w_2,\ w_3,\ w_4)$, and

$$A = \begin{bmatrix} -\frac{\beta_L B_L}{\kappa_L + B_L} - \frac{\beta_H B_H}{\kappa_H + B_H} - b & 0 & -\frac{\beta_H S^* \kappa_H}{(\kappa_H + B_H^*)(\kappa_H + B_H)} & -\frac{\beta_L S^* \kappa_L}{(\kappa_L + B_L^*)(\kappa_L + B_L)} \\ \frac{\beta_L B_L}{\kappa_L + B_L} + \frac{\beta_H B_H}{\kappa_H + B_H} & -(\gamma + b) & \frac{\beta_H S^* \kappa_H}{(\kappa_H + B_H^*)(\kappa_H + B_H)} & \frac{\beta_L S^* \kappa_L}{(\kappa_L + B_L^*)(\kappa_L + B_L)} \\ 0 & \xi & -\chi & 0 \\ 0 & 0 & \chi & -\delta_L \end{bmatrix}. \tag{5.3.9}$$

We can then establish the global asymptotic stability of $X^*$ by proving that the matrix A defined in equation (5.3.9) is Volterra-Lyapunov stable in $\Delta^o \backslash \{X^*\}$. The procedure is similar to that described in Section V.2, with the only complication that A in equation (5.3.9) is a $4 \times 4$ matrix. It is thus best to carry out the procedure by the following three steps. We will omit many algebraic details (which are similar to those in Section V.2), and only present the sketch of the proof in each step.

*Step 1.* We show that the matrix $U = \widetilde{A^{-1}}$ is Volterra-Lyapunov stable. The $3 \times 3$ matrix $U$ can be written as

$$U = \frac{1}{detA} \begin{bmatrix} -\left[(\gamma + b)\chi\delta_L - \frac{\xi\delta_L}{P} - \frac{\xi\chi}{Q}\right] & \frac{\xi\delta_L}{P} + \frac{\xi\chi}{Q} & (\gamma + b)\frac{\delta_L}{P} + (\gamma + b)\frac{\chi}{P} \\ -T\chi\delta_L & -(T + b)\chi\delta_L & -b(\frac{\delta_L}{P} + \frac{\chi}{Q}) \\ -T\xi\delta_L & -(T + b)\xi\delta_L & -(T + b)(\gamma + b)\delta_L \end{bmatrix} \tag{5.3.10}$$

where

$$T = \frac{\beta_L B_L}{\kappa_L + B_L} + \frac{\beta_H B_H}{\kappa_H + B_H},$$

and

$$detA = \chi\delta_L(\gamma + b)(T + b) + b(\frac{\xi\delta_L}{P} + \frac{\xi\chi}{Q}) > 0.$$

Based on Lemma 3, it is easy to observe that the $2 \times 2$ matrix $\widetilde{U}$ is Volterra-Lyapunov stable. Thus, there exists a $2 \times 2$ positive diagonal matrix $\widetilde{M} = diag(m_1,\ m_2)$ such

that $\widetilde{MU} + (\widetilde{MU})^T < 0$. Let $D = -U$ and $E = D^{-1} = -U^{-1}$. We then have $\widetilde{MD} + (\widetilde{MD})^T > 0$, based on which we are able to show $\widetilde{ME} + (\widetilde{ME})^T > 0$ as well. Hence, Lemma 5 guarantees that there exists a $3 \times 3$ positive diagonal matrix $M = diag(m_1, m_2, m_3)$ such that

$$M(-U) + (-U)^T M^T > 0, \tag{5.3.11}$$

which immediately yields $MU + U^T M^T < 0$. This establishes that $U$ is Volterra-Lyapunov stable.

*Step 2.* We show that the same matrix M defined in (5.3.11) satisfies

$$M(\widetilde{-A}) + (\widetilde{-A})^T M^T > 0 \tag{5.3.12}$$

for the matrix A defined in equation (5.3.9).

The key to establish (5.3.12) is to show that the determinant of $M(\widetilde{-A}) + (\widetilde{-A})^T M^T$ is positive; the other requirements are easier to check. In fact, after some tedious algebra, we find

$$\begin{aligned}
&det\{(detA)[M(-U) + (-U)^T M^T]\} \\
&= \Big[T\chi\delta_L^3(\gamma + b) + b\delta_L^2\big[\chi\delta_L(\gamma + b) - \frac{\xi\delta_L}{P} - \frac{\xi\chi}{Q}\big]\Big] det\big[M(\widetilde{-A}) + (\widetilde{-A})^T M^T\big] \\
&- 2m_1m_2^2b^2(\frac{\delta_L}{P} + \frac{\chi}{Q})^2[\chi\delta_L(\gamma + b) - \frac{\xi\delta_L}{P} - \frac{\xi\chi}{Q}] - 2m_1m_2^2Tb\chi\delta_L(\gamma + b)(\frac{\chi^2}{Q^2} + \frac{2\delta_L\chi}{PQ}) \\
&- 4m_1m_2m_3Tb\xi\frac{\delta_L^2}{P}(T + b)[\chi\delta_L(\gamma + b) - \frac{\xi\delta_L}{P} - \frac{\xi\chi}{Q}] - 6m_1m_2m_3T^2\xi\chi\frac{\delta_L^3}{P}(\gamma + b) \\
&- 2m_1m_2m_3Tb\xi\chi\frac{\delta_L^3}{P}(\gamma + b) - 2m_1m_2m_3Tb\xi^2\delta_L(\frac{\delta_L}{P} + \frac{\chi}{Q})^2 \\
&- 4m_1m_2m_3Tb\xi\chi\delta_L^2\frac{\chi}{Q}(\gamma + b) - 4m_1m_2m_3b\xi\delta_L\frac{\chi}{Q}(T + b)[\chi\delta_L(\gamma + b) - \frac{\xi\delta_L}{P} - \frac{\xi\chi}{Q}] \\
&- 2m_1^2m_2T\chi\delta_L(\gamma + b)^2(\frac{\chi^2}{Q^2} + \frac{2\delta_L\chi}{PQ}) - 8m_1m_2m_3T\xi\delta_L^2\frac{\chi^2}{Q}(T + b)(\gamma + b) \\
&- 2m_1^2m_2(T + b)(\gamma + b)(\frac{\chi^2}{Q^2} + \frac{2\delta_L\chi}{PQ})[\chi\delta_L(\gamma + b) - \frac{\xi\delta_L}{P} - \frac{\xi\chi}{Q}].
\end{aligned}$$

Since $M(-U) + (-U)^T M^T > 0$ and $detA > 0$, we have

$$det\{(detA)[M(-U) + (-U)^T M^T]\} > 0.$$

Using the inequality (5.3.6), it is then easy to observe that

$$det\big[M(\widetilde{-A}) + (\widetilde{-A})^T M^T\big] > 0.$$

*Step 3.* We show that the matrix A defined in equation (5.3.9) is Volterra-Lyapunov stable.

Based on Lemma 5 and the results in (5.3.11) and (5.3.12), there exists $m_4 > 0$ such that for $W = diag(w1, w2, w3, w4)$ with $w_i = m_i (1 \leq i \leq 4)$, we have $W(-A) + (-A)^T W^T > 0$; i.e., $WA + A^T W^T < 0$.

Summarizing the above procedure, we have thus established the following result:

**Theorem 19.** *When $R_0 > 1$, the endemic equilibrium of system (3.1.1-3.1.5) is globally asymptotically stable in $\Delta^o$.*

## V.4 Numerical results

We now present some numerical simulations to verify the global asymptotic stability of the endemic equilibria for models analyzed in Section V.2-V.3. We first consider Codeco's model (4.6.1-4.6.3), that is a typical three-dimensional example. We first scale up the total population from 1 to 10,000, and use the same parameter values (for endemic cholera) as in [11], and conduct numerical simulation to this model. We find $R_0 = 1.51$ in this case, and the unique positive endemic equilibrium is located at $I^* \approx 16.98$, $S^* \approx 6606$. Also, we pick another three-dimensional example which is Mukandavire's model (3.1.19-3.1.22) with the same parameter values (for endemic cholera) as in [60]. We scale up the total population from 1 to 13,228. We find $R_0 = 1.23$ in this case, and the unique positive endemic equilibrium is located at $I^* \approx 1.16$, $S^* \approx 10732$. We illustrate the existence of the unique globally asymptotically stable endemic equilibrium for both Codeco's model and Mukandavire's model by using a phase plane portrait which is a useful tool to understand the behavior of a dynamical system, in Figures 5.1 and 5.2. We pick five different initial conditions with $I(0) = 1,\ 100,\ 200,\ 600,\ 1000$, respectively, and plot these five solution curves by the phase plane portrait of $I$ vs. $S$ in Figure 5.1 and 5.2. We clearly see that all these five orbits converge to the endemic equilibrium, showing the global asymptotic stability of the endemic equilibrium.

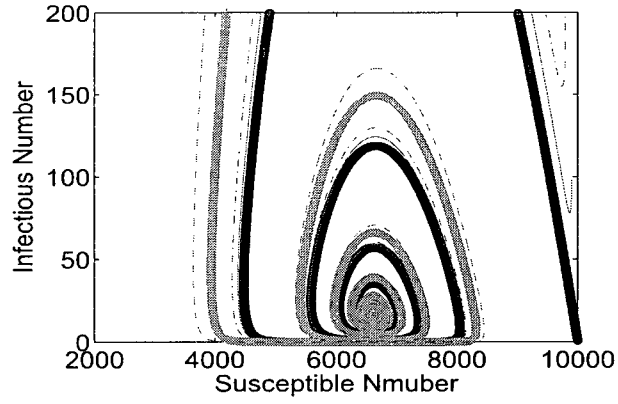


Figure 5.1: The phase plane portrait of $I$ vs. $S$ for Codeco's model with five different initial conditions. The parameter values are taken from [11]. All the curves converge to the endemic equilibrium with $I^* \approx 16.98$, $S^* \approx 6606$.

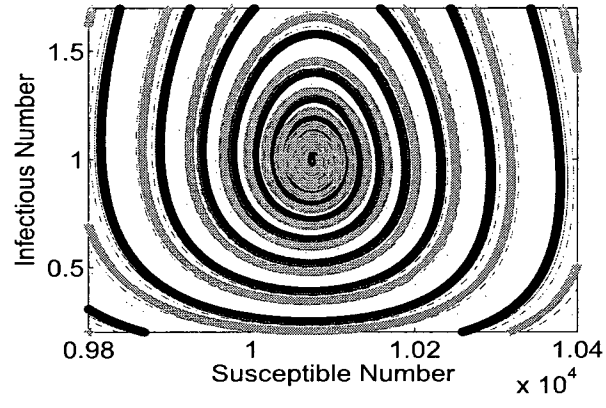


Figure 5.2: The phase plane portrait of $I$ vs. $S$ for Mukandavire's model with five different initial conditions. The parameter values are taken from [60]. All the curves converge to the endemic equilibrium with $I^* \approx 1.16$, $S^* \approx 10732$.

Next, we numerically simulate the model of Hartley *et al.* presented in equations (3.1.1-3.1.5), to illustrate the results for a typical four-dimensional example. The total population is again set as $10,000$ to match the configuration of the original model in [22]. Based on the parameter values from [22], we find $R_0 \approx 18.83$, and the unique endemic equilibrium is $I^* \approx 4.33$, $S^* \approx 534$. We pick the same five

initial conditions as before and plot the phase plane portrait of $I$ vs. $S$ in Figure 5.3. Although these curves appear to closely follow each other and are not clearly distinguishable, we do observe a similar pattern to that in Figures 5.1 and 5.2: the endemic equilibrium attracts all the solution orbits, confirming its global asymptotic stability. We also note that due to the incorporation of the hyperinfectious state, the infection level produced by the model of Hartley *et al.* is extremely high; the peak value of the epidemic is about $3,600$, or 36% of the total population. This can be explained by the unusually high value of $R_0$ (about 18.83) in this case. Thus, under this setting, almost every people will be infected, and eventually the majority of the human population is in the recovered class, $R$. This model thus best suits those extremely severe and fast-spreading cholera epidemics, whereas Codeco's model is better applied to relatively mild or moderate cholera infections.

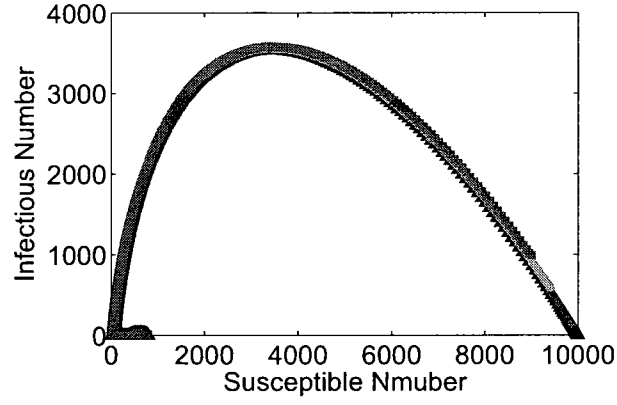


Figure 5.3: The phase plane portrait of $I$ vs. $S$ for Hartley's model with five different initial conditions.

# CHAPTER VI

# MODELS WITH CONTROLS

Although cholera is a severe infection, due to vaccination, advanced water treatment and sanitation practices, which shorten the course of the disease and reduce the severity of the symptoms, cholera is no longer a major health threat in most countries. In this chapter, we aim to modify the models by adding some key control terms. First we will use Codeco's model (4.6.1-4.6.3) to study the local stability of the DFE and endemic dynamics under controls. Then we will apply the controls to the generalized cholera model (4.1.1- 4.1.4). Because the approach to derive the basic reproduction number $R_0$ and the local stability are very similarly to the process described in chapter III, we will omit some algebra, and only present some important results.

## VI.1 Codeco's model with controls

### VI.1.1 The disease-free equilibrium

We modify Codeco's model (4.6.1-4.6.3) by adding three types of controls: vaccination, antibiotic and water sanitation. Also we assume some newborns take vaccination already and only a proportion $P$ of individuals entering the total population are susceptible. To make the equations simpler, we set $m = mb - nb$. The equations become:

$$\frac{dS}{dt} = PnH - nS - \frac{aBS}{K+B} - vS, \tag{6.1.1}$$

$$\frac{dI}{dt} = \frac{aBS}{K+B} - (r+u)I, \tag{6.1.2}$$

$$\frac{dR}{dt} = (1-P)nH + (r-n+u)I - nR + vS, \tag{6.1.3}$$

$$\frac{dB}{dt} = eI - (m+w)B, \tag{6.1.4}$$

where $v$ denotes the rate of vaccination, $u$ denotes the rate of antibiotic treatment, $w$ denotes the rate of bacterial death due to water sanitation.

Equations (6.1.1-6.1.4) have a unique disease-free equilibrium (DFE)

$$X_0 = \big(\frac{PnH}{n+v},\ 0,\ \frac{H(n+v-Pn)}{n+v},\ 0\big)^T. \tag{6.1.5}$$

We denote $\bar{r} = r + u$, $\bar{m} = m + w$. The Jacobian of the ODE system (6.1.1-6.1.4) is

$$\begin{bmatrix} -\frac{aB}{K+B} - n - v & 0 & 0 & -\frac{aSK}{(K+B)^2} \\ \frac{aB}{K+B} & -\bar{r} & 0 & \frac{aSK}{(K+B)^2} \\ v & r+u-n & -n & 0 \\ 0 & e & 0 & -\bar{m} \end{bmatrix}. \tag{6.1.6}$$

After substituting the values for the DFE: $S = \frac{PnH}{n+v}$, $R = \frac{H(n+v-Pn)}{n+v}$, $I = B = 0$, the above matrix becomes

$$J_B = \begin{bmatrix} -n - v & 0 & 0 & -\frac{aPnH}{K(n+v)} \\ 0 & -\bar{r} & 0 & \frac{aPnH}{K(n+v)} \\ v & r+u-n & -n & 0 \\ 0 & e & 0 & -\bar{m} \end{bmatrix}. \tag{6.1.7}$$

The characteristic polynomial of the matrix $J_B$ is

$$\text{Det}\,(\lambda I - J_B) \;=\; (\lambda + n + v)(\lambda + n)\Big[(\lambda + \bar{r})(\lambda + \bar{m}) - \frac{aPnHe}{K(n+v)}\Big].$$

The equilibrium (6.1.5) is locally asymptotically stable if and only if all roots of the above polynomial have negative real parts. Obviously $\lambda = -n - v$ and $\lambda = -n$ are two negative roots. For the quadratic equation inside the brackets,

$$\lambda^2 + \lambda(\bar{r} + \bar{m}) + \Big[\bar{r}\bar{m} - \frac{aPnHe}{K(n+v)}\Big] = 0.$$

According to the Routh-Hurwitz criterion, the sufficient and necessary condition for stability is:

$$\bar{r}\bar{m} - \frac{aPnHe}{K(n+v)} > 0,$$

which yields

$$H < \frac{\bar{r}\bar{m}K(n+v)}{aPne}. \tag{6.1.8}$$

Also, this inequality (6.1.8) provides a threshold for the total population (which is assumed to be completely susceptible initially):

$$S_c = \frac{\bar{r}\bar{m}K(n+v)}{aPne}. \tag{6.1.9}$$

When $H$ is below $S_c$, the DFE is stable and no epidemicity occurs. In contrast, if $H$ is above this critical value, the DFE becomes unstable and any infection entering the population would persist and lead to an epidemic.

We define the basic reproduction number, $R_0$, of this model by

$$R_0 = \frac{N}{S_c} = \frac{aPne}{\bar{r}\bar{m}K(n+v)}H. \tag{6.1.10}$$

Thus, we have established the result below (similar theorems can be seen in chapter III):

**Theorem 20.** *The disease-free equilibrium of the model (6.1.1-6.1.4) is locally asymptotically stable if* $R_0 < 1$, *and unstable if* $R_0 > 1$.

It can be easily observed that the basic reproduction number defined in (6.1.10) is lower in value than that defined in (4.6.4) for the original model, showing the effect of controls.

### VI.1.2 Endemic dynamic

We consider the endemic equilibrium of system (6.1.1-6.1.4) by

$$X^* = \left(S^*, I^*, R^*, B^*\right)^T. \tag{6.1.11}$$

Its components must satisfy

$$I^* = \frac{aPnHe - K\bar{r}\bar{m}(n+v)}{\bar{r}e(a+n+v)}, \tag{6.1.12}$$

$$S^* = \frac{\bar{r}I^*(K+B^*)}{aB^*}, \tag{6.1.13}$$

$$R^* = (1-P)H + \frac{I^*(r-n+u)+vS^*}{n}, \tag{6.1.14}$$

$$B^* = \frac{eI^*}{\bar{m}}. \tag{6.1.15}$$

From equation (6.1.9), it is straightforward to see the endemic equilibrium $I^*$ exists if and only if

$$H > \frac{K\bar{r}\bar{m}(n+v)}{aPne}.$$

That is, $R_0 > 1$, where $R_0$ is defined in (6.1.10).

We have the following result regarding the local stability of the endemic equilibrium.

**Theorem 21.** *When $R_0 > 1$, the positive endemic equilibrium of system (6.1.1-6.1.4) is locally asymptotically stable.*

*Proof.* Consider the Jacobian (6.1.7) at the endemic equilibrium. Set $\frac{aB^*}{K+B^*} = T$, $\frac{aS^*K}{(K+B^*)^2} = Q$, and $T$, $Q$ are all positive. We obtain a Jacobian matrix as

$$J_B^* = \begin{bmatrix} -T-n-v & 0 & 0 & -Q \\ T & -\bar{r} & 0 & Q \\ v & r+u-n & -n & 0 \\ 0 & e & 0 & -\bar{m} \end{bmatrix}.$$

The characteristic polynomial of $J_B^*$ is

$$\text{Det}\,(\lambda I - J_B^*) = (\lambda+n)\Big[(\lambda+n+v+T)(\lambda+\bar{r})(\lambda+\bar{m}) - (\lambda+n+v)Qe\Big].$$

Obviously $\lambda = -n$ is one negative root. For the cubic equation inside the brackets, we have

$$a_0\lambda^3 + a_1\lambda^2 + a_2\lambda^1 + a_3 = 0 \tag{6.1.16}$$

where

$$a_0 = 1, \tag{6.1.17}$$

$$a_1 = \bar{r} + \bar{m} + n + v + T, \tag{6.1.18}$$

$$a_2 = \bar{r}\bar{m} + n\bar{r} + n\bar{m} + v\bar{r} + v\bar{m} + T\bar{r} + T\bar{m} - Qe, \tag{6.1.19}$$

$$a_3 = n\bar{r}\bar{m} + v\bar{r}\bar{m} + T\bar{r}\bar{m} - nQe - vQe. \tag{6.1.20}$$

Based on the Routh-Hurwitz criterion, the sufficient and necessary condition for stability is:

$$a_1 > 0\,, \qquad a_2 > 0\,, \qquad a_3 > 0\,, \qquad a_1 a_2 - a_0 a_3 > 0. \tag{6.1.21}$$

Note $a_1 > 0$ is obvious because all parameters are positive. From equation (6.2.8-6.2.11), we can easily obtain

$$\bar{r} = \frac{aS^* e}{K\bar{m} + eI^*}\,, \qquad Q = \frac{aS^* K\bar{m}^2}{(K\bar{m} + eI^*)^2}.$$

Thus,

$$\bar{r}\bar{m} - Qe = \frac{aS^* e^2 \bar{m} I^*}{(K\bar{m} + eI^*)^2} > 0. \tag{6.1.22}$$

Substitute equation (6.1.22) into equations (6.1.19) and (6.1.20), $a_2 > 0$ and $a_3 > 0$ are easy to see. Also, we write $a_1 a_2 - a_0 a_3$ as follows

$$\begin{aligned} a_1 a_2 - a_0 a_3 \;=\; & \bar{r}^2(n + v + T) + (n + v)\bar{r}\bar{m} \\ & + (\bar{r} + \bar{m})(n + v + T)(\bar{r} + 2\bar{m} + T) \\ & + (\bar{r}^2\bar{m} - \bar{r}Qe) + (\bar{r}\bar{m}^2 - \bar{m}Qe) + (T\bar{r}\bar{m} - TQe). \end{aligned} \tag{6.1.23}$$

Using equation (6.1.22), we can obtain the last three terms in equation (6.1.23) are all positive. Therefore, the sufficient and necessary condition (6.1.21) holds. □

We now present some numerical simulations to compare the cholera epidemics with controls (weak controls and strong controls) and without controls. We assume $P = 0.9$. To impose strong controls on the model, we set $u = 0.5r$, $v = 0.5n$ and $w = 0.5m$. Under this setting, $R_0 = 0.4$. In contrast, if we set $u = 0.1r$, $v = 0.1n$ and $w = 0.1m$, we obtain a weak control model with $R_0 = 1.03$. Figure 6.1 shows the cholera epidemics with weak controls, strong controls and without controls, respectively. The infection curve with strong controls quickly declines to 0 and the disease dies out, due to $R_0 < 1$. The infectious value of the model with weak controls is much lower than that of the original model, showing the controls do weaken the cholera outbreak even though they do not eradicate the outbreak.

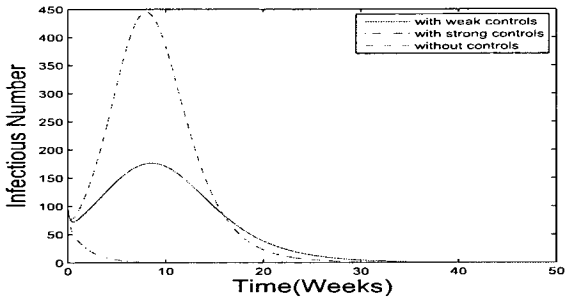


Figure 6.1: The infected population vs. time of Codeco's model. The three curves exhibits the epidemics with weak controls, strong controls and without controls, respectively.

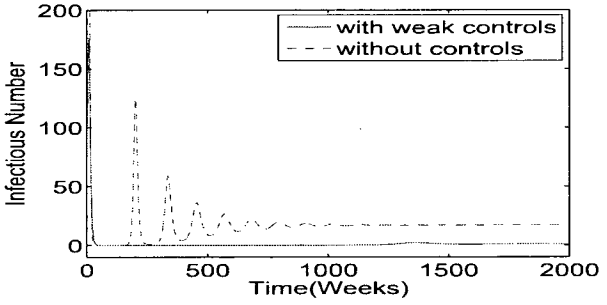


Figure 6.2: The infected population vs. time of Codeco's model. The two curves exhibits the epidemics with weak controls and without controls, respectively.

Figure 6.2 shows the numerical simulation for Codeco's model and the model with weak controls for a longer period of time ( up to 2,000 weeks). The original Codeco's model shows several oscillations after the first outbreak, whereas the model with weak controls, after the first outbreak with lower magnitude, drops to almost the zero level and stays there all time showing no more outbreaks are triggered.

## VI.2 The generalized cholera model with controls

If we put the same controls (vaccination, antibiotic and water sanitation) on Hartley's model [22] and Mukandavire's model [60], we can achieve similar results. Next, we consider the generalized cholera model (4.1.1-4.1.4) with three controls: vaccination,

antibiotic and water sanitation. The equations become:

$$\frac{dS}{dt} = bN - Sf(I,B) - bS - vS, \tag{6.2.1}$$

$$\frac{dI}{dt} = Sf(I,B) - (\gamma + b)I - \mu I, \tag{6.2.2}$$

$$\frac{dR}{dt} = \gamma I - bR + vS + \mu I, \tag{6.2.3}$$

$$\frac{dB}{dt} = \bar{h}(I,B), \tag{6.2.4}$$

where $\bar{h}(I,B) = h(I,B) - wB$. It can be seen that $\bar{h}$ satisfies the same assumptions given in Section IV.1.

Equations (6.2.1-6.2.4) have a unique disease-free equilibrium (DFE)

$$X_0 = \big(\frac{bN}{n+v},\ 0,\ \frac{vN}{b+v},\ 0\big)^T. \tag{6.2.5}$$

Following the same process as in section IV.2, we find the next generation matrix:

$$FV^{-1} = \frac{-1}{\gamma + b + \mu}\begin{bmatrix} -\frac{bN}{b+v}\Big[\frac{\partial f}{\partial I}(0,0) - \frac{\partial f}{\partial B}(0,0)\Big(\frac{\partial \bar{h}}{\partial B}(0,0)\Big)^{-1}\frac{\partial \bar{h}}{\partial I}(0,0)\Big] & \frac{bN}{b+v}(\gamma+b+\mu)\Big(\frac{\partial \bar{h}}{\partial B}(0,0)\Big)^{-1}\frac{\partial f}{\partial B}(0,0) \\ 0 & 0 \end{bmatrix}.$$

Its spectral radius $\rho(FV^{-1})$ can be easily found. Therefore, we obtain the basic reproduction number as

$$R_0 = \frac{bN}{(\gamma+b+\mu)(b+v)}\Big[\frac{\partial f}{\partial I}(0,0) - \frac{\partial f}{\partial B}(0,0)\Big(\frac{\partial \bar{h}}{\partial B}(0,0)\Big)^{-1}\frac{\partial \bar{h}}{\partial I}(0,0)\Big]. \tag{6.2.6}$$

It's clear that this value is lower than that defined in (4.2.2) for the original model. Based on the framework in [80], we immediately obtain the result below

**Theorem 22.** *Let $R_0$ be defined in equation (6.2.6). The disease-free equilibrium of the system (6.2.1)-(6.2.4) is locally asymptotically stable if $R_0 < 1$, and unstable if $R_0 > 1$.*

When $R_0 > 1$, meaning that the controls are not strong enough to eradicate the epidemic, the disease will persist. Thus we consider the endemic equilibrium

$$X^* = \big(S^*,\ I^*,\ R^*,\ B^*\big)^T. \tag{6.2.7}$$

Its components must satisfy

$$I^* = \frac{1}{(\gamma+b+\mu)}\frac{bNf(I^*,B^*)}{b+v+f(I^*,B^*)}, \tag{6.2.8}$$

$$S^* = \frac{bN}{b+v+f(I^*,B^*)}, \tag{6.2.9}$$

$$R^* = \frac{\gamma I^* + \mu I^* + vS^*}{b}, \tag{6.2.10}$$

$$0 = \bar{h}(I^*,B^*). \tag{6.2.11}$$

The Jacobian matrix of the model system (6.2.1)-(6.2.4) is

$$J_B = \begin{bmatrix} -b-f(I,B)-v & -S\frac{\partial f}{\partial I}(I,B) & 0 & -S\frac{\partial f}{\partial B}(I,B) \\ f(I,B) & S\frac{\partial f}{\partial I}(I,B)-(\gamma+b+\mu) & 0 & S\frac{\partial f}{\partial B}(I,B) \\ v & \gamma+\mu & -b & 0 \\ 0 & \frac{\partial \bar{h}}{\partial I}(I,B) & 0 & \frac{\partial \bar{h}}{\partial B}(I,B) \end{bmatrix} \tag{6.2.12}$$

For the convenience of algebraic manipulation, we denote

$$F = f(I^*,B^*), \quad E = \frac{\partial f}{\partial I}(I^*,B^*), \quad P = \frac{\partial f}{\partial B}(I^*,B^*), \quad \bar{Q} = \frac{\partial \bar{h}}{\partial B}(I^*,B^*), \quad \bar{T} = \frac{\partial \bar{h}}{\partial I}(I^*,B^*).$$

From the assumptions (**b**) and (**c**), $F \geq 0,\ E \geq 0,\ P \geq 0,\ \bar{T} \geq 0$, whereas $\bar{Q} \leq 0$. Evaluated at $X^*$, the Jacobian matrix (6.2.12) becomes

$$J_B^* = \begin{bmatrix} -F-b-v & -S^*E & 0 & -S^*P \\ F & S^*E-(\gamma+b+\mu) & 0 & S^*P \\ v & \gamma+\mu & -b & 0 \\ 0 & \bar{T} & 0 & \bar{Q} \end{bmatrix}.$$

The characteristic polynomial of $J_B^*$ is

$$\begin{aligned} \mathrm{Det}\,(\lambda I - J_B^*) &= (\lambda+b)\big[(\lambda+b+F+v)(\lambda+\gamma+b+\mu)(\lambda-\bar{Q}) \\ &\quad -(\lambda+b+v)(S^*E\lambda - S^*E\lambda + S^*P\bar{T})\big]. \end{aligned}$$

Obviously $\lambda = -b$ is one negative root. For the cubic equation inside the brackets,

$$a_0\lambda^3 + a_1\lambda^2 + a_2\lambda^1 + a_3 = 0 \tag{6.2.13}$$

where

$$\begin{aligned}
a_0 &= 1, && (6.2.14)\\
a_1 &= -Q + \gamma + 2b + \mu + F + v - S^*E, && (6.2.15)\\
a_2 &= -\gamma\bar{Q} - 2b\bar{Q} - \mu\bar{Q} + b\gamma + b^2 + b\mu - F\bar{Q} + F\gamma + Fb + F\mu - v\bar{Q}\\
&\quad +v\gamma + vb + v\mu + S^*E\bar{Q} - S^*P\bar{T} - bS^*E - vS^*E, && (6.2.16)\\
a_3 &= -b\gamma\bar{Q} - b^2\bar{Q} - b\mu\bar{Q} - F\gamma\bar{Q} - Fb\bar{Q} - F\mu\bar{Q} - v\gamma\bar{Q} - vb\bar{Q} - v\mu\bar{Q}\\
&\quad +bS^*E\bar{Q} - bS^*P\bar{T} + vS^*E\bar{Q} - vS^*P\bar{T}. && (6.2.17)
\end{aligned}$$

Based on the Routh-Hurwitz criterion, the sufficient and necessary condition for stability is:

$$a_1 > 0\,, \qquad a_2 > 0\,, \qquad a_3 > 0\,, \qquad a_1a_2 - a_0a_3 > 0. \tag{6.2.18}$$

We first establish the following lemma:

**Lemma 12.** *At the endemic equilibrium $X^*$, we have*

$$\begin{aligned}
b + \gamma + \mu - ES^* &\geq 0, && (6.2.19)\\
-Q(b + \gamma + \mu) &\geq PTS^* - EQS^*. && (6.2.20)
\end{aligned}$$

*Proof.* Using equations (6.2.8)(6.2.9), we obtain

$$\begin{aligned}
b + \gamma + \mu - ES^* &= (b + \gamma + \mu) - \frac{\partial f}{\partial I}(I^*, B^*)S^*\\
&= \frac{bNf(I^*, B^*)}{[b + v + f(I^*, B^*)]I^*} - \frac{\partial f}{\partial I}(I^*, B^*)\frac{bN}{b + v + f(I^*, B^*)}\\
&= \frac{bN}{[b + v + f(I^*, B^*)]I^*}\Big[f(I^*, B^*) - \frac{\partial f}{\partial I}(I^*, B^*)I^*\Big]\\
&\geq 0, && (6.2.21)
\end{aligned}$$

and

$$\begin{aligned}
-\bar{Q}(b + \gamma + \mu) &= -\frac{\partial \bar{h}}{\partial B}(I^*, B^*)(b + \gamma + \mu)\\
&\geq \frac{\partial f}{\partial B}(I^*, B^*)\frac{\partial \bar{h}}{\partial I}(I^*, B^*)S^* - \frac{\partial f}{\partial I}(I^*, B^*)\frac{\partial \bar{h}}{\partial B}(I^*, B^*)S^*\\
&= P\bar{T}S^* - E\bar{Q}S^*. && (6.2.22)
\end{aligned}$$

□

**Lemma 13.** *At the endemic equilibrium $X^*$, all the four inequalities in (6.2.18) hold.*

*Proof.* First, using the inequality (6.2.19), we obtain

$$\begin{aligned} a_1 &= \bar{Q} + \gamma + 2b + \mu + F + v - S^*E \\ &= -\frac{\partial \bar{h}}{\partial B}(I^*, B^*) + \gamma + 2b + \mu + f(I^*, B^*) + v - \frac{\partial f}{\partial I}(I^*, B^*)S^* \\ &> (b + \gamma + \mu) - \frac{\partial f}{\partial I}(I^*, B^*)S^* \\ &> 0. \end{aligned} \tag{6.2.23}$$

Next, using both results in (6.2.19) and (6.2.20), we obtain

$$\begin{aligned} a_2 &= -\gamma\bar{Q} - 2b\bar{Q} - \mu\bar{Q} + b\gamma + b^2 + b\mu - F\bar{Q} + F\gamma + Fb + F\mu - v\bar{Q} \\ &= (b + v)(b + \gamma + \mu - ES^*) + (-\bar{Q}b - \bar{Q}\gamma - \bar{Q}\mu - PS^*\bar{T} + E\bar{Q}S^*) \\ &\quad +(Fb + F\gamma + F\mu - v\bar{Q} - F\bar{Q} - b\bar{Q}) \\ &> 0. \end{aligned} \tag{6.2.24}$$

Similarly, we have

$$\begin{aligned} a_3 &= -b\gamma\bar{Q} - b^2\bar{Q} - b\mu\bar{Q} - F\gamma\bar{Q} - Fb\bar{Q} - F\mu\bar{Q} - v\gamma\bar{Q} - vb\bar{Q} - v\mu\bar{Q} \\ &\quad +bS^*E\bar{Q} - bS^*P\bar{T} + vS^*E\bar{Q} - vS^*P\bar{T} \\ &= (b + v)(-\bar{Q}b - \bar{Q}\gamma - \bar{Q}\mu + E\bar{Q}S^* - PS^*\bar{T}) + (-b\mu\bar{Q} - F\gamma\bar{Q} - Fb\bar{Q} - F\mu\bar{Q}) \\ &> 0. \end{aligned} \tag{6.2.25}$$

Finally, note that $a_1 > -Q > 0$ and that

$$\begin{aligned} (-Q)a_2 - a_0a_3 &= \left(\bar{Q}^2b + \bar{Q}^2\gamma + \bar{Q}^2\mu - E\bar{Q}^2S^* + P\bar{T}\bar{Q}S^*\right) \\ &\quad +\left(F\bar{Q}^2 + \bar{Q}^2b + \bar{Q}^2v + bS^*P\bar{T} + vS^*P\bar{T}\right) \\ &> 0. \end{aligned} \tag{6.2.26}$$

It is thus clear to see $a_1a_2 > a_0a_3$ holds. □

**Theorem 23.** *The endemic equilibrium of the system (6.2.1-6.2.4) is locally asymptotically stable if $R_0 > 1$, where $R_0$ is defined in (6.2.6).*

Our results from these preliminary studies show that incorporation of control measures weakens the infection, and may also eradicate the disease provided the control is strong enough. We note, however, from a practical point of view, that the use of antibiotics is not a recommended course of action for an outbreak as cholera will become antibiotic resistant extremely quickly. Oral rehydration therapy is a cheap and standard treatment without other intervention strategies.

# CHAPTER VII

# CONCLUSION AND FUTURE WORK

In this dissertation, we have presented an in-depth mathematical study of several epidemic cholera models. We have presented three basic mathematical cholera models including Codeco's model [11] in 2001, Hartley, Morris and Smith's model [22] in 2006 and Mukandavire, Liao, Wang and Gaff's model *et al.* [60] in 2010. We have formally derived the basic reproduction number $R_0$ by computing the spectral radius of the next generation matrix, and through a stability analysis which directly relates $R_0$ to the stability of the disease-free equilibrium, providing important guidelines for the prevention and control strategies on cholera epidemics [23; 14]. We also have studied the stability property at both the disease-free equilibrium (which determines the short-term epidemic behavior) and the endemic equilibrium (which determines the long-term disease dynamics). Moreover, although it is difficult to construct specific Lyapunov functions to approach the global stability analysis, we have incorporated the Volterra-Lyapunov matrix theory into Lyapunov functions to overcome this challenge, and this method can be applied to general epidemic models. In another key part of this dissertation, we have presented a new and unified deterministic model, which incorporates a general incidence rate and a general formulation of the pathogen concentration, to analyze the dynamics of cholera. And also, we have conducted equilibrium analysis to study the complex epidemic and endemic behavior of the disease. Finally, we have briefly discussed the dynamics of cholera models with control measures incorporated.

At the beginning of chapter III, we introduced Hartley's model [22] where a hyperinfectious state was incorporated. We recall that the next generation matrix approach is used to derive the basic reproduction number $R_0$, and a useful theorem is established: The disease-free equilibrium of the model (3.1.6) is locally asymptotically stable if $R_0 < 1$, and unstable if $R_0 > 1$ (see Theorem 4). This theorem appears frequently. Besides, we are also interested in understanding the stability of the disease-free equilibrium (DFE) that is directly related to the threshold of disease transmission. We conducted the stability analysis and applied the Lemma introduced by Castillo-Chavez *et al.* [9] to verify the local stability and global stability (see Theorem 5).

The middle part of chapter III is about endemic dynamics. In this section, our main concern is the stability of an endemic state of the model. Endemic state is a steady state solution of the model for which the number of infected individuals stays at a positive level. For Hartley's model [22], Theorems 6 and 7 are obtained to explain the existence and local stability of endemic equilibrium. In addition, we analyzed another model which was proposed by Mukandavire, Liao, Wang and Gaff *et al.* [60]. Similarly, Theorem 8 is obtained. Next, we focus on the Zimbabwean cholera outbreak as a real-world application of Hartley's model. As we mentioned before, two important parameters $\beta_h$ and $\beta_L$ are hard to determine. We adjusted these two parameters to match the reported infections in Zimbabwe. The data fitting is shown in Fig 3.2 and more detailed numerical simulation results for a much longer period of time (up to 7,000 weeks) for $I$, $S$ and $R$ are shown in Figs 3.3 and 3.4. The results for both epidemic and endemic dynamics are consistent with the analytical predictions. The findings in chapter III have several implications to the real-world cholera. Not only can the model well fit the Zimbabwean data, our results also confirm that the hyperinfectious state plays an important role in the transmission of the disease, especially for the onset of an epidemic. This point was also carefully discussed in [22].

In chapter IV, we have presented a generalized mathematical cholera model (4.1.1 -4.1.4) under five necessary assumptions (see assumption a-e) and conducted an analysis for the epidemic and endemic dynamics. By introducing general incidence and pathogen functions, our model (4.1.1-4.1.4) can unify several cholera studies into a single framework of modeling, simulation and analysis. Thus, the complication of cholera dynamics lies in the coupling between human hosts and environmental components which leads to a combined human-environment epidemiological model. Nonetheless, the basic reproduction number was derived by using the next generation matrix analysis again. The stability analysis in chapter IV (see Section IV.5) showed that under biologically feasible conditions, a regular (i.e., forward) transcritical bifurcation occurs at $R_0 = 1$. Specifically, we have established that for $R_0 < 1$, there is a unique DFE which is both locally and globally asymptotically stable; this equilibrium becomes unstable when $R_0 > 1$. Meanwhile, there is a unique positive endemic equilibrium which is locally asymptotically stable when $R_0 > 1$. Theorem 13 is obtained finally.

We have to note that it is more difficult to show the global stability. We have conducted global stability analysis of a class of deterministic epidemiological models which involve both human and environmental components (SIR-B), constituting high-dimensional nonlinear systems, by using the method of Lyapunov functions combined with the theory of Volterra-Lyapunov stable matrices. By incorporating the Volterra-Lyapunov matrix theory, this method essentially transfers the analysis from differentiable functions to related matrices. Consequently, this method circumvents the (long-standing) difficulty of determining specific coefficient values for the Lyapunov functions, thus advances this classical approach toward wider and more successful applications in dynamical systems. The disadvantage, however, of this method lies in the demand of algebraic and matrix manipulation, especially in the process of proving Volterra-Lyapunov matrix stability. As can be expected, the implementation of this method will likely be hindered for epidemiological models with more complex incidence rates, or those with even higher dimensions, though such difficulty remains the same for all other existing methods in global stability analysis. As far as the current method is concerned, some symbolic computation software (such as Mathematica, Maple and Matlab) can be possibly used to leverage some of the algebraic difficulty. Besides, in this dissertation, in chapter IV, we have only considered Lyapunov functions of the most common form, i.e., square sums. Other types of Lyapunov functions, such as those proposed in [35], can be constructed as well when using the Volterra-Lyapunov matrix analysis. This can possibly improve the efficiency and enable better implementation of this method. Though this method has been demonstrated in the application to a pretty general class of epidemiological models, it is not clear at present what properties, in precise terms, a dynamical system needs to have to ensure the success of this method. Thus, like all other approaches, this method works well for some (or many) types of dynamical systems but may not for other types. A general sufficient condition for the applicability of this method would be worth exploring, and, if found, would provide useful guidelines.

It remains to show the global asymptotic stability for the endemic equilibrium of our cholera model (4.1.1-4.1.4). This is generally difficult for high-dimensional nonlinear systems, such as ours in (4.1.1)-(4.1.4) no matter we use the classic Lyapunov functions or the approach we used in chapter V. Quite a few efforts [18; 19; 38; 55; 70; 73; 75] have been devoted to extend the classical Poincaré-Bendixson framework [21] to high-dimensional systems, using theory of monotone

flows, competitive systems, and Lipschitz manifolds, etc., though such extensions are in general highly nontrivial. Finally, in a series of papers [42; 44; 45; 43], M.Y. Li and his co-workers analyzed the global stability of high-dimensional endemic equilibria based on the theory of monotone dynamical systems and geometric approaches. Similar work of epidemiological global dynamics has also been conducted in [40; 58; 83]. These studies provide useful directions for our future work on the global endemic stability of the cholera model.

In addition to the analysis, the cholera model (4.1.1-4.1.4) can be applied in a number of ways. For example, climatic impacts (such as rainfall, monsoon, flood, drought, and water temperature) on cholera epidemics [32; 51] can be studied by incorporating seasonally variational factors into the incidence function $f$. Meanwhile, several recent studies [17; 28; 62] have suggested that cholera dynamics is closely related to the prevalence of bacteriophages in the environment; the effects of those vibriophages on cholera can be easily added to the environmental function $h$ in our model. Furthermore, prevention and intervention strategies, such as vaccination, water sanitation, hydration therapy and antibiotic treatment, can be naturally represented by modifying the two functions $f$ and $h$ in our model, so as to seek possible optimal control strategies [37] against cholera outbreaks. We note a recent work by Neilan, Schaefer, Gaff *et al.* [62] on the optimal control study of cholera dynamics, which provides useful direction for our future study.

All numerical experiments in this dissertation were done with the Matlab program and they were run on a personal computer with 2.0GHz CPU and 4 GB memory.

# REFERENCES

[1] A. Alam, R.C. Larocque, J.B. Harris, et al., Hyperinfectivity of human-passaged Vibrio cholerae can be modeled by growth in the infant mouse, *Infection and Immunity*, 73: 6674-6679, 2005.

[2] K. Beck, J.P. Keener and P. Ricciardi, The effects of epidemics on genetic evolution, *J. Math. Biol*, 19: 79-94, 1984.

[3] E. Beretta and V. Capasso, On the general structure of epidemic systems: Global asymptotic stability, *Computers and Mathematics with Applications*, 12: 677-694, 1986.

[4] A. Berman, R.J. Plemmons, Nonnegative matrices in the mathematical sciences, *Academic Press, New York*, 1970.

[5] S.M. Blower and H. Dowlatabadi, Sensitivity and uncertainty analysis of complex models of disease transmission: an HIV model, as an example, *International Statistical Review*, 62: 229-243, 1994.

[6] B. Buonomo and D. Lacitignola, On the use of the geometric approach to global stability for three dimensional ODE systems: A bilinear case, *Journal of Mathematical Analysis and Applications*, 348: 255-266, 2008.

[7] V. Capasso and S.L. Paveri-Fontana, A mathematical model for the 1973 cholera epidemic in the european mediterranean region, *Revue dépidémoligié et de santé Publiqué*, 27: 121-132, 1979.

[8] V. Capasso and G. Serio, A generalization of the Kermack-Mckendrick deterministic epidemic model, *Mathematical Biosciences*, 42: 43-61, 1978.

[9] C. Castillo-Chavez, Z. Feng and W. Huang, On the Computation of $R_0$ and its role on global stability, *math.la.asu.edu/chavez/2002/JB276.pdf*, 2002.

[10] N. Chitnis, J.M. Cushing and J.M. Hyman, Bifurcation analysis of a mathematical model for malaria transmission, *SIAM Journal on Applied Mathematics*, 67: 24-45, 2006.

[11] C.T. Codeco, Endemic and epidemic dynamics of cholera: the role of the aquatic reservoir, *BMC Infectious Diseases*, 1:1, 2001.

[12] G.W. Cross, Three types of matrix stability, *Linear Algebra and its Applications*, 20: 253-263, 1978.

[13] O. Diekmann, J.A.P. Heesterbeek and J.A.J. Metz, On the definition and the computation of the basic reproduction ratio $R_0$ in models for infectious diseases in heterogrnrous population, *J. Math. Biol.* 578: 365-382, 1990.

[14] K. Dietz, The estimation of the basic reproduction number for infections diseases, *Statistical Methods in Medical Research*, 2: 23-41, 1993.

[15] J. Dushoff, W. Huang and C. Castillo-Chavez, Backwards bifurcation and catastrophe in simple models of fatal diseases, *Journal of Mathematical Biology*, 36: 227-248, 1998.

[16] M. Fan, M.Y. Li, K.Wang, Global stability of an SEIS epidemic model with recruitment and a varying total population size, *Mathematical Boiscience*, 170: 199-208, 2001.

[17] S.M. Faruque, I.B. Naser, M.J. Islam, *et al.*, Seasonal epidemics of cholera inversely correlate with the prevalence of environmental cholera phages, *Proceedings of the National Academy of Sciences*, 102: 1702-1707, 2005.

[18] M. Feckan, A generalization of Bendixson's criterion, *Proceedings of the American Mathematical Society*, 129: 3395-3399, 2001.

[19] M. Feckan, Criteria on the nonexistence of invariant Lipschitz submanifolds for dynamical systems, *Journal of Differential Equations*, 174: 392-419, 2001.

[20] M. Ghosh, P. Chandra, P. Sinha and J. B. Shukla, Modeling the spread of carrier-dependent infectious diseases with environmental effect, *Applied Mathematics and Computation*, 152: 385-402, 2004.

[21] P. Hartman, Ordinary dikerential equations, John Wiley, New York, 1980.

[22] D.M. Hartley, J.G. Morris and D.L. Smith, Hyperinfectivity: a critical element in the ability of V. cholerae to cause epidemics? *PLoS Medicine*, 3: 0063-0069, 2006.

[23] H.W. Hethcote, The mathematics of infectious diseases, *SIAM Review*, 42: 599-653, 2000.

[24] H.W. Hethcote, Qualitative analysis of communicable disease models, *Mathematical Biosciences*, 28: 335-356, 1976.

[25] H.W. Hethcote and S.A. Levin, Periodicity in epidemiological models, in *Applied Mathematical Ecology*, Levin, Hallam, Gross (Eds.), Springer-Verlag, 1989.

[26] T.R. Hendrix, The pathophysiology of cholera, *Bulletin of the New York Academy of Medicine*, 47: 1169-1180, 1971.

[27] M.W. Hirsch, System of differential equations that are competitive or coorperative. VI: A local Cr closing lemma for 3-dimensional systems, *Ergodic Theory and Dynamical Systems*, 11: 443-454, 1991.

[28] M.A. Jensen, S.M. Faruque, J.J. Mekalanos and B.R. Levin, Modeling the role of bacteriophage in the control of cholera outbreaks, *Proceedings of the National Academy of Sciences*, 103: 4652-4657, 2006.

[29] J.B. Kaper, J.G. Morris and M.M. Levine, Cholera, *Clinical Microbiology Reviews* 8: 48-86, 1995.

[30] H.K. Khalil, *Nonlinear systems*, Prentice Hall, NJ, 1996.

[31] A.A. King, E.L. Lonides, M. Pascual and M.J. Bouma, Inapparent infections and cholera dynamics, *Nature*, 454: 877-881, 2008.

[32] K. Koelle, X. Rodo, M. Pascual, Md. Yunus and G. Mostafa, Refractory periods and climate forcing in cholera dynamics, *Nature*, 436: 696-700, 2005.

[33] G.A. Korn and T.M. Korn, *Mathematical handbook for scientists and engineers: definitions, theorems, and formulas for references and review*, Dover Publications, Mineola, NY, 2000.

[34] A. Korobeinikov and P. Maini, A Lyapunov function and global properties for SIR and SEIR epidemiolgical models with nonlinear incidence, *Mathematical Biosciences and Engineering*, 1: 57-60, 2004.

[35] A. Korobeinikov and P.K. Maini, Non-linear incidence and stability of infectious disease models, *Mathematical Medicine and Biology*, 22: 113-128, 2005.

[36] A. Lajmanovich and J. Yorke, A deterministic model for gonorrhea in a nonhomogeneous population, *Mathematical Biosciences*, 28: 221-236, 1976.

[37] S. Lenhart and J. Workman, *Optimal control applied to biological models*, Chapman Hall/CRC, 2007.

[38] B. Li, Periodic orbits of autonomous ordinary differential equations: theory and applications, *Nonlinear Analysis: Theory, Methods and Applications*, 5: 931-958, 1981.

[39] G. Li, W. Wang and Z. Jin, Global stability of an SEIR epidemic model with constant immigration, *Chaos, Solitons and Fractals*, 30: 1012-1019, 2006.

[40] G. Li and J. Zhen, Global stability of an SEI epidemic model with general contact rate, *Chaos, Solitons and Fractals*, 23: 997-1004, 2005.

[41] C. C. McCluskey and D. J. D. Earn, Attractivity of coherent manifolds in metapopulation models, *Journal of Mathematical Biology* , 2010.

[42] M.Y. Li, J.R. Graef, L. Wang and J. Karsai, Global dynamics of a SEIR model with varying total population size, *Mathematical Biosciences*, 160: 191-213, 1999.

[43] M.Y. Li and J.S. Muldowney, On Bendixson's criterion, *Journal of Differential Equations*, 106: 27-39, 1994.

[44] M.Y. Li and J.S. Muldowney, Global stability for the SEIR model in epidemiology, *Mathematical Biosciences*, 125: 155-164, 1995.

[45] M.Y. Li and J.S. Muldowney, A geometirc approach to global-stability problems, *SIAM Journal on Mathematical Analysis*, 27: 1070-1083, 1996.

[46] M.Y. Li, J.S. Muldowney and P.V.D. Driessche, Global stability of SEIRS models in epidemiology, *Canadian Applied Mathematics Quarterly*, 7: 409-425, 1999.

[47] M.Y. Li, H.L. Smith and L. Wang, Global dynamics of an SEIR epidemic model with vertical transmission, *SIAM Journal on Mathematical Analysis*, 62: 58-69, 2001.

[48] M.Y. Li and L. Wang, Global stability in some SEIR epidemic models, *IMA Volumes in Mathematics and its Application*, Spring-Verlag, 126: 295311, 2002.

[49] X. Lin and J.W.H. So, Global stability of the endemic equilibrium and uniform persis- tence in epidemic models with subpopulations, *Journal of the Australian Mathematical Society*, Ser. B, 34: 282-295, 1993.

[50] J. Liu, A First Course in the Qualitative Theory of Differential Equations, *Pearson Education, Inc., Upper Saddle River, New Jersey*, 2003.

[51] B. Lobitz, L. Beck, B. Huq, *et al.*, Climate and infectious disease: use of remote sensing for detection of Vibrio cholerae by indirect measurement, *Proceedings of the National Academic Society USA*, 97: 1438-1443, 2000.

[52] A. Lyapunov, Problemes general de la stabilite du mouvment, *Communications of the Mathematical Society of Kharkow*, 1892; republished in *Annals of Mathematics Studies*, No. 17, Princeton Press, 1947.

[53] S. Marino, I. Hogue, C.J. Ray and D.E. Kirschner, A methodology for performing global uncertainty and sensitivity analysis in system biology, *Journal of Theoretical Biology*, 254: 178-196, 2008.

[54] P.R. Mason, Zimbabwe experiences the worst epidemic of cholera in Africa, *Journal of Infection in Developing Countries*, 3: 148-151, 2009.

[55] V.S. Medvedev, Sufficient conditions for dynamical systems on manifolds to have no integral cycles, *Differential Equations*, 6: 454-466, 1970.

[56] J. Mena-Lorca and H.W. Hethcote, Dynamic models of infectious diseases as regulator of population sizes, *Journal of Mathematical Biology*, 30: 693-716, 1992.

[57] D.S. Merrell, S.M. Butler, F. Qadri, et al., Host-induced epidemic spread of the cholera bacterium, *Nature*, 417: 642-645, 2002.

[58] S.M. Moghadas and A.B. Gumel, Global stability of a two-stage epidemic model with generalized non-linear incidence, *Mathematics and Computers in Simulation*, 60: 107-118, 2002.

[59] I. Mugoya, *et al.*, Rapid spread of Vibrio cholerae 01 throughout Kenya, 2005. *Am. J. Trop.Med.Hyg.*,, 78(3): 527-533, 2008

[60] Z. Mukandavire, S. Liao, J. Wang, H. Gaff, D.L. Smith and J.G. Morris, Estimating the basic reproductive number for the 2008-2009 cholera outbreak in Zimbabwe, preprint, 2010.

[61] R.L.M. Neilan, E. Schaefer, H. Gaff, K.R. Fister and S. Lenhart, Modeling optimal intervention strategies for cholera, *Bulletin of Mathematical Biology*, 2010.

[62] E.J. Nelson, J.B. Harris, J.G. Morris, S.B. Calderwood and A. Camilli, Cholera transmission: the host, pathogen and bacteriophage dynamics, *Nature Reviews: Microbiology*, 7: 693-702, 2009.

[63] R.M. Nisbet and W.S.C. Gurney, *Modeling fluctuating populations*, John Wiley & Sons: New York, 1982.

[64] M. Pascual, M. Bouma, and A. Dobson, Cholera and climate: revisiting the quantiative evidence, *Microbes and Infections*, 4: 237-245, 2002.

[65] E. Pourabbas, A. d'Onofrio and M. Rafanelli, A method to estimate the incidence of communicable diseases under seasonal fluctuations with application to cholera, *Applied Mathematics and Computation*, 118: 161-174, 2001.

[66] R. Redheffer, Volterra multipliers I, *SIAM Journal on Algebraic and Discrete Methods*, 6: 592-611, 1985.

[67] R. Redheffer, Volterra multipliers II, *SIAM Journal on Algebraic and Discrete Methods*, 6: 612-623, 1985.

[68] T.C. Reluga, J. Medlock and A.S. Perelson, Backward bifurcation and multiple equilibria in epidemic models with structured immunity, *Journal of Theoretical Biology*, 252: 155-165, 2008.

[69] F. Rinaldi, Global stability results for epidemic models with latent period, *IMA Journal of Mathematics Applied in Medicine & Biology*, 7: 69-75, 1990.

[70] L.A. Sanchez, Existence of periodic orbits for high-dimensional autonomous systems, *Journal of Mathematical Analysis and Applications*, 363: 409-418, 2010.

[71] C.P. Simon and J.A. Jacquez, Reproduction numbers and the stability of equilibria of SI models for heterogeneous populations, *SIAM Journal on Applied Mathematics*, 52: 541-576, 1992.

[72] B.H. Singer and D. Kirschner, Influence of backward bifurcation on interpretation of $R_0$ in a model of epidemic tuberculosis with reinfection, *Mathematical Biosiences and Engineering*, 1: 91-93, 2004.

[73] H.L. Smith, Monotone Dynamical Systems: An Introduction to the Theory of Compet- itive and Cooperative Systems, *American Mathematical Society, Providence*, 1995.

[74] H.L. Smith and H.R. Zhu, Stable periodic orbits for a class of three dimensional com- petitive systems, *Journal of Differential Equations*, 110: 143-156, 1994.

[75] R.A. Smith, Orbital stability for ordinary differential equations, *Journal of Differential Equations*, 69: 265-287, 1987.

[76] A. Taylor and A. Crizer, A Modified Lotka-Volterra Competition Model with a Non-Linear Relationship Between Species, 2005.

[77] D. Terman, An introduction to dynamical systems and neuronal dynamics, *Tutorials in Mathematical Biosciences I*, Springer, Berlin/Heidelberg, 2005.

[78] J.H. Tien and D.J.D. Earn, Multiple transmission pathways and disease dynamics in a waterborne pathogen model, *Bulletin of Mathematical Biology*, 72: 1506-1533, 2010.

[79] V. Tudor and I. Strati, *Smallpox, cholera*, Tunbridge Wells: Abacus Press, 1977.

[80] P. van den Driessche and J. Watmough, Reproduction numbers and subthreshold endemic equilibria for compartmental models of disease transmission, *Mathematical Biosciences*, 180: 29-48, 2002.

[81] E. Vynnycky, A. Trindall and P. Mangtani, Estimates of the reproduction numbers of spanish influenza using morbidity data, *International Journal of Epidemiology*, 36: 881-889, 2007.

[82] J. Wang and S. Liao, A generalized cholera model and epidemic/endemic analysis, Submitted, 2010.

[83] J. Zhang and Z. Ma, Global dynamics of an SEIR epidemic model with saturating contact rate, *Mathematical Biosciences*, 185: 15-32, 2003.

[84] Center for Disease Control and Prevention web page: www.cdc.gov.

[85] The Wikipedia: en.wikipedia.org.

[86] World Health Organization web page: www.who.org.

# VITA

Shu Liao
Department of Computational And Applied Mathematics
Old Dominion University
Norfolk, VA 23529

## PREVIOUS DEGREES:

M.S. Old Dominion University, Norfolk, VA. (2009)
Major: Computational And Applied Mathematics

B.S. Chengdu University of Technology, Chengdu, China. (2003)
Major: Computational And Applied Mathematics

## SCHOLARSHIP AND EXPERIENCE:

Modeling and Simulation scholarship (08/2009 - 12/2010)
Old Dominion University, Norfolk, VA

Teaching Assistant (08/2007 - 12/2010)
Old Dominion University, Norfolk, VA

## PUBLICATIONS

**S. Liao** and J. Wang, *"A Computational Study of Avian Influenza"*, *Discrete and Continuous Dynamical Systems*, Accepted, 2009.

**S. Liao** and J. Wang, *"Stability Analysis and Application of a Mathematical Cholera Model"*. Submitted, 2010.

Z. Mukandavire, **S. Liao**, J. Wang, H. Gaff, D. L. Smith and J. G. Morris, *"Estimating the basic reproductive number for the 2008-2009 cholera outbreak in Zimbabwe"*. Preprint, 2010.

J. Wang and **S. Liao**, *"A generalized cholera model and epidemic/endemic analysis"*. Submitted, 2010.

**S. Liao** and J. Wang, *"Global stability analysis of epidemiological models based on Volterra-Lyapunov stable matrices"*. Submitted, 2010.

Typeset using LaTeX.